9642

NATIONAL LIBRARY
OTTAWA

CANADA

BIBLIOTHÈQUE NATIONALE
OTTAWA

NAME OF AUTHOR SUSHIL K. SARNA

TITLE OF THESIS Computer models of gastrointestinal electrical control activity.

UNIVERSITY OF ALBERTA

DEGREE FOR WHICH THESIS WAS PRESENTED Ph. D

YEAR THIS DEGREE GRANTED 1971

Permission is hereby granted to THE NATIONAL LIBRARY OF CANADA to microfilm this thesis and to lend or sell copies of the film.

The author reserves other publication rights, and neither the thesis nor extensive extracts from it may be printed or otherwise reproduced without the author's written permission.

(Signed) S K Sarna

PERMANENT ADDRESS:

c/o Electrical Engineering Dept.
U of A, Edmonton-7
Alta

DATED July 26 1971

NL-91 (10-68)

THE UNIVERSITY OF ALBERTA

COMPUTER MODELS OF GASTROINTESTINAL ELECTRICAL CONTROL ACTIVITY

by

© SUSHIL K. SARNA

A THESIS

SUBMITTED TO THE FACULTY OF GRADUATE STUDIES

IN PARTIAL FULFILMENT OF THE REQUIREMENTS FOR THE DEGREE

OF DOCTOR OF PHILOSOPHY

DEPARTMENT OF ELECTRICAL ENGINEERING

EDMONTON, ALBERTA

FALL, 1971

UNIVERSITY OF ALBERTA

FACULTY OF GRADUATE STUDIES

The undersigned certify that they have read, and recommend to the Faculty of Graduate Studies for acceptance, a thesis entitled "Computer Models of Gastrointestinal Electrical Control Activity" submitted by Sushil K. Sarna in partial fulfilment of the requirements for the degree of Doctor of Philosophy.

E. E. Daniel Y. J. Kingma
Supervisors
Keith A. Stromsmoe

....

....

R. B. Stein

G B Walker

Thomas S. Ar
External Examiner

Date 22 June 1974

....

ABSTRACT

The characteristics of the electrical control activity in the gastrointestinal tract were studied in anesthetized dogs and simulated on analog and hybrid computers. A chain of relaxation oscillators was used to model the electrical control activity of the small intestine and an array of oscillators to model the electrical control activity of the stomach. Each oscillator was represented by a system of two first order nonlinear differential equations and was bidirectionally coupled to its adjacent oscillators. The models simulated the following:

a) The frequency gradients and the phase lag patterns observed in the stomach and the small intestine of dog;

b) The effects of complete and partial circumferential cuts on the frequency and the phase relationships of control waves;

c) The intrinsic frequency gradients observed in these organs;

d) The effects of close intraarterial injections of acetylcholine in the stomach and the small intestine of dog. Close intraarterial injections of acetylcholine in the small intestine produced response activity, while those in the stomach produced no effect, prolonged wave cycle, or a premature control potential depending on the phase at which acetylcholine was injected;

e) The effects of local heating and sympathetic reflex activity on the frequency of control waves and the direction of phase lag.

When the gastric and the intestinal models were coupled, the effects of one activity on the other were similar to those observed in the pyloric region of the dog. The models suggested that the gastrointestinal electrical control activity behaves like a system of coupled relaxation oscillators.

ACKNOWLEDGEMENTS

The author would like to express his sincere gratitude to Dr. E. E. Daniel and to Prof. Y. J. Kingma for their guidance and valuable suggestions throughout the course of this work. The animal operations were done in the Department of Pharmacology with the guidance of Dr. E. E. Daniel. The author is grateful to Dr. Daniel for the use of his MRC research grant for the animal operations. The author also wishes to thank the National Research Council of Canada, the Isaac Wilton Killam Memorial Fellowship Trust, and the Department of Electrical Engineering for financial support.

The cooperation received from Mr. Dave Rudyk of the Electrical Engineering Department, Mr. Fred Loeffler and Mr. Ken Burt of the Pharmacology Department is gratefully appreciated.

The author owes a debt of gratitude to his parents, brother and sister for their best wishes, and to his wife Rajni for her encouragement and understanding during this work.

TABLE OF CONTENTS

PAGE

Chapter I INTRODUCTION 1

Chapter II METHODS, MATERIALS AND EQUIPMENT 2

2.1 Animal Studies 2

2.2 Computer Studies 11

Chapter III ELECTRICAL CONTROL ACTIVITY OF THE SMALL INTESTINE 18

3.1 General 18

3.2 Animal Studies 18

3.21 Frequency gradients 18

3.22 Phase lag pattern 26

3.23 Single cuts 28

3.24 Sympathetic reflex and local heating 28

3.25 Intraarterial injections of acetylcholine 33

3.26 Summary of results 36

3.3 Computer Model of Intestinal Electrical Control Activity 37

3.31 Frequency gradients 37

3.32 Phase lag pattern 49

3.33 Single cuts 52

3.34 Local heating and sympathetic reflex 56

3.35 Effects of the occurrence of response activity on control activity 57

3.4 Discussion 63

Chapter IV ELECTRICAL CONTROL ACTIVITY OF THE STOMACH 73

4.1 General 73

PAGE

4.2 Animal Studies 74

4.21 Electrical control activity of the dorsal and ventral walls 74

4.22 Intact frequency gradient 76

4.23 Phase lag pattern 77

4.24 Intrinsic frequency gradient 80

4.25 Partial circumferential cuts 84

4.26 Premature control potentials 94

4.27 Summary of results 101

4.3 Computer Model of Gastric Electrical Control Activity 103

4.31 Arrangement of oscillators 103

4.32 Frequency gradients 103

4.33 Phase lag pattern 107

4.34 Complete circumferential cuts 107

4.35 Partial circumferential cuts 111

4.36 Premature control potentials 114

4.37 Effect of response activity on control activity 115

4.38 Refractoriness of oscillators 121

4.39 Frequency of coupled oscillators 129

4.40 Interaction between duodenal and antral control activities 129

4.4 Discussion 141

Chapter V MATHEMATICAL ANALYSIS 148

5.1 Necessary and Sufficient Conditions for the Existence of a Limit Cycle 148

5.11 Necessary conditions 148

5.12 Sufficient conditions 151

5.13 Coupling of oscillators 157

		PAGE
Chapter VI	CONCLUSIONS, LIMITATIONS AND APPLICATIONS	160
BIBLIOGRAPHY		165
APPENDIX	PDP-8 COMPUTER PROGRAM FOR MULTIPLIERS	172

LIST OF TABLES

TABLE		PAGE
3.1	Effects of intraarterial injections of acetylcholine in the duodenum	35
3.2	Parameters of oscillators for the first intestinal model	47
3.3	Parameters of oscillators for the second intestinal model	48
4.1	Effects of the isolation of dorsal and ventral sides on gastric electrical control activity	76
4.2	Results of partial circumferential cuts in the stomach	95
4.3	Effects of intraarterial injections of acetylcholine on the greater curvature side	99
4.4	Summary of the effects of intraarterial acetylcholine injections on greater curvature sides of 5 dogs	100
4.5	Parameters of oscillators for the gastric electrical control activity model	106
4.6	Effects of complete circumferential cuts in the stomach	110
4.7	Premature control potentials in the gastric model	116
4.8	Effect of the coupling factor between gastric and intestinal models on the frequency of a small isolated segment of antrum	140

LIST OF FIGURES

FIGURE PAGE

2.1 Diagram showing a close intraarterial cannula 10

2.2 Analog computer diagram of an oscillator 13

2.3 Hybrid computer diagram of an oscillator 14

2.4 Diagram showing the circuit to control the time of application of pulses (response activity) and their duration 17

3.1 Diagram of the gastrointestinal tract 19

3.2 Control waves recorded from the frequency plateau region of the small intestine 21

3.3 Control waves recorded from the variable frequency region of the small intestine 22

3.4 Frequency gradients of the electrical control activity in the small intestine of a normal dog 24

3.5 Phase lag pattern in the frequency plateau region of a normal dog 27

3.6 Effects of a single cut in the frequency plateau region of a normal dog 29

3.7 Effect of sympathetic reflex activity on the direction of phase lag 31

3.8 Close intraarterial injections of acetylcholine in the small intestine of a dog 34

3.9 Block diagram for the first intestinal model 38

3.10 Block diagram for the second intestinal model 38

3.11 Frequency gradients in the first intestinal model 41

3.12 Frequency gradients in the second intestinal model 42

3.13 Outputs of oscillators in the frequency plateau region of the second intestinal model 43

3.14 Outputs of oscillators in the variable frequency region of the second intestinal model 44

3.15 Effect of varying bidirectional coupling factor on the frequency of the plateau and its length (first intestinal model) 45

FIGURE		PAGE
3.16	Effect of varying phase shifted coupling factor on the frequency of the plateau and its length (first intestinal model)	46
3.17	Effect of varying parameter b_0 on the resultant frequency of two bidirectionally coupled relaxation oscillators	50
3.18	Phase lag pattern in the frequency plateau region of the second intestinal model	51
3.19	Phase lag between two bidirectionally coupled oscillators as a function of bidirectional coupling factor	53
3.20	A single cut in the frequency plateau region of the first intestinal model	54
3.21	A single cut in the frequency plateau region of the second intestinal model	55
3.22	Simulated local heating in the second intestinal model	58
3.23	Simulated sympathetic reflex activity in the first intestinal model	59
3.24	Effect of response activity on control activity in the second intestinal model. Response activity occurred 2.0 sec after the positive going zero crossing of the control wave	61
3.25	Effect of response activity on control activity in the second intestinal model. Response activity occurred 1.0 sec after the positive going zero crossing of the control wave	62
3.26	Diagram showing the difference in the manner of interaction between longitudinal and circular muscle layers in the duodenum and ileum	70
4.1	Positions of electrodes to record the electrical control activity from the dorsal and the ventral walls of the stomach	75
4.2	The shape of the electrically active region in the dog stomach	78
4.3	Control waves recorded from 6 electrodes near the greater curvature	79
4.4	Phase lag patterns along the greater curvatures of two dogs	81
4.5	Longitudinal and transverse cuts in the stomach to determine the intrinsic frequency gradients	82

FIGURE		PAGE
4.6	Intrinsic frequency gradients in the stomach	83
4.7	A recording showing frequency pulling of distal control waves after a partial cut	86
4.8	Positions of partial cuts in the stomach	92
4.9	Proximal and distal propagation of a premature control potential	97
4.10	Lengthening of wave period due to an intraarterial injection of acetylcholine in the early part of the wave cycle	98
4.11	Block diagram for the gastric electrical control activity model	104
4.12	Intrinsic frequency gradients in the gastric model	105
4.13	Uncoupled and coupled outputs of oscillators representing the greater curvature	108
4.14	The phase lag pattern in the gastric model	109
4.15	The phenomenon of frequency pulling in the gastric model	112
4.16	Occurrence of a premature control potential in the gastric model (no effect on control waves)	117
4.17	Occurrence of a premature control potential in the gastric model (period lengthened)	118
4.18	Occurrence of a premature control potential in the gastric model (propagated proximally and distally)	119
4.19	Occurrence of a premature control potential in the gastric model (propagated distally only)	120
4.20	Effect of response activity on control activity in the gastric model	122
4.21	Definition of a premature control potential	123
4.22	Refractory curve of a single oscillator	125
4.23	Refractory curves of coupled oscillators	126
4.24	Arrangement of coupled oscillators referred to in Fig. 4.23	127
4.25	Refractory curves for different coupling factors	128

FIGURE		PAGE
4.26	Refractory curves when input pulse applied to more than one oscillator	130
4.27	Effect of varying parameter b_0 on the resultant frequency of two bidirectionally coupled oscillators	131
4.28	Block diagram showing the coupling of intestinal and gastric models	132
4.29	Effects of antral control activity on duodenal control activity	134
4.30	Effects of antral control activity on the most proximal duodenal oscillator when it is uncoupled from the rest of intestinal oscillators	137
4.31	Effects of duodenal control activity on antral control activity	138
4.32	Effects of duodenal control activity on antral control activity after a complete simulated circumferential cut in the antrum	139
4.33	Diagram explaining the reason for the proximal and distal propagation of a premature control potential	145

CHAPTER I

INTRODUCTION

The presence of a rhythmic electrical activity in the stomach and the small intestinal muscle layers was first reported by Alvarez et al. (1) in 1921. Puestow (2) in 1932 confirmed the presence of this activity in isolated intestinal segments and reported another activity called spike activity superimposed on the rhythmic activity. The relationship between rhythmic activity, spike activity and mechanical contractions was first cited by Bozler (3) in 1946. Since then, several investigators in this field have studied the nature, the origin and the spread of these activities, using a variety of techniques (1-28, 32, 33, 35-42, 46-55).

It is now generally agreed that the gastrointestinal muscle layers exhibit two distinct types of electrical activity. The first type is a rhythmic activity known as slow wave activity (32), pacesetter activity (33) or basic electrical rhythm (10). This activity does not by itself cause contractions. It is present all over the small intestine and distal two-thirds of the stomach at all times. The intestinal waveform recorded with monopolar extracellular electrodes is a rapid positive going spike followed by a plateau before decay (7, 12). The stomach waveform recorded with similar electrodes (7, 13, 14) is a triphasic potential (positive, negative, positive). When recorded with intracellular electrodes, the intestinal waveform is non-sinusoidal (7) and the stomach waveform is a monophasic positive spike (15, 16). This activity has been referred to as Electrical Control Activity (ECA) in this thesis.

The second type of electrical activity, known as fast activity or action potentials, is of intermittent nature. This activity can be recorded from a segment only when it is mechanically active. The waveform of this activity when recorded with extracellular electrodes is a negative going spike, but when recorded with intracellular electrodes it is a positive going spike (37). This activity has been referred to as Electrical Response Activity (ERA) in this thesis.

The electrical control activity is so designated because it controls the occurrence of electrical response activity (7, 8) and hence of contractions. The response activity is initiated when the control activity is in a relatively positive phase. This, in other words, means that the frequency of local contractions and their sequence depend on the frequency of control activity and its phase lag pattern. These two factors occur appropriately in the small bowel and the stomach for effective mixing and/or propulsive movements.

Various experiments support the view that the control activity of the stomach and the small intestine is myogenic in nature (19). Isolated segments of small intestine and stomach continue to show control activity. The control activity of the small intestine is not affected by section of extrinsic nerves, sympathetic and vagal stimulation (20). The activity is not suppressed by blocking agents like atropine or phenoxybenzamine in their effective concentrations (6, 8) or by nicotine, hexamethonium and cocaine in doses which normally interfere with nerve conduction or transmission (7, 8, 20). Also the activity is not abolished by moderate doses of drugs which stimulate or inhibit intestinal motility; e.g., acetylcholine, 5-HT or adrenaline (6, 7). The frequency and amplitude of control activity are, however, very sensitive to temperature, a decrease in temperature decreasing the amplitude and frequency (7, 17). This suggests that the generation of ECA may be related to some metabolic process.

Daniel *et al.* (17) showed by using microelectrodes that the origin of control activity is in the longitudinal muscle layers. This view is supported by the observations of others who studied isolated strips of longitudinal and circular muscle layers (11, 21). Isolated longitudinal muscle strips continue to show ECA at the original frequency in some species like rabbits and at a lower frequency in some other species like cats (38). Circular muscle cells show control activity only when connected to longitudinal muscle cells (21, 39). It has been suggested that the control activity is generated in the longitudinal muscle cells and spreads electrotonically into the circular muscle cells. Another possibility that has been suggested is that the circular muscle cells are potential oscillators but oscillate only when driven by the control activity of longitudinal muscle cells (27). The ionic basis of generation of either the control activity or the response activity is not clear yet.

The electrical control activity in the stomach and the small intestine has been studied in isolated muscle, in isolated segments and in intact organs. There are still several controversial points regarding the nature and behavior of this activity. For instance, both a stepwise and a continuous frequency gradient have been reported in the intestine (22-24, 33, 40-42), various specialized conduction paths have been suggested for the stomach control potentials (48-50) and so on. To clarify some of these points we carried out a study of gastrointestinal ECA characteristics. The purpose of this project, therefore, was to study the nature and behavior of ECA in the gastrointestinal tract, and to make computer models of it consistent with the experimental data. The models were also used to interpret available physiological data and to make predictions which could be tested in the animals. Effects of the occurrence of ERA on ECA were also studied.

The results of most of the previous studies have been interpreted in terms of cable theory or a core conductor model. Two kinds of explanations based on cable theory have been given for the spread of electrical activity in the small intestine. The first explanation assumes a single pacemaker in the duodenum. Control wave of this pacemaker may propagate throughout the intestine, tending to excite all regions. Different regions will then respond to this stimulus at a maximum frequency determined by their inherent frequency and other factors. This explanation is favored by investigators who did experiments to locate a single pacemaker in the duodenum (4, 5, 23). The second explanation was that there may be multiple pacemakers located along the length of the intestine. This explanation is favored by the group of workers who found a stepwise frequency gradient in the intestine (24, 25). In this case the control wave from one pacemaker would propagate up to the second pacemaker and then the control wave of the second pacemaker would take over. Termination of propagation would be due to the inability of the distant pacemaker to respond to the first pacemaker due to depletion in the strength of the stimulus or due to its low inherent frequency.

The hypothesis assumed in this thesis is that the gastrointestinal electrical control activity is caused by a large number of relaxation oscillators (23, 26-28). Nelson and Becker (23) were the first to propose that the intestinal electrical activity behaves like a chain of loosely coupled relaxation oscillators. They simulated the frequency gradients of the small intestine by two forward coupled Van der Pol oscillators. They used this model to study the phenomenon of frequency pulling, fequency entrainment, etc., between relaxation oscillators and concluded that the gradient of ECA frequency in the intestine could be determined by a variable degree of frequency pulling due to variation in the coupling factor. Their model could not simulate other intestinal ECA characteristics (see Chapter III) due to the use of only two oscillators. Addition of backward coupling in their dual oscillator model pulled down the frequency of the proximal higher frequency oscillator unless the ratio of forward to backward coupling was more than 10 to 1. The inference drawn was that in the smooth muscle of the gut with a normally functioning pacemaker, refractoriness to backward conduction is more than 10 times the excitability in the resting state, immediately after the passage of an impulse, since distal bowel frequency had no effect on duodenal frequency. Such a degree of refractoriness was obviously not present in the model, since with equal magnitudes of forward and backward couplings the distal oscillator pulled down the frequency of the proximal oscillator.

Recently Diamant et al. (26) simulated the ECA frequency gradient of the small intestine by using a chain of 10 forward coupled Van der Pol oscillators. They studied properties like length of frequency plateau as a function of the coupling factor, waxing and waning zones, formation of multiple frequency plateaus, etc. A similar model was tried in the early stages of this work, but was found to be inadequate because it could not simulate all the intestinal ECA characteristics. Also forward coupling alone was not acceptable on a priori and ultrastructural grounds (Daniel, E. E., Duchon, G. and Henderson, R., in press). When backward coupling was added in the above model of forward coupled Van der Pol oscillators, the distal lower frequency oscillators pulled down the frequency of proximal higher frequency oscillators. No similar observation has ever been reported for the small intestine. However, due to the junctional symmetry of the connections among cells, backward coupling must always be present.

Models of the stomach and the small intestinal ECA proposed in this thesis use relaxation oscillators represented by a system of two first order nonlinear differential equations. The oscillators were arranged in the form of a chain for the intestinal model and in the form of an array for the stomach model. Each oscillator was bidirectionally coupled to its adjacent oscillators. The models simulated all the characteristics observed in the small intestine and the stomach of dogs. Use of relaxation oscillators to model the stomach ECA is novel.

Several examples exist of the occurrence of relaxation oscillations in biological systems and in nature. Van der Pol and Van der Mark (29) were the first to use relaxation oscillators to make an electrical model of the heart. Roberge and Nadeau (34) destroyed the sinus node in heart and simulated its rhythmic activity by an electronic relaxation oscillator forward coupled to the beating heart. The output of the relaxation oscillator was used to stimulate the right atrium, and the ventricular response was returned to the input of the relaxation oscillator. Other familiar examples of the occurrence of relaxation oscillations in nature are the periodic recurrence of epidemics, the periodic density of two species of animals living together, and one species serving as food to the other, sleeping of flowers, etc. (29, 31).

The methods, materials and equipment used during the course of this research are explained in the second chapter. The small intestine and the stomach models are described in the third and fourth chapters, respectively. Each of these chapters is divided into three sections; namely, animal studies, computer model studies and discussion. Mathematical analysis is given in the fifth chapter. Conclusions, applications and limitations of these models, and possible future work, are described in the sixth chapter.

CHAPTER II

METHODS, MATERIALS AND EQUIPMENT

2.1 Animal Studies

Healthy female dogs weighing 10-20 kg were used in all experiments. Dogs were fasted for 24 hours before the experiment. A mixture of chloralose (2%) urethane (10%) (3 ml/kg) given intravenously was used as the anesthetizing agent. Subsequent to this, sodium pentobarbital (60 mg each time) was given intravenously if needed. Reserpinized dogs (0.1 mg/kg intravenously for 3 days before use) were used in some experiments to suppress the reflex release of norepinephrine when the intestine was cut or constricted at a point along its length.

Access to the abdominal cavity was obtained by a midline opening from sternum to pelvis. Rectal or abdominal temperature was monitored with a thermometer and maintained between 38.5 and 40 °C by heat radiation and control of room temperature.

Silver wire electrodes (0.15 mm diameter) were implanted in the seromuscular layers of the stomach and the small intestine to record electrical activity. The indifferent or ground electrode was placed subcutaneously in the left thigh to minimize cardiac electrical activity. As far as possible, all the electrodes were implanted simultaneously to minimize handling of the organs and the fall in temperature. After placement of electrodes 30-45 minutes were allowed for these organs to recover from the above effects.

All recordings were made on a 6-channel Beckman Dynograph model R recorder with a curvilinear ink writer (R-C coupled, time constant 0.3 or 1 sec, high frequency filter setting at 3). Repeated records were taken at proximal electrodes to guarantee that their frequencies did not change as the activity at distal electrodes was recorded. Frequencies were averaged over 1-minute periods in the intestinal records, and over 5-minute periods in the stomach records. Minimum recording period at each electrode was 10 minutes.

If a small segment of the intestine or the stomach is isolated electrically from the rest of the organ, it continues to show an ECA frequency of its own called intrinsic frequency. Three procedures were tried to determine the intrinsic frequency gradient in the small intestine. In the first procedure, the intestine was constricted by a 4 mm diameter rubber tube; in the second procedure, it was transected; and in the third procedure, the muscle layers were cut and peeled back 5-10 mm. All these procedures cited in order of decreasing intensity of the reflex led to sympathetic activity in unreserpinized dogs, causing increased ECA frequency and reversal in the direction of phase lag distal to the affected area. Even after reserpinization, which led to severe diarrhea, a brief period of reflex sympathetic activity was sometimes observed. Eventually section of muscle layers was adopted as the routine procedure because of the milder trauma produced, less reflex activity, the avoidance of leakage of bowel contents into the abdominal cavity, and because the procedure was easy to perform. Section of muscle layers was the only method used in the stomach. Electrodes implanted in the submucosa after removal of muscle layers did not record any rhythmic electrical activity which indicated that the segments proximal and distal to the cut were electrically uncoupled.

Premature control potentials in the stomach and ERA in the intestine were induced by intraarterial injections of acetylcholine (0.05 to 0.5 μg in heparinized Krebs Ringer solution at 41 °C). One of the vasa recta that perfused 1-2 cm length of intestine was selected (Fig. 2.1). The artery was separated from the adjacent vein and nerve, and cannulated with a small polythene cannula (inner diameter 0.58 mm, outer diameter 0.96 mm). To overcome the effect of dead space, each injection of acetylcholine was flushed with 0.5-1 cc of Krebs. A similar procedure was used for the acetylcholine perfusion in the stomach. The artery used was usually the gastroepiploic. On a few occasions a branch of the right gastric artery near the lesser curvature was cannulated.

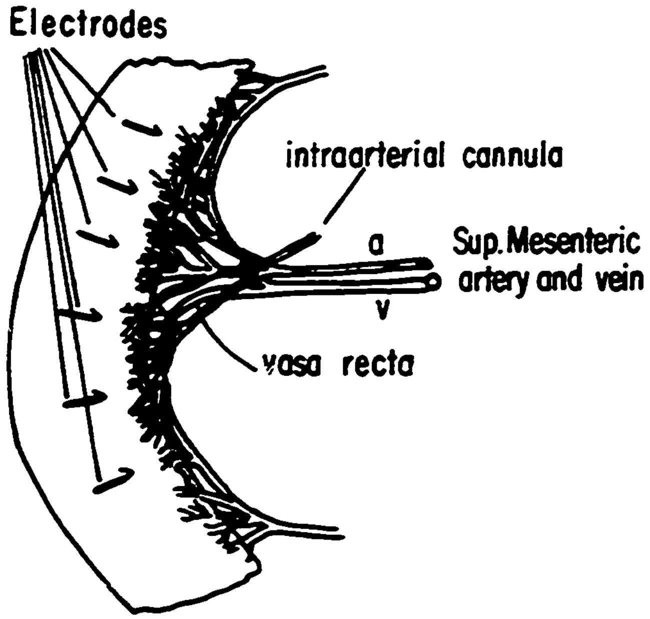
Electrodes
intraarterial cannula
a
v
Sup. Mesenteric artery and vein
vasa recta

Figure 2.1

Diagram showing a close intraarterial cannula in the small intestine.

2.2 Computer Studies

Seventeen relaxation oscillators were programmed on analog and hybrid computers (PACE 231R, TR-48, 4 TR-20's, 4 SLAC-6's, Redcor interface and PDP-8). The intestinal electrical control activity was modelled by a chain of these oscillators and the gastric control activity by an array. Each oscillator was represented by the following system of two first order nonlinear differential equations:

$$\dot{x} = k(a_1 y + a_2 x + a_3 x^2 + a_4 x^3) \tag{2.1}$$

$$\dot{y} = \frac{-1}{k}(b_1 y + b_2 x + b_3 x^2 + b_4 x^3 - b_0) \tag{2.2}$$

These equations are a generalized form of the Van der Pol equation (29):

$$\ddot{x} - k(1 - x^2)\,\dot{x} + b_2 x = 0 \tag{2.3}$$

where k is the damping coefficient and $\sqrt{b_2}$ is the undamped natural frequency in radians per second.

Fitzhugh (30) used Lienard's transformation to obtain a system of two first order differential equations as follows:

$$\text{Let} \quad y = \frac{\dot{x}}{k} + \frac{x^3}{3} - x \tag{2.4}$$

then

$$\dot{y} = \frac{\ddot{x}}{k} + x^2\dot{x} - \dot{x}$$

Using equation (2.3),

$$\dot{y} = -\frac{b_2 x}{k} \tag{2.5}$$

Terms were added to equation (2.5) to give

$$\dot{y} = -\frac{1}{k}(b_2 x - b_0 + b_1 y) \tag{2.6}$$

Also from equation (2.4)

$$\dot{x} = k(y + x - \frac{x^3}{3}) \tag{2.7}$$

Equations (2.6) and (2.7) are known as Bonhoeffer-Van der Pol (BVP) or Fitzhugh equations. Fitzhugh used these equations to make models of nerve membrane (with $b_2 = 1$). Equations (2.1) and (2.2) were obtained by adding terms to equations (2.6) and (2.7) and generalizing them. Roberge (43) used a similar system of equations to simulate the phenomenon of concealed conduction in the heart. In the phase plane analysis of the nerve membrane model, Fitzhugh derived conditions such that the system rested at a stable point, but when stimulated by an impulse, it would exhibit the all-or-none phenomenon of an action potential. In the gastrointestinal models, parameters in equations (2.1) and (2.2) were adjusted such that a limit cycle existed in the phase plane.

The computer diagram for one oscillator is shown in Figure 2.2. A PDP-8 digital computer was used in place of multipliers in 6 oscillators (Fig. 2.3). The digital program in assembly language is given in the appendix. The oscillators were coupled through potentiometers so that any desired coupling factor between 0 and 1 could be obtained.

Preliminary investigations of the solution to equations (2.1) and (2.2) showed that the peak amplitude of oscillations was less than 3. The equations were magnitude scaled for greater accuracy as follows:

Let $x_{max} = y_{max} = 10V$.

$\dot{x}_{max} = \dot{y}_{max} = 10V/sec$; then

$$10\left[\frac{\dot{x}}{10}\right] = k(10a_1\left[\frac{y}{10}\right] + 10a_2\left[\frac{x}{10}\right] + 100a_3\left[\frac{x}{10}\right]^2 + 1000a_4\left[\frac{x}{10}\right]^3)$$

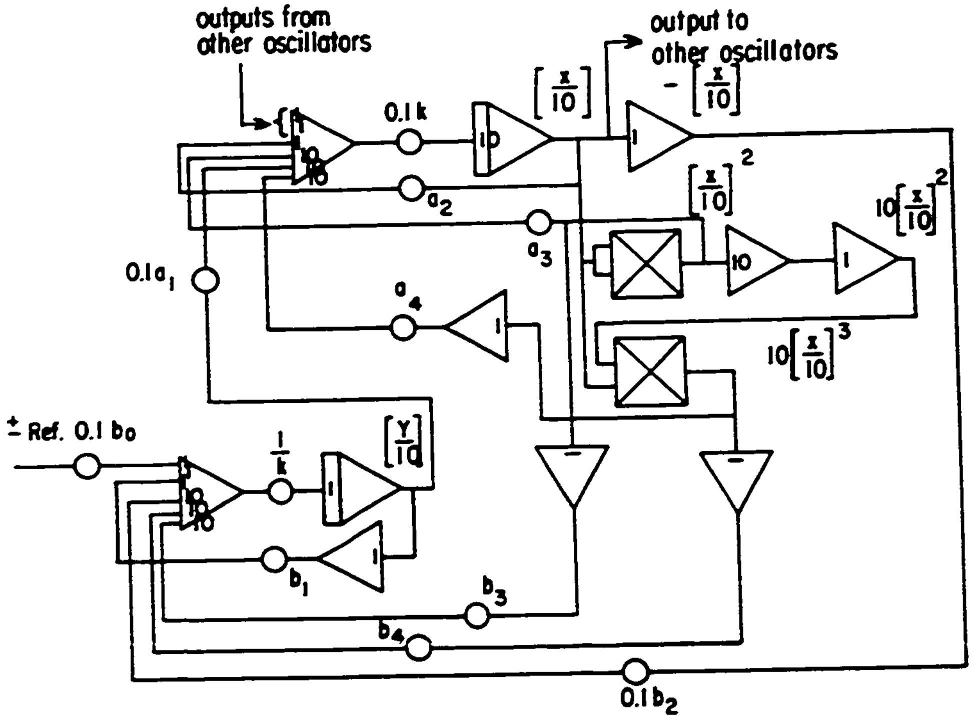
outputs from other oscillators
output to other oscillators
[x/10]
- [x/10]
0.1k
10
1
10
10
a2
a3
a4
0.1a1
[x/10]^2
10[x/10]^2
10[x/10]^3
± Ref. 0.1 bo
1/k
[Y/10]
b1
b3
b4
0.1b2

Figure 2.2

Analog computer diagram of an oscillator (see ref. 62 for symbols used). The forcing function (outputs from other oscillators) is added according to equation 3.1. The addition of forcing function as shown here is equivalent to adding the forcing function and its first derivative to the second order differential equation representing the oscillator (see section 5.2).

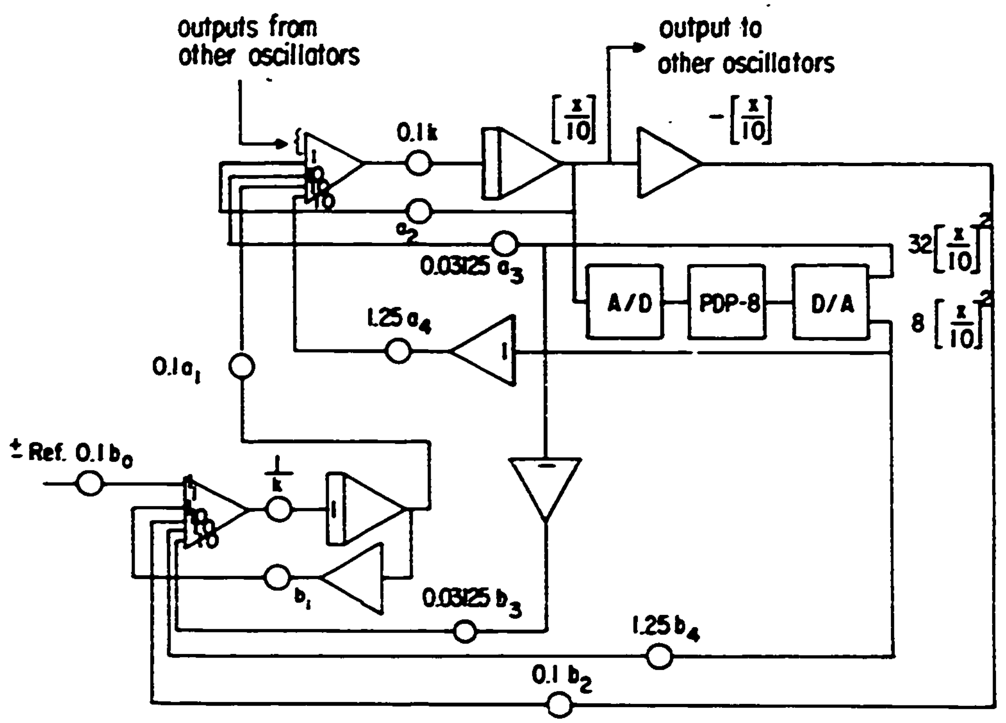
outputs from
other oscillators
output to
other oscillators
$\left[\frac{x}{10}\right]$
$-\left[\frac{x}{10}\right]$
0.1k
a_2
$0.03125\ a_3$
$32\left[\frac{x}{10}\right]^2$
$8\left[\frac{x}{10}\right]^2$
A/D
PDP-8
D/A
$1.25a_4$
$0.1a_1$
± Ref. $0.1b_0$
$\frac{1}{k}$
b_1
$0.03125\ b_3$
$1.25b_4$
$0.1\ b_2$

Figure 2.3

Hybrid computer diagram of an oscillator (see ref. 62 for symbols used). The forcing function (outputs from other oscillators) is added according to equation 3.1. The addition of forcing function as shown here is equivalent to adding the forcing function and its first derivative to the second order differential equation representing the oscillator (see section 5.2)

$$10\left[\frac{\dot{y}}{10}\right] = -\frac{1}{k}\left(10b_1\left[\frac{y}{10}\right] + 10b_2\left[\frac{x}{10}\right] + 100b_3\left[\frac{x}{10}\right]^2 + 1000b_4\left[\frac{x}{10}\right]^3 - b_0\right)$$

or

$$\left[\frac{\dot{x}}{10}\right] = k\left(a_1\left[\frac{y}{10}\right] + a_2\left[\frac{x}{10}\right] + 10a_3\left[\frac{x}{10}\right]^2 + 100a_4\left[\frac{x}{10}\right]^3\right)$$

$$\left[\frac{\dot{y}}{10}\right] = -\frac{1}{k}\left(b_1\left[\frac{y}{10}\right] + b_2\left[\frac{x}{10}\right] + 10b_3\left[\frac{x}{10}\right]^2 + 100b_4\left[\frac{x}{10}\right]^3 - \frac{b_0}{10}\right)$$

Analog computers were preferred to digital computers to solve the nonlinear differential equations because of the ease with which the parameters in the equations could be varied and their effect studied. Except for the overall characteristics of the oscillators in the stomach and the small intestine, very little is known about them. Processes responsible for the periodic depolarization of smooth muscle cells are uncertain yet. Determination of equations, similar to those of Hodgkin and Huxley (44, 45) for squid axon, in the case of smooth muscle, is difficult and incomplete for experimental and other reasons. A general system of differential equations was, therefore, chosen to represent relaxation oscillations. Its parameters were varied such that independent oscillations of desired frequency existed in the uncoupled oscillators, but when coupled the characteristics of the gastric or the intestinal control activity were obtained. The search for the appropriate parameters would be very difficult and time-consuming if the effect of variation of each parameter or a number of them simultaneously could not be observed side by side.

The effect of intraarterial injections of acetylcholine in the stomach and the intestine was studied on the model by feeding pulses at the inputs of oscillators. Single pulses of 0.5 or 1 sec duration were fed to initiate premature control potentials in the stomach, and to draw refractoriness curves (Chapter IV). Bursts of spikes consisting of pulses at a frequency of 10/sec and pulse duration of 30 msec were fed into the oscillators to study the effect of ERA on ECA in the small intestine and the stomach. These values are close to those observed in the animal records. A TR-20 analog computer and 4 comparators (Fig. 2.4) were used to control the duration of pulses and to feed them at various phases of the wave cycle.

The oscillator used to trigger comparator C_1 was the same as that into which the pulses were to be fed. The time of onset of the pulse at A06 was measured from the positive going zero crossing of the oscillator output.

$$\text{Time of onset of pulse} = \frac{\text{setting of P02}}{10(\text{setting of P01})}\ \text{sec}$$

$$\text{Duration of pulse} = \frac{\text{setting of P03} - \text{setting of P02}}{10(\text{setting of P01})}\ \text{sec}$$

The use of a separate analog computer (TR-20) allowed repeated feedings of pulses without interfering with the working of the model.

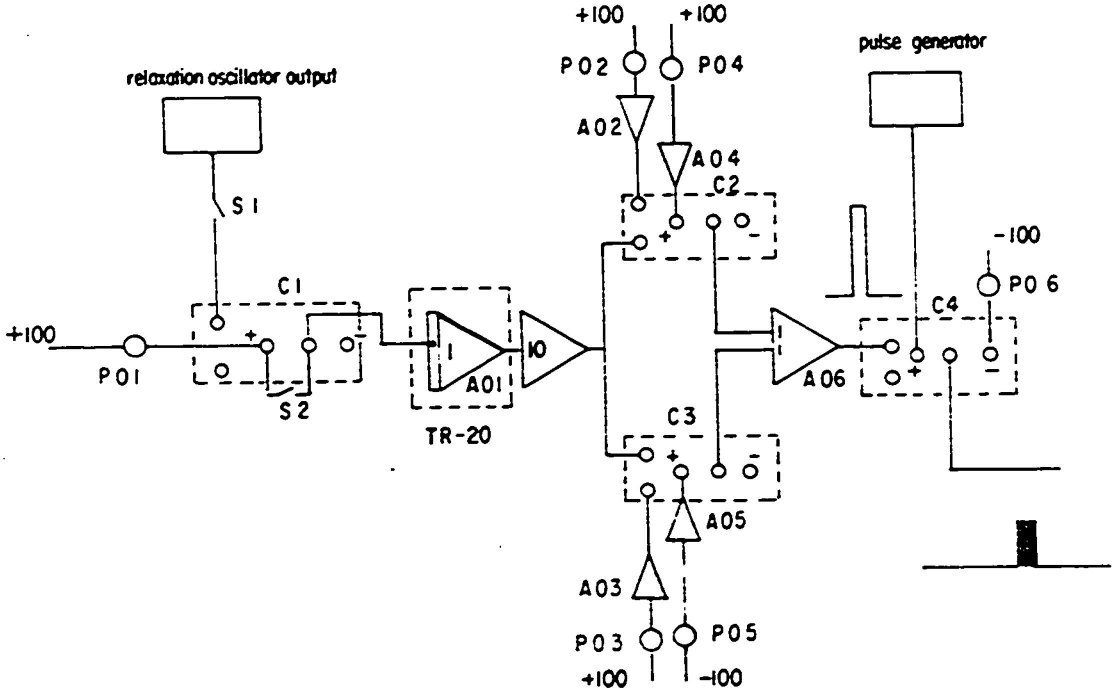
+100
+100
P02
P04
A02
A04
C2
pulse generator
relaxation oscillator output
S1
-100
P0 6
C1
C4
+100
P01
S2
A01
TR-20
10
A06
C3
A05
A03
P03
P05
+100
-100

Figure 2.4

Diagram showing the circuit to control the time of application of pulses and their duration. Time was measured from the positive going zero crossing of the control wave.

CHAPTER III

ELECTRICAL CONTROL ACTIVITY OF THE SMALL INTESTINE

3.1 General

The small intestine is a convoluted tube extending from the pylorus of the stomach to the ileocecal orifice (Fig. 3.1). It is divided into 1) the duodenum, 2) the jejunum and 3) the ileum. The duodenum, about 20 cm in length in the dog, is the most proximal part. The remainder of the intestine is divided arbitrarily into a jejunum (proximal two-fifths) and an ileum distally.

The intestinal wall has two major muscle layers: one is longitudinally oriented and called the outer or longitudinal muscle layer; the other is circumferentially oriented and called the inner or circular muscle layer. The origin of ECA has been shown to be in the longitudinal muscle layer (11, 17, 21).

3.2 Animal Studies

3.21 Frequency gradients

Frequency gradients were determined in 9 dogs. Up to 55 electrodes were implanted (approximately 5 cm apart) throughout the entire length of the small intestine in each dog.

Control waves in the duodenum and the proximal jejunum were phase locked and hence of the same frequency (18.0-21 c/min in 9 dogs, mean 19.0 ± 0.675 s.e.). This region of the small intestine was defined as the frequency plateau. Two waves were considered phase locked if the maximum deviation in phase from the initial phase difference did not exceed 360°. This definition of phase locking

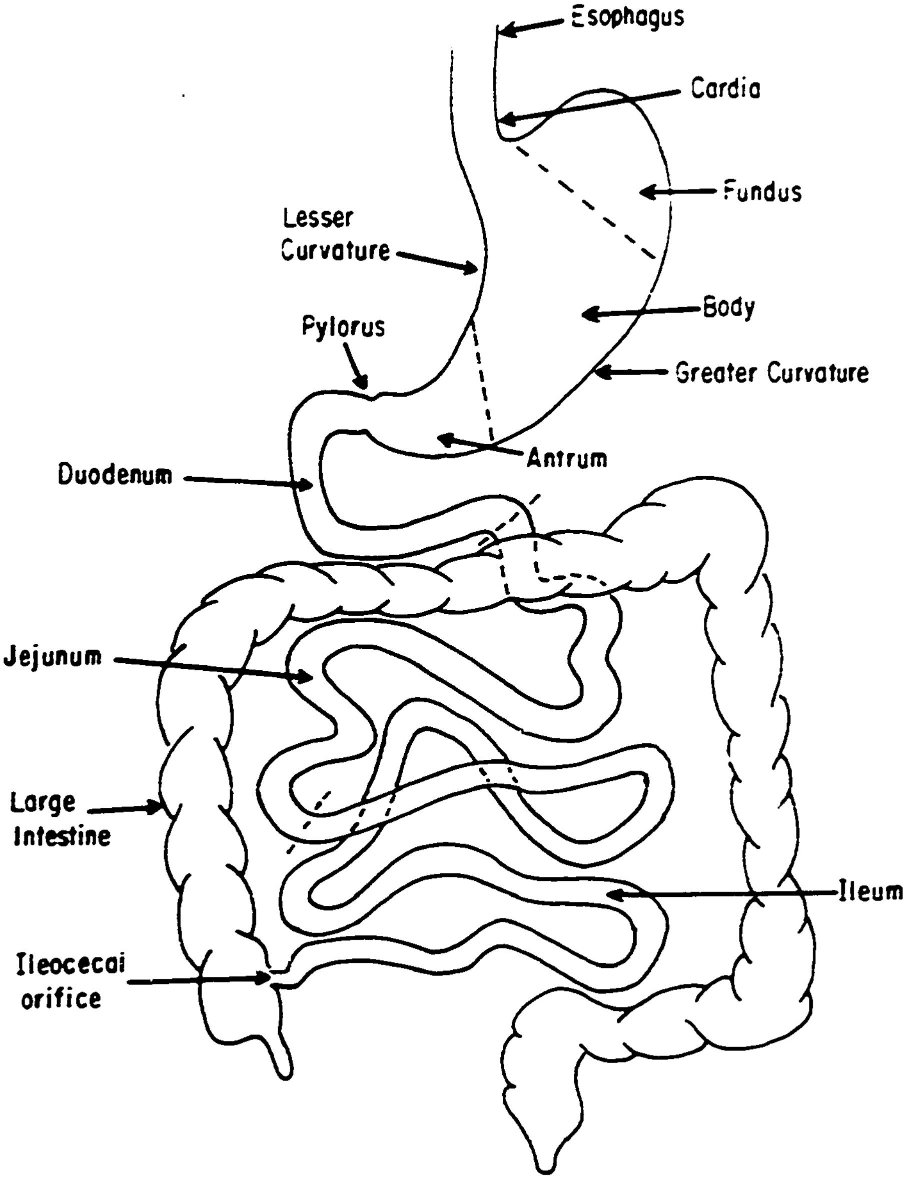
Esophagus
Cardia
Fundus
Lesser Curvature
Body
Pylorus
Greater Curvature
Duodenum
Antrum
Jejunum
Large Intestine
Ileum
Ileocecal orifice

Figure 3.1

Diagram of gastrointestinal tract.

was adopted to allow for the variable time period of waves recorded from biological systems like the small intestine. The length of the frequency plateau varied from 60 to 80 cm in different dogs. Figure 3.2 shows the phase locked control waves recorded from 6 electrodes implanted in the proximal 30 cm length of the small intestine.

There were no frequency plateaus (as defined above) distal to the first one in the 9 dogs investigated for this purpose. The control waves distal to the frequency plateau showed temporal variation in average frequency, and were not phase locked. From the end of the frequency plateau to the end of the small intestine, the average frequency reduced to 12-14 c/min in different dogs. This region was defined as the variable frequency region. Figure 3.3 shows the recording obtained from 6 electrodes implanted in the variable frequency region. Electrode 1 was at a distance of 75 cm from the pylorus, and the distance between successive electrodes in the distal direction was 5 cm. It is seen that the control waves recorded at electrodes 4, 5 and 6 fall behind by one cycle from the control waves recorded at electrodes 1, 2 and 3 during the time interval shown by arrows.

The end of the frequency plateau was not clearly defined. Near the end, the waves remained phase locked for most of the time, but occasionally fell out of phase. As a result, the average frequency in this region was only slightly lower than the plateau frequency. The waves in this region and in those distal to it showed more irregularity in amplitude and in instantaneous frequency than the waves inside the frequency plateau region.

The variable frequency region was studied in further detail to detect the presence of any short plateaus. Up to 40 electrodes were implanted (1-5 cm apart) in the ileum and the jejunum of 2 dogs. Control

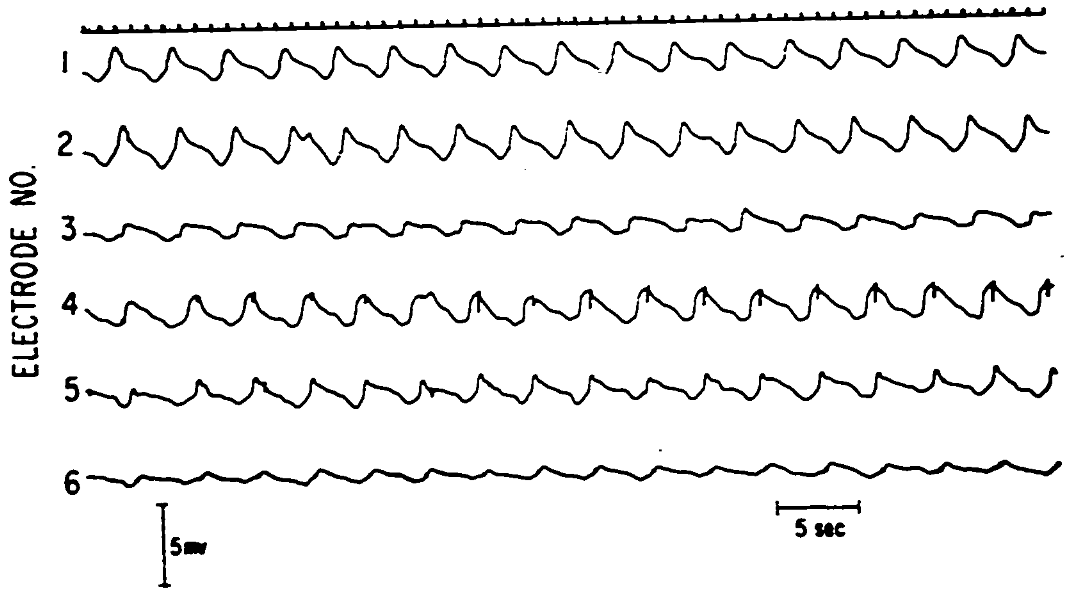

Figure 3.2

Control waves recorded from 6 electrodes implanted in the proximal 30 cm length of the small intestine. Distances of electrodes 1 to 6 from the pylorus were 5, 10, 15, 20, 25 and 30 cm, respectively. Note that the control waves are phase locked.

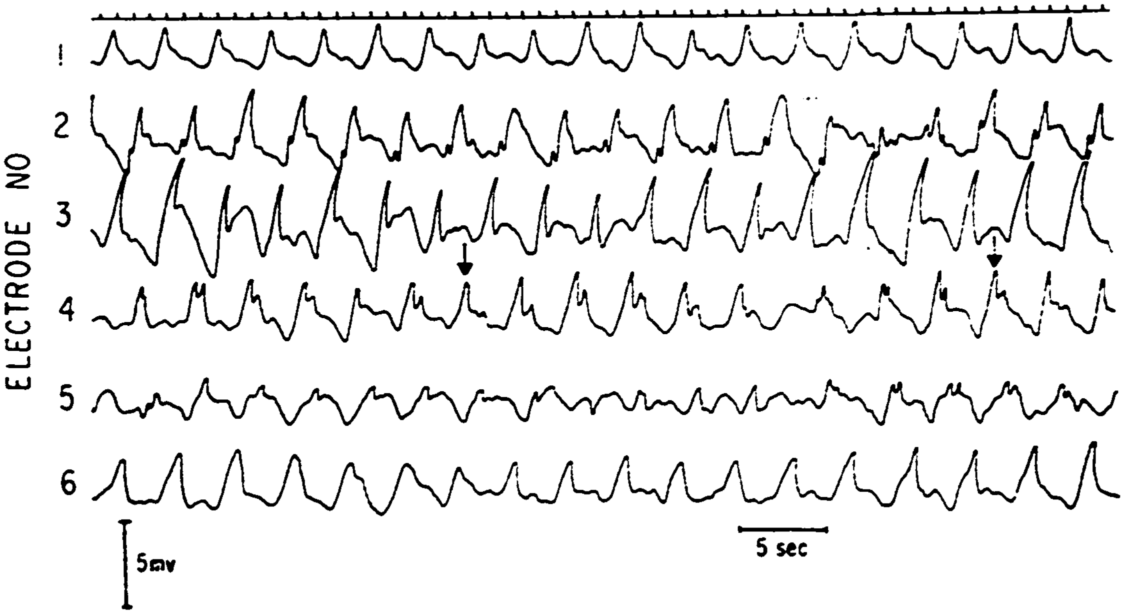

Figure 3.3

Control waves recorded from 6 electrodes implanted in the variable frequency region of the small intestine. Distances of electrodes 1 to 6 from the pylorus were 75, 80, 85, 90, 95 and 100 cm, respectively. Control waves recorded at electrodes 4, 5 and 6 became unlocked from the control waves recorded at electrodes 1, 2 and 3 during the time interval shown by two arrows.

waves recorded from electrodes less than 5 cm apart were phase locked for variable lengths of time. In one dog, where the distal 100 cm length of the small intestine was studied, three regions less than 5 cm in length were found where the control waves were phase locked for more than 10 minutes. In general, however, the phase lag increased gradually, and the waves got unlocked in less than 10 minutes (Fig. 3.3). It seemed that there was a critical value of phase lag beyond which the two waves could not remain phase locked. When this value of phase lag was reached, the waves became unlocked for one or two cycles, and then locked again to repeat the process of increasing the phase lag. The distal 70 cm length of the small intestine in the above-mentioned dog was then isolated into small segments, 5 cm in length. This increased the tendency of waves to become phase locked for longer periods. In 5 isolated segments, the waves remained phase locked for more than 10 minutes.

In the second dog, two regions less than 5 cm in length were found where the control waves were phase locked for more than 10 minutes. The distal region under study (110 cm in length) was then isolated from the proximal region by a single cut. As for the first dog, it increased the tendency of control waves to remain phase locked for longer periods. Two regions 10 cm in length were found where the waves remained phase locked over a 10-minute recording period. These regions were found immediately distal to the cut. These experiments suggested that coupling with higher frequency oscillators was one of the factors that prevented the formation of a stable frequency plateau in the distal small intestine.

The shape of the frequency gradient in the intestine of a normal dog is shown in Figure 3.4. The frequency plateau length for the dog was 60 cm, and the plateau frequency 21 c/min. Variations in the

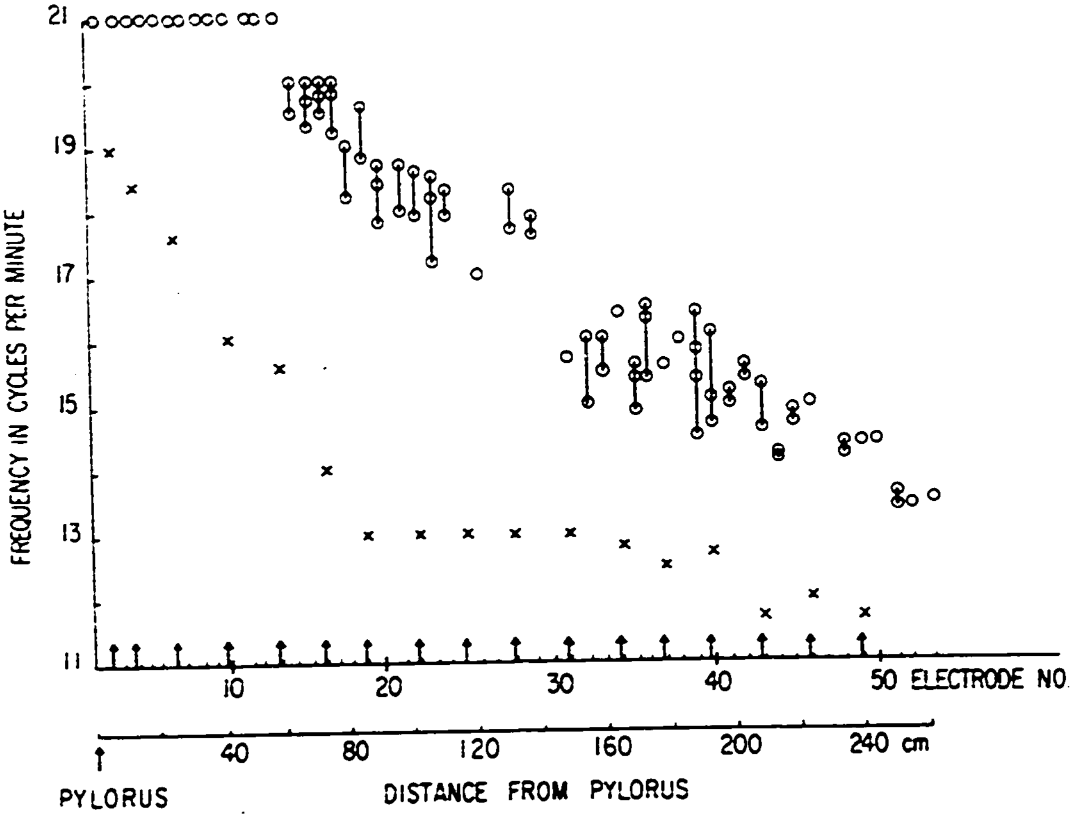

Figure 3.4

Frequencies (○) recorded at 53 electrodes implanted simultaneously throughout the entire length of the small intestine. All frequencies were averaged over 1-minute periods. Height of each vertical line shows the range of variation of 1-minute average frequency over a minimum time interval of 10 minutes. Intrinsic frequencies (×) of regions just distal to the cuts (at arrows) are shown.

average frequencies distal to the frequency plateau are shown by vertical lines. The length of each vertical line shows the range of variation of 1-minute average frequency over a 10-minute interval. Similar frequency gradients were observed in the other 4 normal dogs and in 4 reserpinized dogs (27).

Figure 3.4 also shows the intrinsic frequencies in the same dog after section of the muscle layers at 15 cm intervals (shown by arrows) and recovery from the sympathetic reflexes and temperature decrease which followed surgery. The intrinsic frequencies shown are of regions immediately distal to the cuts. It was confirmed by making further cuts within the 15 cm segments that the frequencies of the proximal regions were not being pulled down by the distal lower frequency regions in the isolated segment. Intrinsic frequencies were determined in this way in 6 dogs. It was invariably found, as in this dog, that the intrinsic frequencies decreased rapidly in the proximal part (90-120 cm from the pylorus) and gradually in the distal part of the small intestine. Diamant and Bortoff (24) reported a linear intrinsic frequency gradient.

Closely spaced cuts were made in the region 5-10 cm from the pylorus to determine the highest intrinsic frequency in the small intestine (3 dogs). The intrinsic frequency gradient in this region was not as steep as in the rest of the duodenum. The highest intrinsic frequency measured was less than the plateau frequency in all cases. Diamant and Bortoff (24) have reported similar findings.

The control waves in the isolated segments which previously formed the frequency plateau were still phase locked, and the phase lag was in the aboral direction. In the distal isolated segments, the frequencies recorded were nearly the same at all the electrodes, but the waves were generally not phase locked despite being uncoupled from higher frequency proximal oscillators. For instance, in one dog, the control waves were phase locked in only 3 out of 12 distal isolated segments. This implies that coupling and/or some other parameter differed in these segments, compared to the segments in the frequency plateau.

3.22 Phase lag pattern

The phase differences among control waves in the frequency plateau region were measured in two experiments, one with a normal dog and the other with a reserpinized dog. 50-55 electrodes were implanted 1-2 cm apart in the proximal part of the small intestine. The direction of the phase lag was aboral. Figure 3.5 shows the phase lag pattern in the normal dog. Phase lag/cm was of the order of 5-15° in the proximal part of the frequency plateau, and 30-40° in the distal part. That phase lag increased towards the end of the plateau agrees with the observations of others (35), but they interpreted this finding as a decrease in propagation velocity on the basis of a cable model. Similar phase lag pattern was observed in the reserpinized dog.

Electrodes were implanted along the circumference in the duodenum to determine the phase differences in this direction (3 dogs). Very little or no phase lag was observed among control waves recorded at these electrodes. This implied that all the cells along the circumference were oscillating in phase and could, therefore, functionally be considered as one oscillator.

Electrodes were also implanted along the circumference in the ileums of 3 dogs (at 2 locations in each dog). It was found that at 5 locations the control waves along the circumference were phase locked.

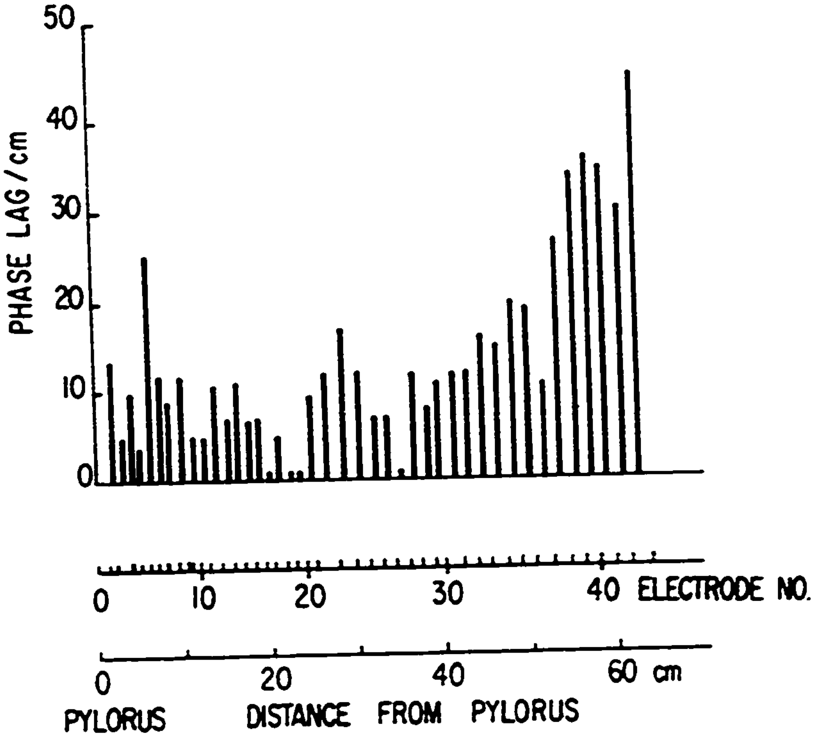

Figure 3.5

55 electrodes were implanted simultaneously to study the phase lag pattern in the frequency plateau. The electrodes were approx. 1 cm apart up to the ligament of Treitz, and approx. 2 cm apart distal to it. Phase lags were measured up to the control wave at 43rd electrode which was the last one to be entrained in the frequency plateau. Phase lag between two successive electrodes was divided by the distance between them, and plotted at the mean distance of the two electrodes from the pylorus.

However, they were not in phase as in the duodenum. The value of phase difference between the most leading control wave and the most lagging control wave was different at different locations; e.g., the values were 72° and 54.5° at two locations in the ileum of the same dog. At one location close to the end of the ileum (20 cm from the ileocecal valve) the control waves were not phase locked. These observations suggested that two or more independent oscillators existed along the circumference in the distal part of the small intestine.

3.23 Single cuts

A single cut of muscle layers was made in the frequency plateau region of the small intestine in 4 dogs. Recordings were made 30-45 minutes after the cut. ECA proximal to the cut was unaffected in frequency and in phase relationships. ECA frequency distal to the cut fell and formed another frequency plateau which extended into the variable frequency region. Distal to this new frequency plateau, temporal variations of average frequencies existed as before (Fig. 3.6). Results were consistent in all dogs.

Partial cuts along the circumference were made, and extended stepwise in the duodenum of two dogs. Results of these experiments showed that in the region 10-15 cm distal to the pylorus, approximately 1 cm length of the muscle layers along the circumference was enough to keep the proximal and distal ECA waves phase locked. If a length of muscle layers smaller than 1 cm was left, frequency pulling occurred.

3.24 Sympathetic reflex and local heating

It was observed on several occasions, that when a cut or a

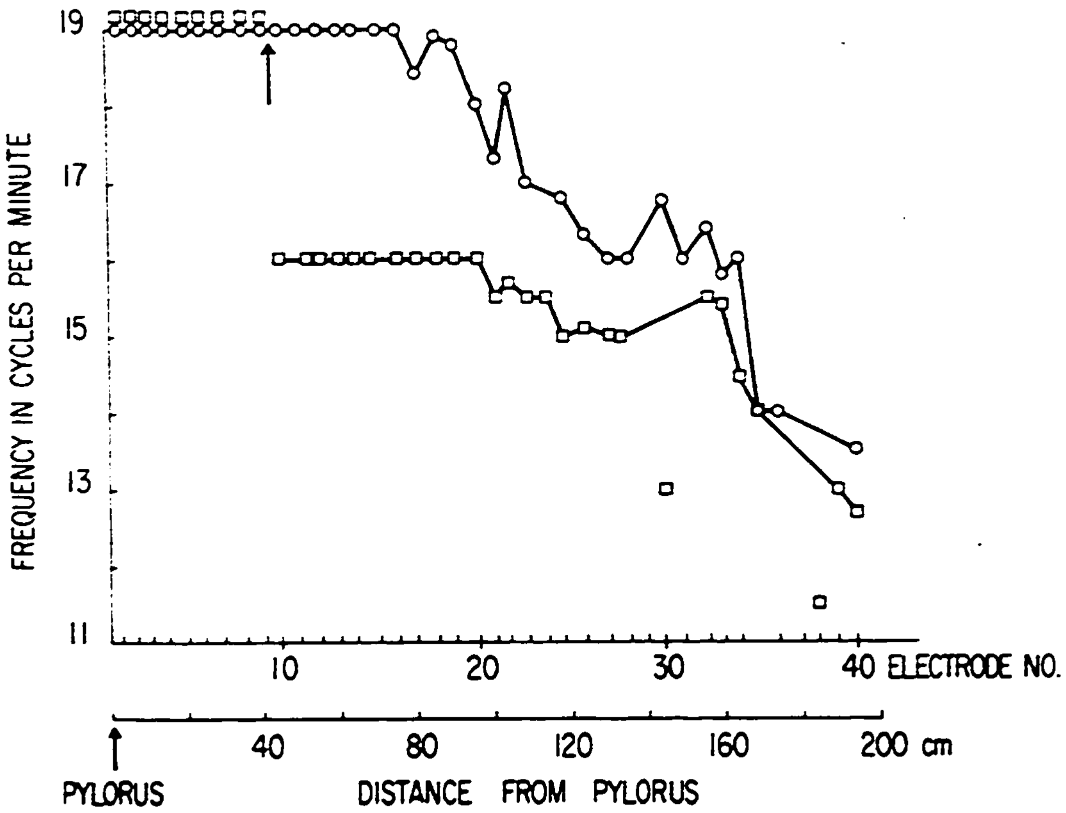

Figure 3.6

Effect of making a single cut in the frequency plateau region of the intestine of a normal dog. Frequencies recorded before the cut (shown by arrow) are indicated by (○) and those after the cut by (□). The second lower frequency plateau formed distal to the cut extended into the variable frequency region before cutting. The average frequencies distal to the second frequency plateau varied with time as before.

constriction was made in the frequency plateau region of a normal dog, the frequency distal to the cut did not immediately fall to its intrinsic value. Instead, the frequency remained at a higher value for variable lengths of time. When this situation occurred, a phase lead instead of a phase lag existed in the aboral direction (Fig. 3.7). Figure 3.7(a) shows the control waves recorded from the plateau region of a normal dog. The direction of phase lag was aboral. Figure 3.7(b) shows the control waves recorded from the same electrodes when a cut was made between electrodes 2 and 3. There was no change in the direction of phase lag proximal to the cut, while distal to it the direction of phase lag reversed; i.e., the phase lag was in the oral direction. In some dogs the above phenomenon existed for as long as 3 hours, and hence seemed stable. In other dogs, the phenomenon disappeared after variable lengths of time, or did not occur at all.

Within the duration of this phenomenon, if a second cut was made distal to the first cut (the second cut was made 10-15 cm from the first cut in these experiments), the ECA frequency between the two cuts immediately fell to its intrinsic value. Distal to the cut, the same phenomenon of a higher frequency and reversed direction of phase lag was then observed. On making further cuts in the aboral direction, the phenomenon repeated itself. During all these experiments the frequencies proximal to the first cut remained unaffected.

Reversal in the direction of phase lag also occurred if the intestine was handled. For instance, on several occasions when the vasa recti of the intestine were cannulated to study the effect of injecting acetylcholine, the direction of phase lag in the regions of cannulations reversed. When this situation occurred, cutting the muscle layers 15-20

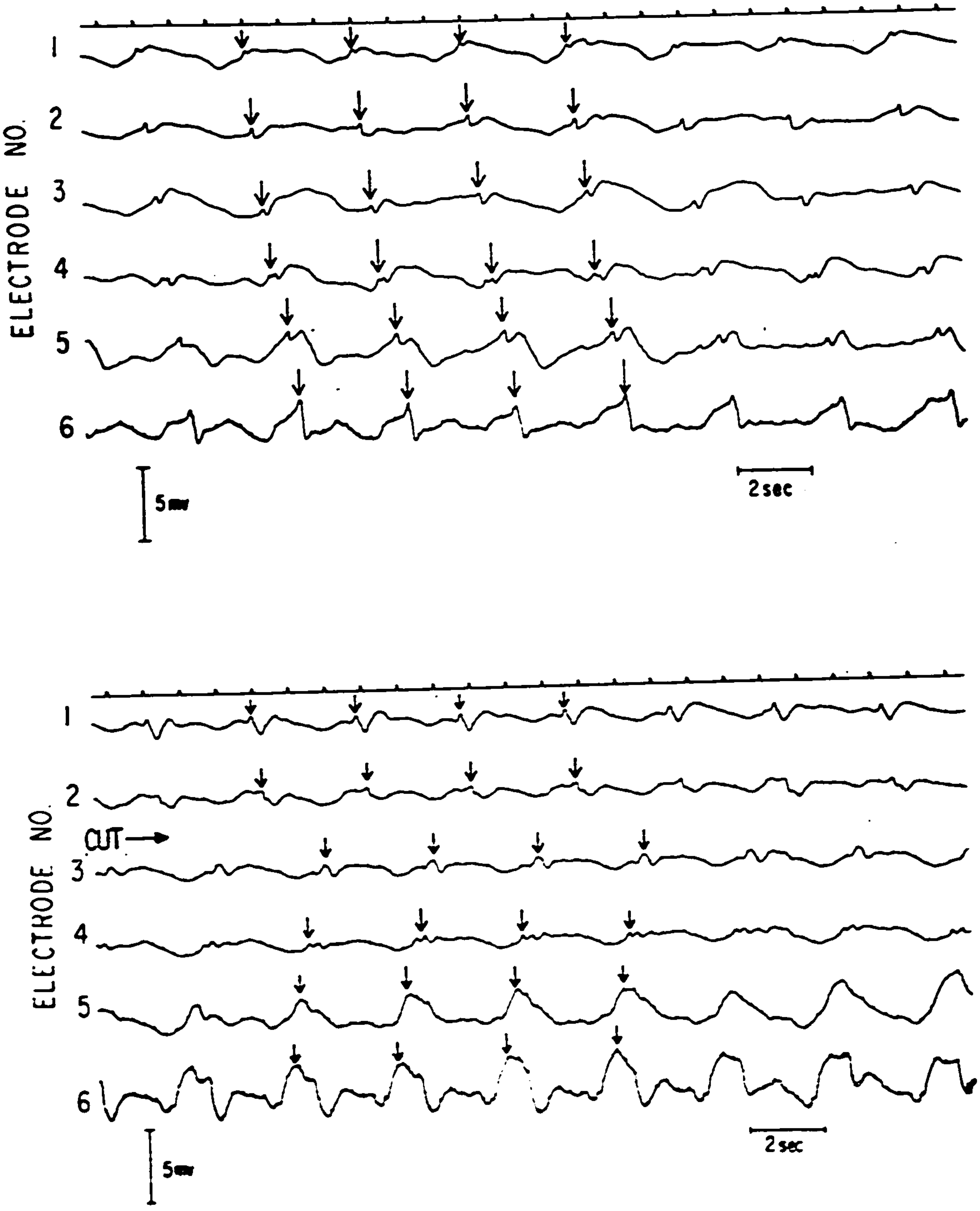

Figure 3.7

Recording showing the reversal in the direction of phase lag due to sympathetic reflex activity caused by a cut: (a) recording made before any cut; (b) recording made at the same electrodes after a cut had been made between electrodes 2 and 3. Distances of electrodes 1 to 6 from the pylorus were 41.75, 43.25, 45.00, 46.50, 48.25, and 50.25, respectively. The arrows show successive cycles.

cm distal to the cannulated areas returned the phase lags to normal. Both of the above-mentioned observations indicated that the raised frequencies and the reversal in the direction of phase lag were caused by some phenomenon occurring distal to the source of disturbance, such as a cut or a cannulation.

These phenomena were absent in reserpinized dogs, or occurred for very brief periods only (5 dogs). Furthermore, the phenomenon was more frequent and longer lasting during the winter months than during the summer months. Norepinephrine released reflexly on cutting or handling of the intestine of an unreserpinized dog may have caused the observed increase in frequencies. Norepinephrine, when infused intraarterially, has been shown to cause a rise in frequencies (8). In reserpinized dogs, norepinephrine was almost absent (Khin Kyi Kyi, J. and Daniel, E. E., unpublished). A probable reason for this phenomenon to occur more frequently during the winter months could be that dogs have more sympathetic activity during those months to maintain their normal body temperature.

The intestinal ECA frequency and amplitude are sensitive to temperature (7, 17). However, when small segments (1-2 cm in length) of intact jejunum (35-40 cm from the pylorus) were heated in two dogs, no change in either the ECA frequency or the direction of phase lag was observed. Diamant et al. (25) transected the small intestine and heated the region immediately distal to the cut after its frequency had fallen to its intrinsic value. Heat raised the frequency of that region, and that in turn raised the frequency of distal regions. Milton et al. (4) heated small segments of intact duodenum and found that it not only raised the ECA frequency of that region but also reversed the direction of phase lag proximal to the heated segment.

3.25 Intraarterial injections of acetylcholine

The purpose of injecting acetylcholine (0.05–0.5 μg) intraarterially was to induce ERA at different phases of the ECA cycle and study its effect. Two dogs were used in these experiments. Each small intestine was cannulated at two sites, one in the duodenum and one in the jejunum. Both sites were inside the frequency plateau region. Acetylcholine was injected repeatedly at various phases of the ECA wave cycle.

The results of one experiment are given in Table 3.1. The perfusion site was 10.5 cm from the pylorus. Time was measured from the positive going zero of the control wave, and was expressed as a percentage of the time period of the wave. The following observations were made in these experiments:

1) The response activity was more often produced in the earlier part of the ECA cycle than in the later part. In the earlier part of the cycle, known as the plateau, the control wave was in a relatively more positive phase than in the rest of the cycle, known as the trough.
2) When the response activity occurred in the plateau, it had less tendency to unlock distal control waves from the proximal ones than when it occurred in the trough (see Table 3.1).
3) During the unlocked stage, the distal waves fell to a lower frequency for a few cycles, and then became phase locked with the proximal ones with the normal phase lag. The proximal control waves were unaffected in frequency or phase relationship. Figure 3.8 shows the unlocking of waves when 0.1 μg of acetylcholine was injected. Naturally occurring response activity over several consecutive cycles also caused similar unlocking.

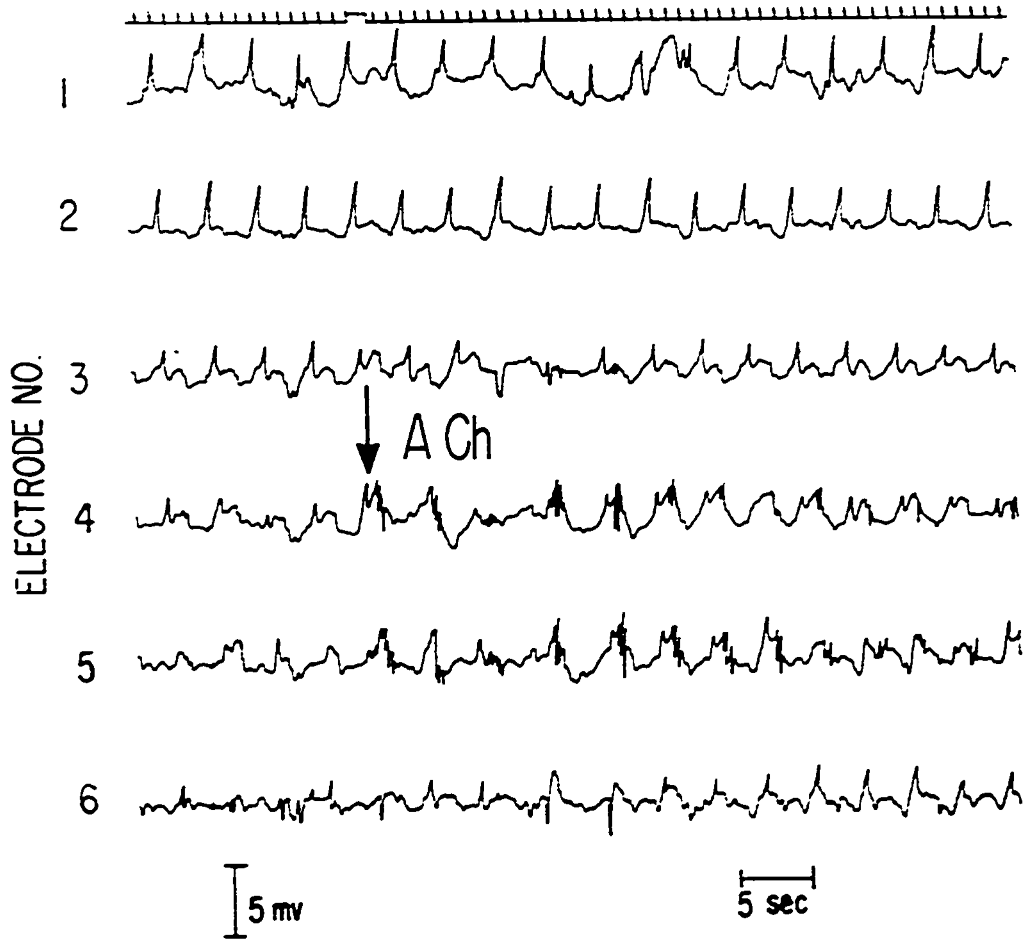

Figure 3.8

Effect of injecting acetylcholine intraarterially. Acetylcholine was injected into the region of electrode 4 at the time shown by arrow. The control waves recorded at electrodes 4, 5 and 6 were unlocked from those recorded at electrodes 1, 2 and 3. Distances of electrodes 1 to 6 from the pylorus were 7.0, 9.0, 10.2, 11.7, 13.7 and 15.7 cm, respectively.

Table 3.1

INTRAARTERIAL INJECTIONS OF ACETYLCHOLINE IN DUODENUM

Perfusion no.	Dose in μg	Response activity started at	Response activity ended at	Uncoupled distal waves or not
1	0.10	18.8%	74.8%	yes
2	0.10	11.8%	53.0%	no
3	0.05	0.0%	17.6%	no
4	0.05	17.6%	53.0%	no
5	0.05	0.0%	54.0%	no
6	0.05	0.0%	31.2%	no
7	0.05	12.5%	37.5%	no
8	0.05	18.8%	37.5%	no
* 9	0.05	56.2% 50.0%	75.0% 75.0%	yes
10	0.05	33.3%	60.0%	no
11	0.05	50.0%	60.5%	no
12	0.10	31.4%	63.0%	no
13	0.05	37.5%	62.5%	no
*14	0.10	12.5% 0.0%	43.7% 43.7%	no
15	0.10	27.4%	47.0%	no
*16	0.10	11.8% 0.0%	100.0% 53.0%	yes
17	0.10	12.5%	43.7%	no
*18	0.10	31.2% 40.0%	50.0% 75.0%	yes
19	0.10	0.0%	37.5%	no

*The second set of values for these perfusions indicate the occurrence of ERA on the next cycle.

3.26 Summary of results

To sum up the results of animal studies, any model of the intestinal control activity of dogs must show the following:

1) One frequency plateau in the proximal part where the control waves are phase locked.
2) Temporal variation of average frequencies distal to this frequency plateau.
3) The plateau frequency should be higher than the highest intrinsic frequency.
4) A single complete cut in the frequency plateau region should not affect the ECA frequency of the proximal part, but the ECA frequency of the distal part should fall and form another frequency plateau. A single cut in the variable frequency region should not cause any long frequency plateau to be formed distal to the cut.
5) The model should be capable of showing appropriate phase lags in the oral and in the aboral directions.
6) When response activity occurs in the later part of the control wave cycle, the distal control waves should fall to a lower frequency, but the proximal ones should not be affected. Response activity in the earlier part of the cycle should not cause unlocking.

3.3 Computer Model of Intestinal ECA

3.31 Frequency gradients

A chain of bidirectionally coupled relaxation oscillators is proposed as a model of the intestinal electrical control activity. The length of intestine of dogs in our experiments varied from 200 to 250 cm. A hypothetical intestine 200 cm long was assumed for the model. The oscillators were distributed over this length in the form of a chain. Parameters were chosen (Tables 3.2 and 3.3) such that oscillations existed at the output of each oscillator, and their intrinsic frequencies decreased (Figs. 3.11 and 3.12) in a manner similar to that observed in dogs; i.e., the gradient was steep in the proximal part and flattened out towards the end. This uncoupled chain of oscillators was, in fact, the model of the small intestine when it was electrically uncoupled into small segments.

To simulate the control activity of the intact intestine, the oscillators were coupled. Two models which simulate the intact frequency gradients are proposed. The differences between these models were:

a) in their oscillator parameter values; and
b) in the manner in which the oscillators were coupled in the chain.

The first model (Fig. 3.9) had three types of coupling between adjacent oscillators: forward coupling, backward coupling and phase shifted coupling. The second model (Fig. 3.10) had only forward and backward couplings. Both models showed the characteristics of control activity observed in the dog intestine.

Forward coupling means that the output of an oscillator is feeding into the next distal oscillator. The physical analog of this coupling in the intestine may be that a proximal cell is affecting the membrane potential of the next distal cell either by altering the voltage across a nexal

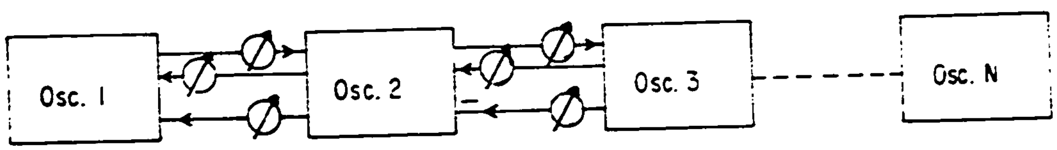
Osc. 1
Osc. 2
Osc. 3
Osc. N
–

Figure 3.9

Block diagram illustrating the arrangement of oscillators in the first intestinal model.

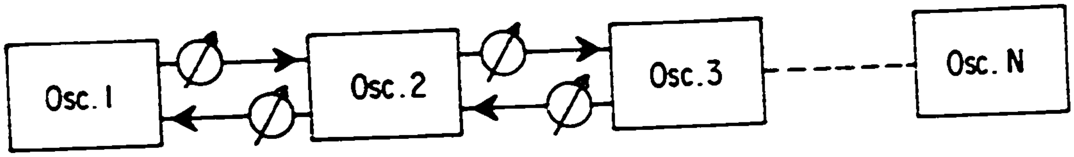
Osc. 1
Osc. 2
Osc. 3
Osc. N

Figure 3.10

Block diagram illustrating the arrangement of oscillators in the second intestinal model.

contact (36) or by setting up currents in the extracellular fluid as a result of potential variations across its membrane. In the former case, where the coupling is due to potential difference across the nexus, the cells may be considered as voltage coupled. In the latter case, where currents are responsible for coupling, they may be considered as current coupled.

Backward coupling, the counterpart of forward coupling, means that an oscillator is affecting the next proximal oscillator. These two couplings together have been referred to as bidirectional coupling. In both models, the magnitude of these two couplings was kept the same between adjacent oscillators, as would be expected among adjacent cells because of symmetry.

Phase shifted coupling was obtained by inverting the output of an oscillator and feeding it back to the next proximal oscillator. The physical analog of phase shifted coupling may be the interaction between longitudinal and circular muscle cells, as discussed later.

In a chain of coupled oscillators, the equation of the n^{th} oscillator will be:

$$\dot{x}_n = k(a_1 y_n + a_2 x_n + a_3 x_n^2 + a_4 x_n^3 + C_{n-1} x_{n-1} + C_{n+1} x_{n+1} + \bar{C}_{n+1} \bar{x}_{n+1}) \qquad (3.1)$$

$$\dot{y}_n = -\frac{1}{k}(b_1 y_n + b_2 x_n + b_3 x_n^2 + b_4 x_n^3 - b_0) \qquad (3.2)$$

C_{n-1} = coupling factor for forward coupling.

C_{n+1} = coupling factor for backward coupling.

$\bar{C}_{n+1}$ = coupling factor for phase shifted coupling.

$\bar{x}_{n+1}$ = phase shifted output of the $(n+1)^{th}$ oscillator.

The parameters of oscillators and the coupling factors in the two models are given in Tables 3.2 and 3.3. $\bar{C}_{n+1}$ was kept 0 for the second model.

The frequency gradients when the oscillators in the chain were coupled for the first model (Fig. 3.11) or for the second model (Fig. 3.12) were similar. In either model a frequency plateau was formed in the proximal part of the chain. The oscillator outputs were phase locked in this region. The plateau frequency in both cases was 18.7 c/min, and was higher than the highest intrinsic frequency of 18.0 c/min in the chain. The outputs of oscillators distal to the frequency plateau showed a variable 1-minute average frequency. The process of falling out of phase was similar to that observed in dogs. Phase lag increased gradually until a critical value was reached. At this stage unlocking occurred for one or two cycles. The outputs of oscillators in the frequency plateau region and the variable frequency region of the second model are shown in Figures 3.13 and 3.14 respectively. The two models were similar in demonstrating all characteristics of intestinal ECA.

The capability of a relaxation oscillator to entrain others to form a frequency plateau depends upon the amount of coupling available, and on the difference between the plateau frequency and the intrinsic frequency of the oscillator to be entrained. This property is illustrated in Figures 3.15 and 3.16 for the first model. The phase shifted coupling factor was kept constant at 0.170 in Figure 3.15, and the bilateral coupling factor was varied. In Figure 3.16 the bilateral coupling factor was kept constant at 0.140 and the phase shifted coupling factor was varied. Curves I and II in the two figures show the plateau frequency and the lowest intrinsic frequency oscillator entrained in the plateau respectively. The bilateral

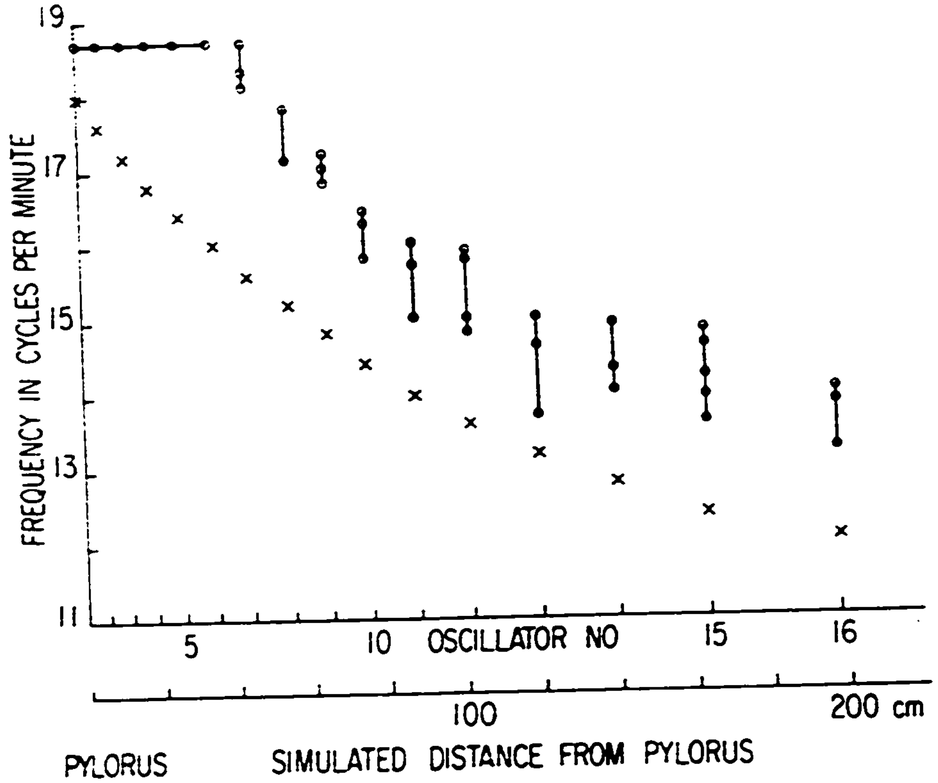

Figure 3.11

Frequency gradients in the first intestinal model. (x) shows the intrinsic frequency of an oscillator, and (o) shows the frequency when it was coupled with other oscillators as shown in Figure 3.9. Frequencies shown are 1-minute average frequencies over a minimum 10-minute recording time.

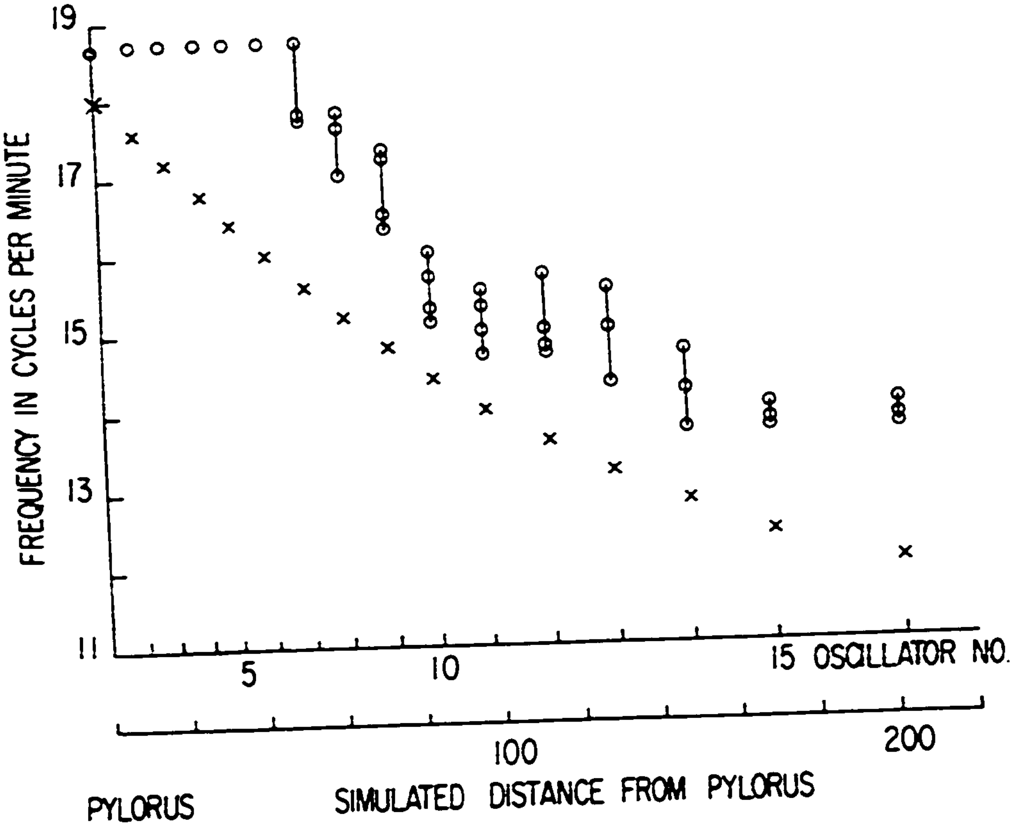

Figure 3.12

Frequency gradients in the second intestinal model. (x) shows the intrinsic frequency of an oscillator and (○) shows the frequency when it was coupled with others as shown in Figure 3.10. Frequencies shown are 1-minute average frequencies over a minimum 10-minute recording time.

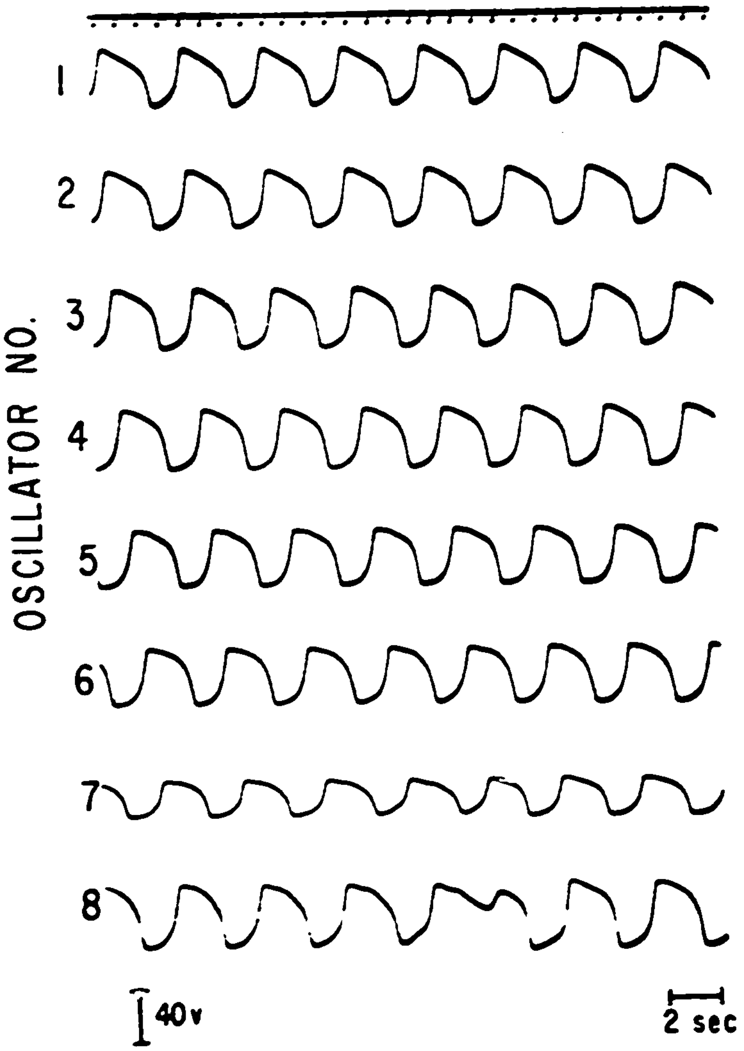

Figure 3.13

Outputs of oscillators 1 to 8 in the second intestinal model. Oscillators 1 to 6 were in the frequency plateau. Labelling as in Figure 3.12.

NOTE: The voltage scales shown in this and the subsequent recordings on PACE recorder do not apply to channel 7 from the top. This channel could not be calibrated.

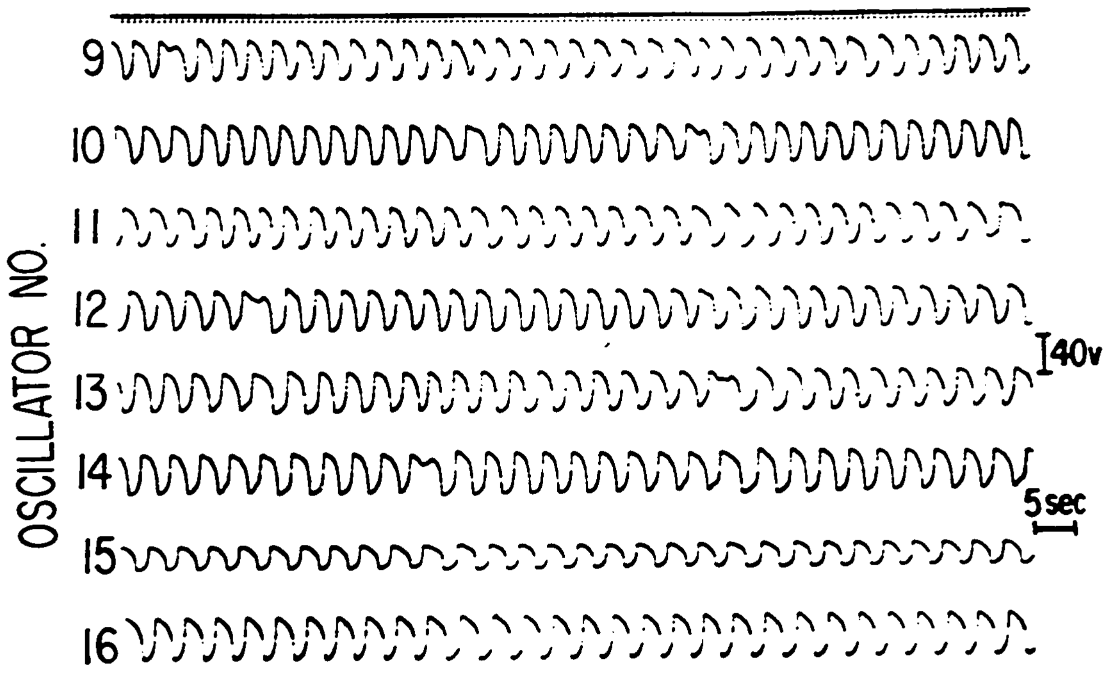

Figure 3.14

Outputs of oscillators 9 to 16 in the second intestinal model. All oscillators were in the variable frequency region. Labelling as in Figure 3.12.

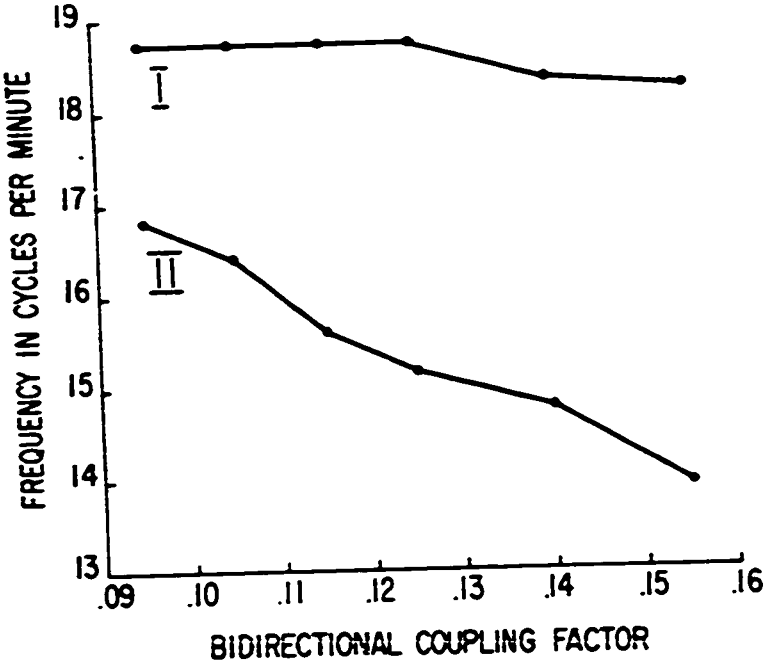

Figure 3.15

Diagram illustrating the effect of varying bidirectional coupling factor on the length of plateau and its frequency. Phase shifted coupling factor was kept constant at 0.170. Trace I shows the plateau frequency, and Trace II shows the lowest intrinsic frequency oscillator entrained in the plateau. The most proximal oscillator in the chain had the highest intrinsic frequency of 18.0 c/min.

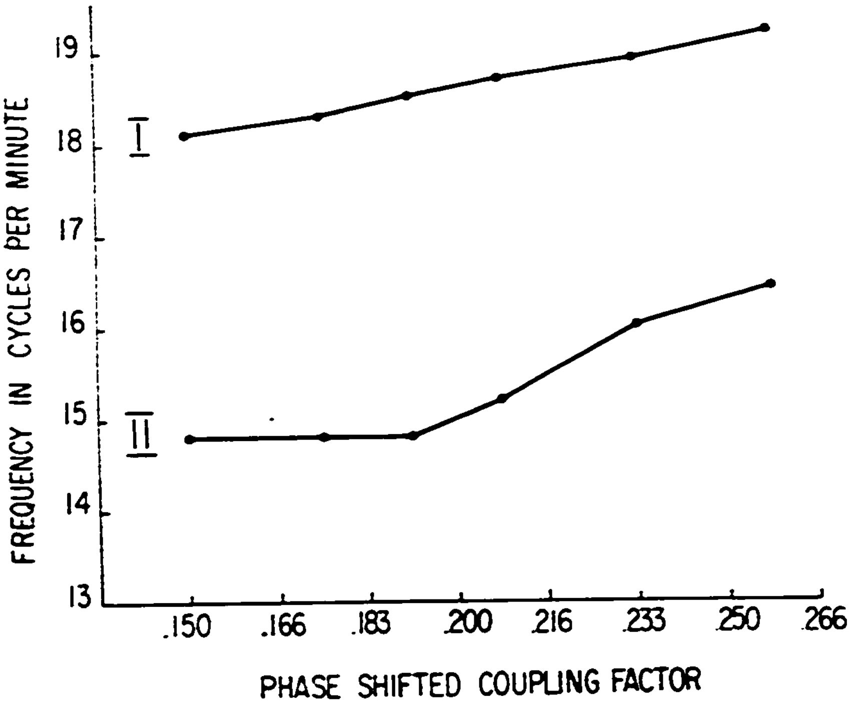

Figure 3.16

Diagram showing the effect of varying phase shifted coupling factor on the length of plateau and its frequency. Bidirectional coupling factor was kept constant at 0.140. Trace I shows the plateau frequency, and Trace II shows the lowest intrinsic frequency oscillator entrained in the plateau. The most proximal oscillator in the chain had the highest intrinsic frequency of 18.0 c/min.

Table 3.2

PARAMETERS OF OSCILLATORS FOR THE FIRST INTESTINAL MODEL

$a_1 = 1.0$, $a_2 = 1.0$, $a_3 = 0.2$, $a_4 = -0.333$,

$b_1 = 0.2$, $b_3 = 0.0$, $b_4 = 0.0$, $k = 6$

for all oscillators.

Oscillator No.	Intrinsic frequency c/min	b_0	b_2	C_{n-1}	C_{n+1}	$\bar{C}_{n+1}$
1	18.0	6.0	8.020	—	0.120	0.170
2	17.6	6.0	7.904	0.120	0.120	0.170
3	17.2	6.0	7.702	0.120	0.120	0.170
4	16.8	6.0	7.512	0.120	0.120	0.170
5	16.4	6.0	7.264	0.120	0.120	0.170
6	16.0	6.0	6.520	0.120	0.120	0.170
7	15.6	6.0	6.260	0.120	0.120	0.170
8	15.2	3.0	5.820	0.120	0.120	0.170
9	14.8	3.0	5.712	0.120	0.120	0.170
10	14.4	3.0	5.412	0.120	0.110	0.170
11	14.0	3.0	5.216	0.110	0.110	0.170
12	13.6	2.0	5.066	0.110	0.090	0.170
13	13.2	2.0	4.220	0.090	0.090	0.170
14	12.8	2.0	4.120	0.090	0.090	0.170
15	12.4	2.0	5.800	0.090	0.090	0.170
16	12.0	2.0	5.600	0.090	—	—

Table 3.3

PARAMETERS OF OSCILLATORS FOR THE SECOND INTESTINAL MODEL

$a_2 = 1.0$, $a_3 = 0.3725$, $a_4 = -0.3725$,
$b_1 = 0.0$, $b_2 = 2.40$, $b_3 = 0.6$, $b_4 = 0.75$
$k = 5$ for all oscillators.

Oscillator No.	Intrinsic frequency c/min	a_1	b_0	C_{n-1}	C_{n+1}
1	18.0	1.339	6.00	--	0.190
2	17.6	1.283	5.98	0.190	0.190
3	17.2	1.234	5.96	0.190	0.190
4	16.8	1.198	5.94	0.190	0.190
5	16.4	1.225	5.92	0.190	0.190
6	16.0	1.056	5.90	0.190	0.190
7	15.6	1.030	5.88	0.190	0.190
8	15.2	0.970	5.86	0.190	0.190
9	14.8	0.930	5.84	0.190	0.190
10	14.4	0.840	5.80	0.190	0.190
11	14.0	0.780	5.76	0.190	0.190
12	13.6	0.740	5.72	0.190	0.190
13	13.2	0.730	5.68	0.190	0.160
14	12.8	0.710	5.64	0.160	0.140
15	12.4	0.640	5.60	0.140	0.110
16	12.0	0.630	5.56	0.110	--

coupling factor was dominant in determining the plateau length, while the phase shifted coupling factor was dominant in determining the plateau frequency. The two coupling factors were appropriately chosen to obtain the desired frequency and length of the plateau.

In the second model, the bidirectional coupling factor determined the length of the plateau. It was observed that a plateau frequency higher than, equal to, or lower than the highest intrinsic frequency could be obtained by an appropriate choice of parameters. The effect of variation of one such parameter, b_0 , on the resultant frequency of two bidirectionally coupled oscillators was studied. The results are shown in Figure 3.17. The frequency of one oscillator was kept constant at 18.0 c/min, while that of the other was kept at 17.0, 17.5 and 18.0 c/min (curves 1, 2 and 3, respectively). The coupling factor was 0.190 in all three cases. It is seen that, as the value of b_0 increases, the resultant frequency also increases. For the same coupling factor and value of b_0, the resultant frequency is higher for less difference in intrinsic frequencies. In the second model, the value of b_0 was set at 6.0.

3.32 Phase lag pattern

The phase lag pattern among oscillators in the frequency plateau region was similar to that observed in dogs. Phase lag between the outputs of adjacent oscillators for the same difference of intrinsic frequency, and for the same coupling factor, was less in the proximal part of the chain and increased distally. The phase lag pattern in the frequency plateau region of the second model is shown in Figure 3.18. A similar phase lag pattern existed in the frequency plateau region of the first model (27).

The phase lag between two entrained oscillators depends upon the

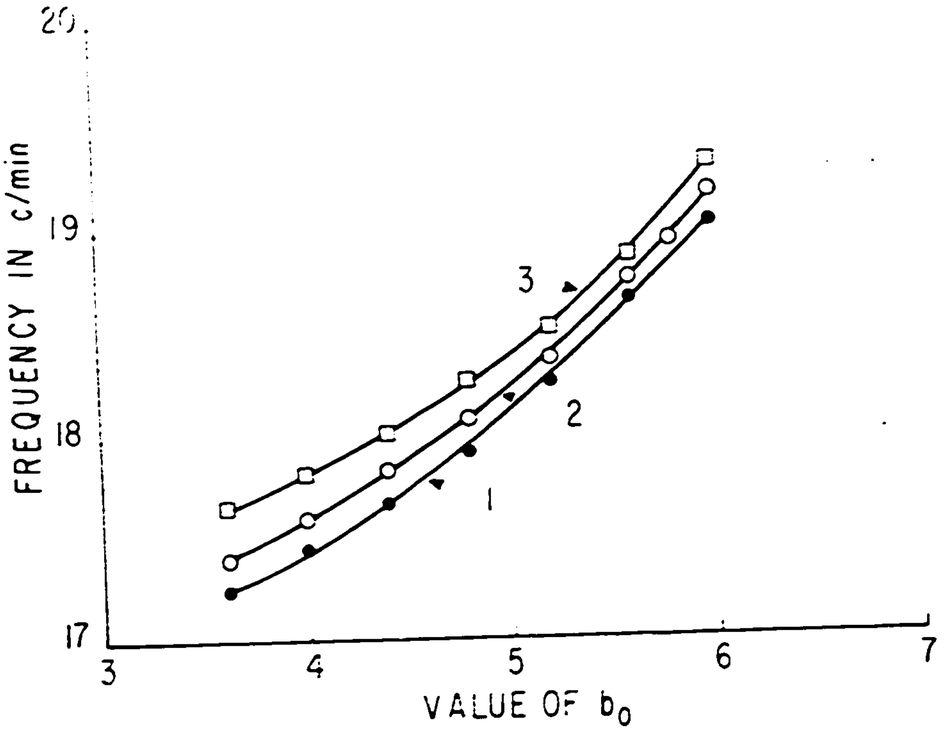

Figure 3.17

Diagram showing the effect of varying parameter b_0 on the resultant frequency of two bidirectionally coupled relaxation oscillators. The frequency of one of the oscillators was kept constant at 18.0 c/min, while that of the other was kept at 17.0, 17.5 and 18.0 c/min (curves 1, 2 and 3, respectively). The coupling factor was kept constant at 0.190.

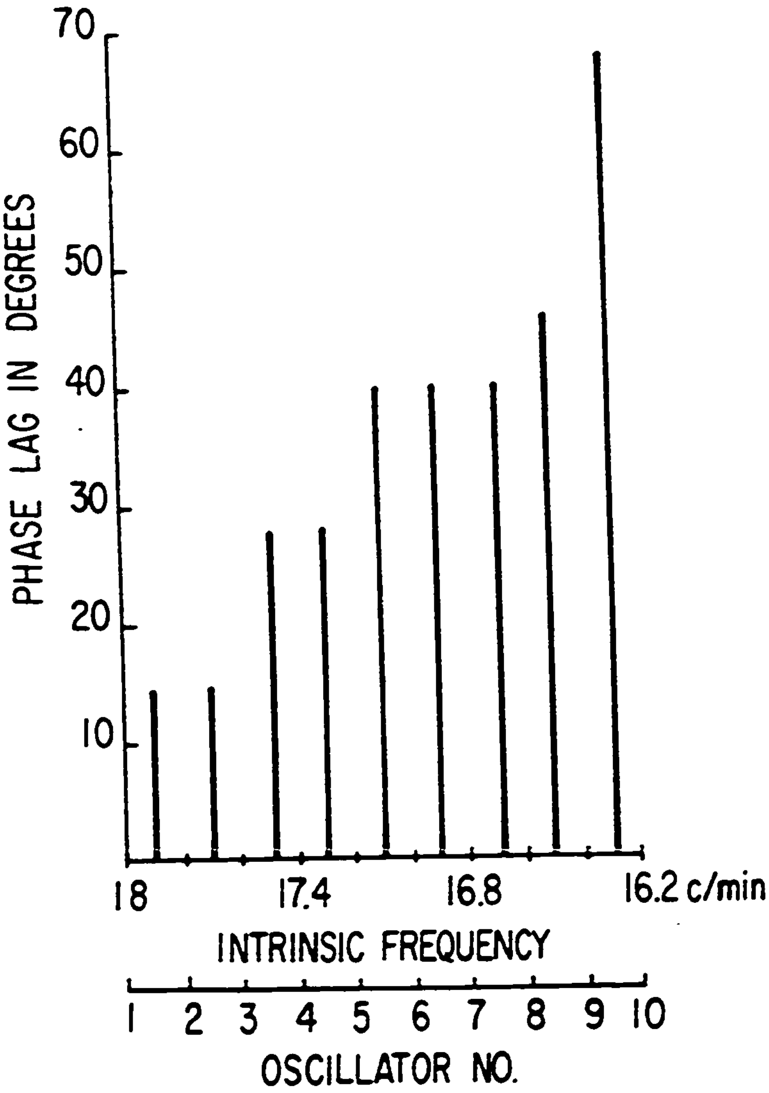

Figure 3.18

Phase lag pattern among oscillators in the frequency plateau region of the second intestinal model. Coupling factor was 0.190 for all the oscillators. Phase lag for the same difference of intrinsic frequency increased distally in the frequency plateau.

difference between their intrinsic frequencies and upon the coupling factor. Figure 3.19 shows the phase lag between two entrained oscillators (second model) as a function of the coupling factor. Oscillator 1 was kept at 18.0 c/min, while oscillator 2 was kept at 15, 16 and 17 c/min (curves 1, 2 and 3, respectively). The end points of the curves on the left side show the minimum amount of coupling factor required for frequency entrainment of the oscillators for the given intrinsic frequency difference. Once entrained, the phase lag reduced when the coupling factor was increased. Also, for the same coupling factor, the phase lag was more for larger intrinsic frequency differences. These observations suggest that the larger phase lag/cm among distal control waves in the frequency plateau region of the dog intestine is due to the larger difference between the intrinsic frequency of distal regions and the plateau frequency.

3.33 Single cuts

A single cut in the model was simulated by reducing the coupling factors between two oscillators to 0. The cut was simulated between oscillators 3 and 4 in both models (Fig. 3.20 for the first model, and Fig. 3.21 for the second model). The frequencies of oscillators proximal to the cut were not affected, but those of the distal oscillators dropped to a lower value and formed another frequency plateau. The new frequency plateau extended into the region of variable frequencies before the cut. Distal to the new frequency plateau, oscillators showed variable average frequencies as before. When the cut was made between the first and second oscillators, frequencies dropped on both sides of the cut. Similar results were obtained in the dog intestine when a single cut was made just distal to the pylorus (C. F. Code, personal communication to Dr. E. E. Daniel).

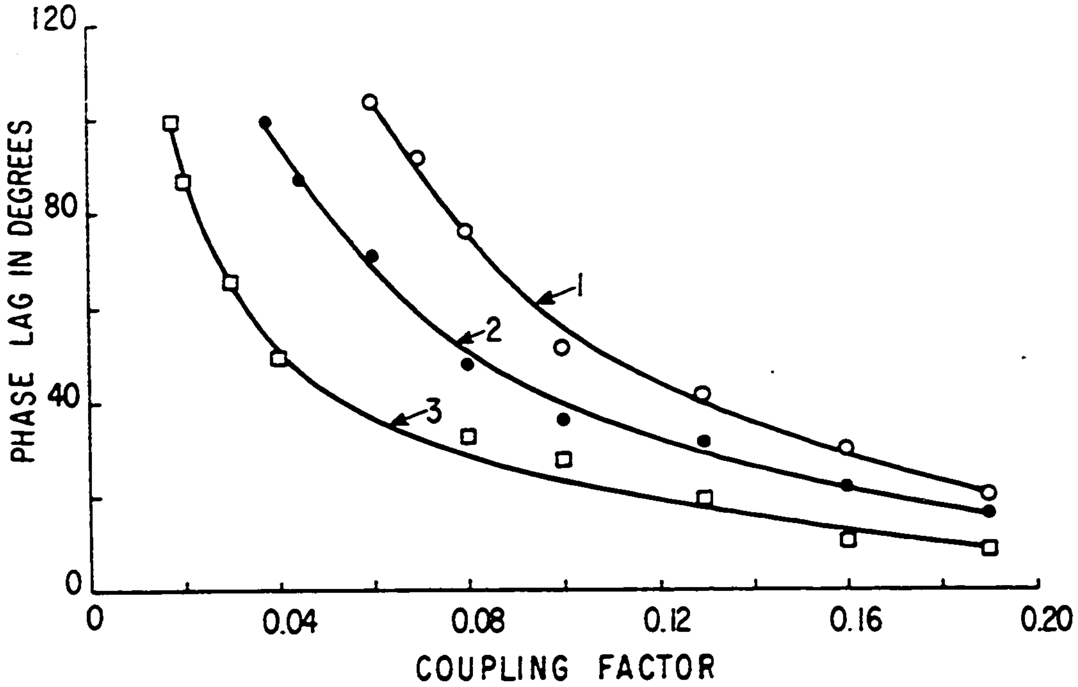

Figure 3.19

Diagram showing the effect of varying coupling factor on the phase lag between two bidirectionally coupled relaxation oscillators. The frequency of one of the oscillators was kept constant at 18.0 c/min, while that of the other was kept at 15.0, 16.0 and 17.0 c/min (curves 1, 2 and 3, respectively). The end points of curves on the left side show the minimum coupling factor required for frequency entrainment in each case.

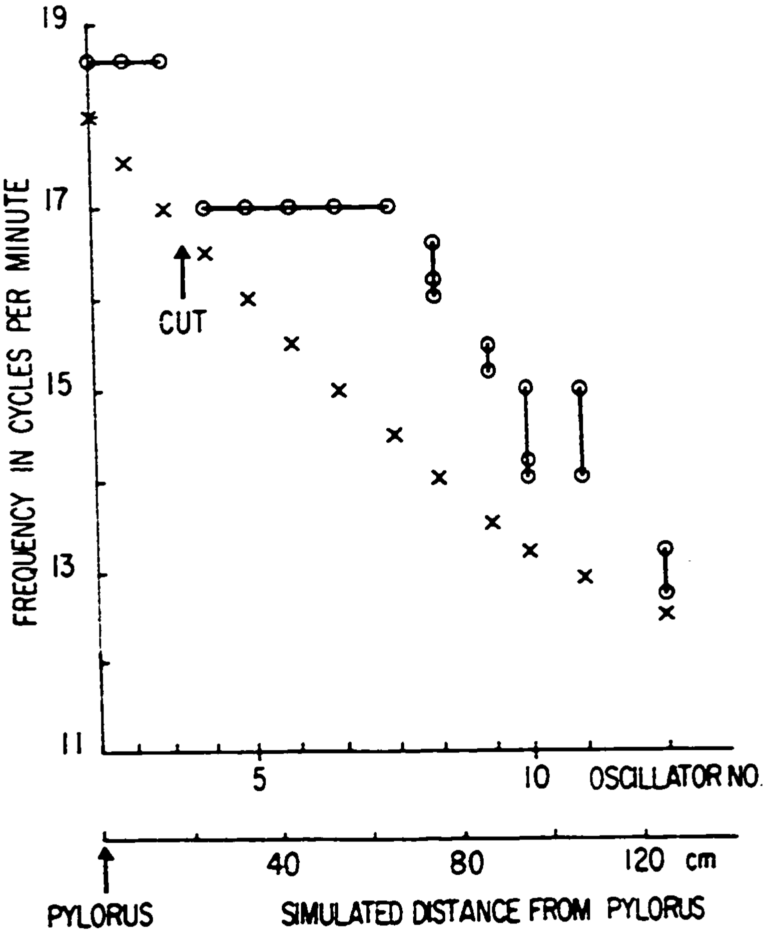

Figure 3.20

Effect of making a single cut in the frequency plateau region of the first intestinal model. The cut was made between oscillators 3 and 4 by reducing the coupling factors between them to zero. The frequencies of proximal oscillators were not affected. Another frequency plateau was formed distal to the cut. The second frequency plateau extended into the variable frequency region before cutting (see Figure 3.11).

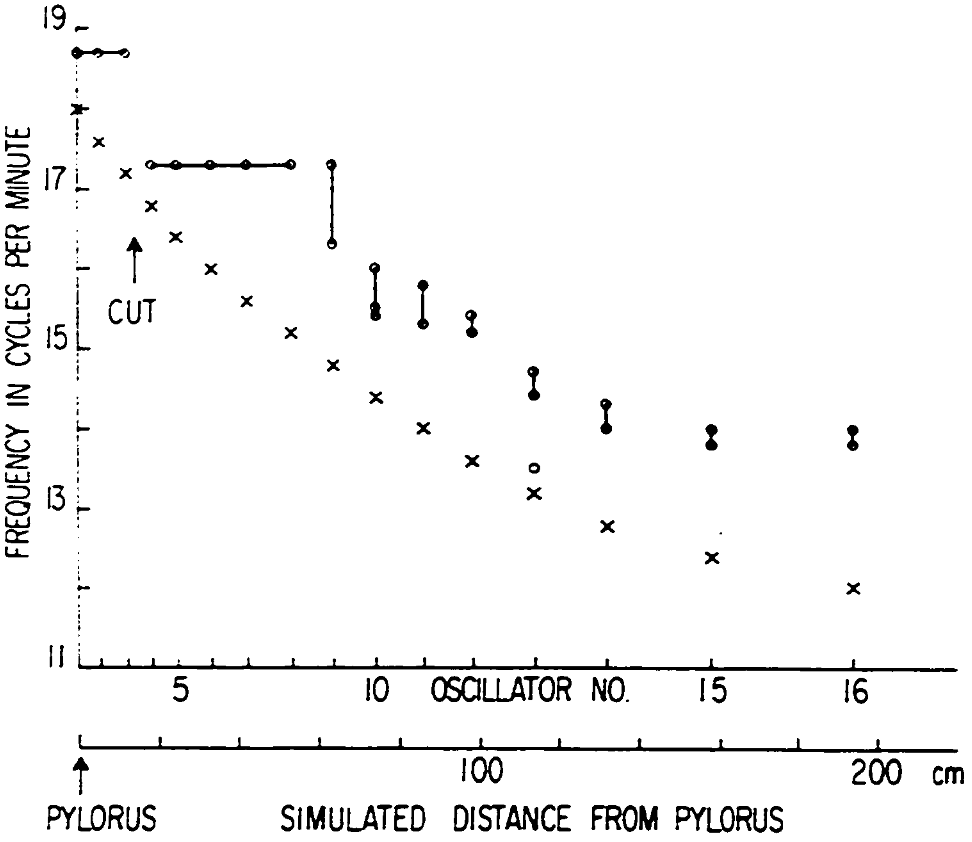

Figure 3.21

Effect of making a single cut in the frequency plateau region of the second intestinal model. The cut was made between oscillators 3 and 4 by reducing the coupling factors between them to zero. The frequencies of proximal oscillators were not affected. Another frequency plateau was formed distal to the cut. The second frequency plateau extended into the variable frequency region before cutting (see Figure 3.12).

When a single cut was made in the variable frequency region in either model, the outputs of all distal oscillators were phase locked. This did not happen in the dog intestine where only a small region immediately distal to the cut showed phase locked control waves. Possible reasons for this discrepancy in the models are discussed later.

A partial cut was simulated by reducing the coupling factor between oscillators 2 and 3 in the second model. It was found that the coupling factor could be reduced to 0.05 from the normal value of 0.190 before unlocking occurred. Even after further reduction of the coupling factor, frequency pulling of the distal oscillators occurred.

3.34 Local heating and sympathetic reflex

Local heating was simulated in models by raising the intrinsic frequency of an oscillator in the chain. The intrinsic frequency of oscillator 4 in the second model was 16.8 c/min. It was raised in steps to 18 c/min, 19 c/min, 20 c/min, 21 c/min and 22 c/min. No change in the plateau frequency (18.7 c/min) or in the direction of phase lag was observed until the intrinsic frequency of oscillator 4 was 20 c/min. At this time the plateau frequency rose to 19.2 c/min. Oscillator 4 led oscillator 3. Oscillators 3 and 2 had no phase lag, and oscillator 1 led oscillator 2. When the intrinsic frequency of oscillator 4 was raised to 21 c/min, the plateau frequency rose to 20 c/min. A complete reversal in the direction of phase lag was observed; i.e., oscillator 4 led oscillator 3, oscillator 3 led oscillator 2, and oscillator 2 led oscillator 1. Distal to oscillator 4 the phase lag was in the aboral direction as before. The outputs of 8 oscillators when oscillator 4 was at its normal frequency of 16.8 c/min, when it was at 20 c/min, and when it was at 21 c/min are shown in Figure 3.22. When the intrinsic frequency of oscillator 4 was raised to 22 c/min, the plateau frequency rose to 20.5 c/min. Similar results were obtained with the first model.

The sympathetic reflex activity also caused increased frequencies and reversal of the normal direction of phase lag. If norepinephrine, released reflexly, raised the frequency of only a small distal segment, then its simulation on the model will be similar to that described above for local heating. The increased intrinsic frequency of one distal oscillator will cause reversal in the direction of phase lag, and increased ECA frequencies.

It is also probable that norepinephrine acted on a longer length of intestine and, instead of raising the intrinsic frequency of a small segment, it raised the intrinsic frequencies of the intestine over a longer length. This could have caused an upward intrinsic frequency gradient. Such a gradient was simulated distal to a cut in the frequency plateau region of the first model, as shown in Figure 3.23. It was observed that the highest intrinsic frequency oscillator had the most leading control wave. Control waves proximal to it (shown by □'s) showed phase lag in the oral direction, and those distal to it (shown by ○'s) showed phase lag in the aboral direction. The arrow in the diagram shows the position of the simulated cut. Similar results were obtained for the second model.

3.35 Effects of the occurrence of response activity on control activity

Pulses (to simulate spikes) at a frequency of 10/sec and a pulse width of 30 msec were fed into oscillator 4 of the second model. The pulses lasted for 1.0 sec. The pulses were fed at various phases of the

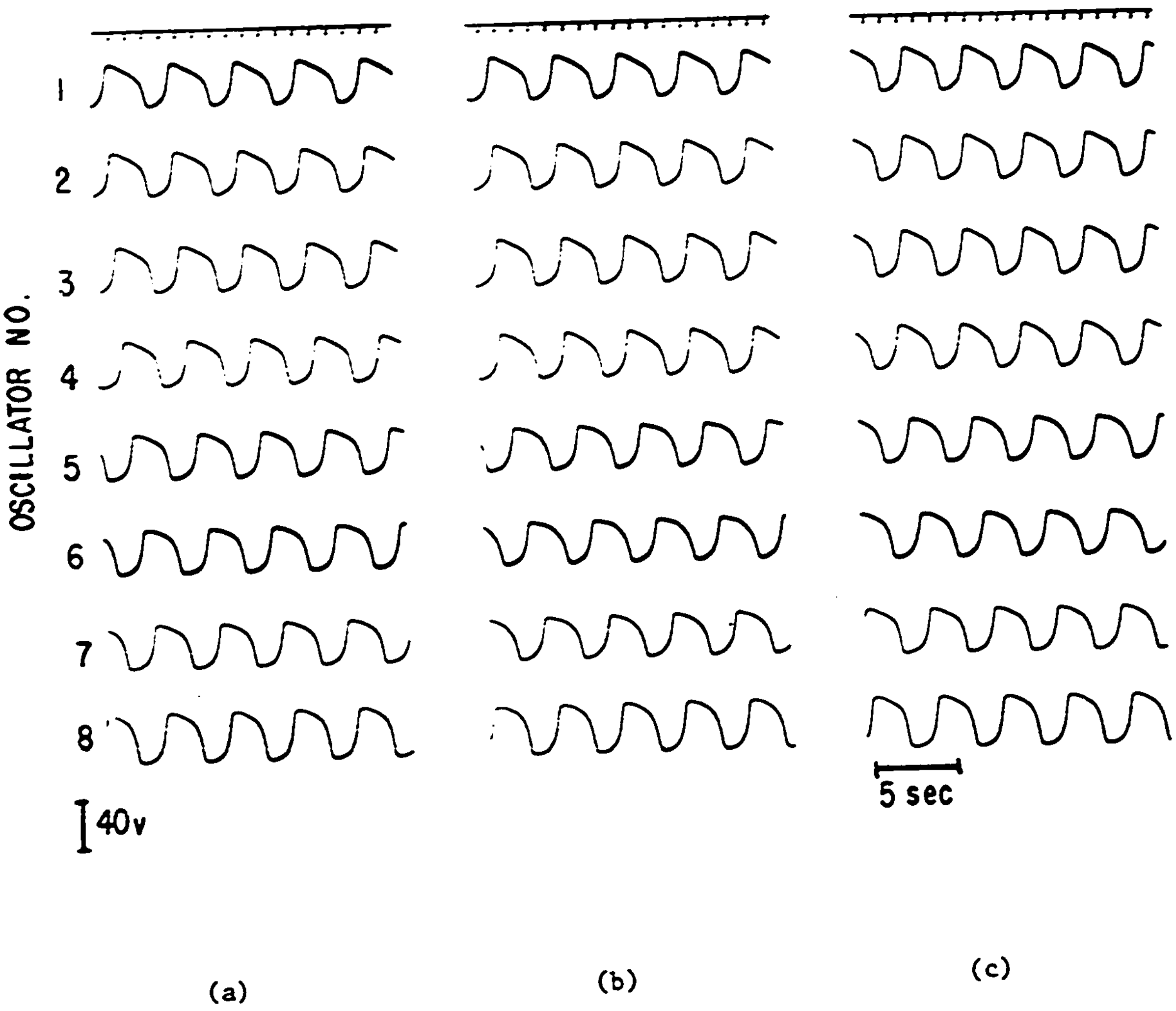

Figure 3.22

Local heating was simulated by raising the intrinsic frequency of oscillator 4. (a) Intrinsic frequency of oscillator 4 was 16.8 c/min; (b) intrinsic frequency of oscillator 4 was raised to 20 c/min; (c) intrinsic frequency of oscillator 4 was raised to 21 c/min. The recording shown is for the second intestinal model. Labelling as in Figure 3.12.

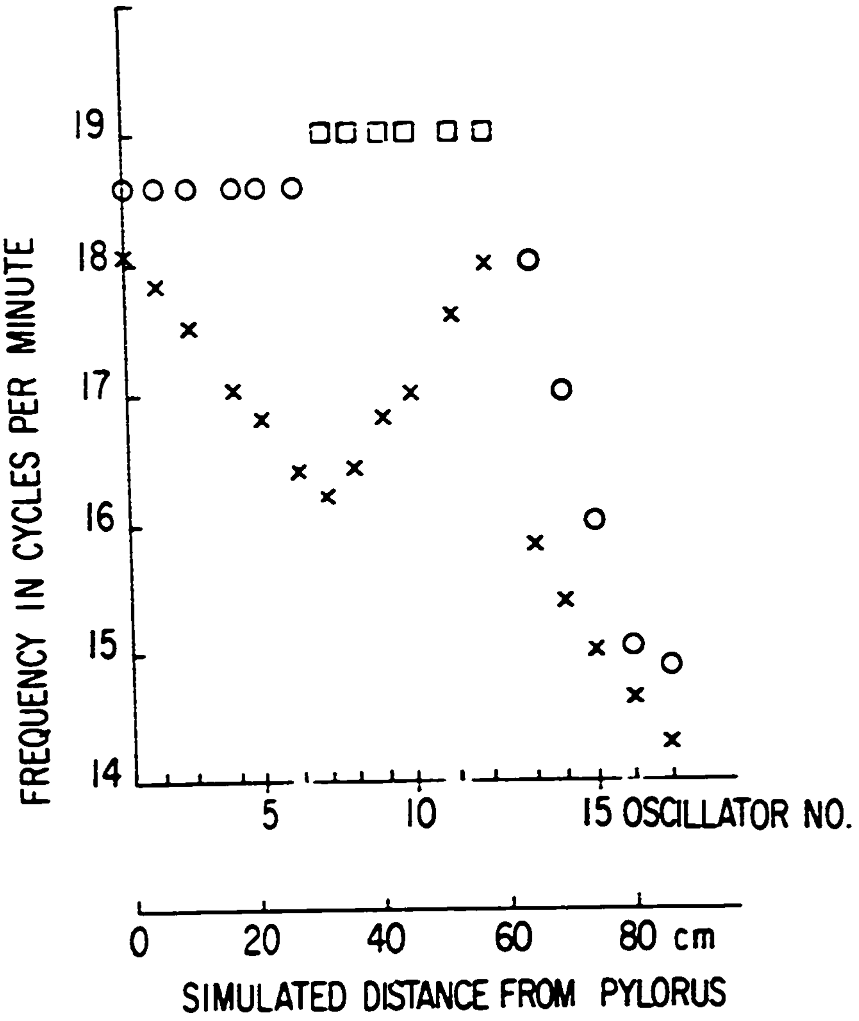

Figure 3.23

Simulation of sympathetic reflex activity in the first intestinal model by forming an upward intrinsic frequency (×) gradient distal to a cut (shown by arrow). The highest intrinsic frequency in the upward gradient was 18.0 c/min. (○) indicates the frequencies of oscillators among which phase lag existed in the aboral direction, and (□) shows the frequencies of oscillators among which phase lag existed in the oral direction.

control wave cycle. The time of onset of the pulses was measured from the positive going zero of the oscillator control wave, as described in section 2.2. Control wave period was 3.20 sec. Pulses introduced in one cycle, at or after 2.0 seconds unlocked the distal control waves from the proximal ones. Unlocking was also caused if pulses were applied during several consecutive cycles at 1.5 sec. Pulses applied at less than 1.5 sec did not cause unlocking. During unlocking, the frequency of distal waves dropped to a lower value, while the proximal waves were unaffected in frequency. After a few cycles, the waves were phase locked again with the normal phase lag. Figure 3.24 shows the case where the pulses were applied at 2.0 sec (second model). Figure 3.25 shows the case where the pulses were applied at 1.0 sec (second model). Similar results were determined for the first model.

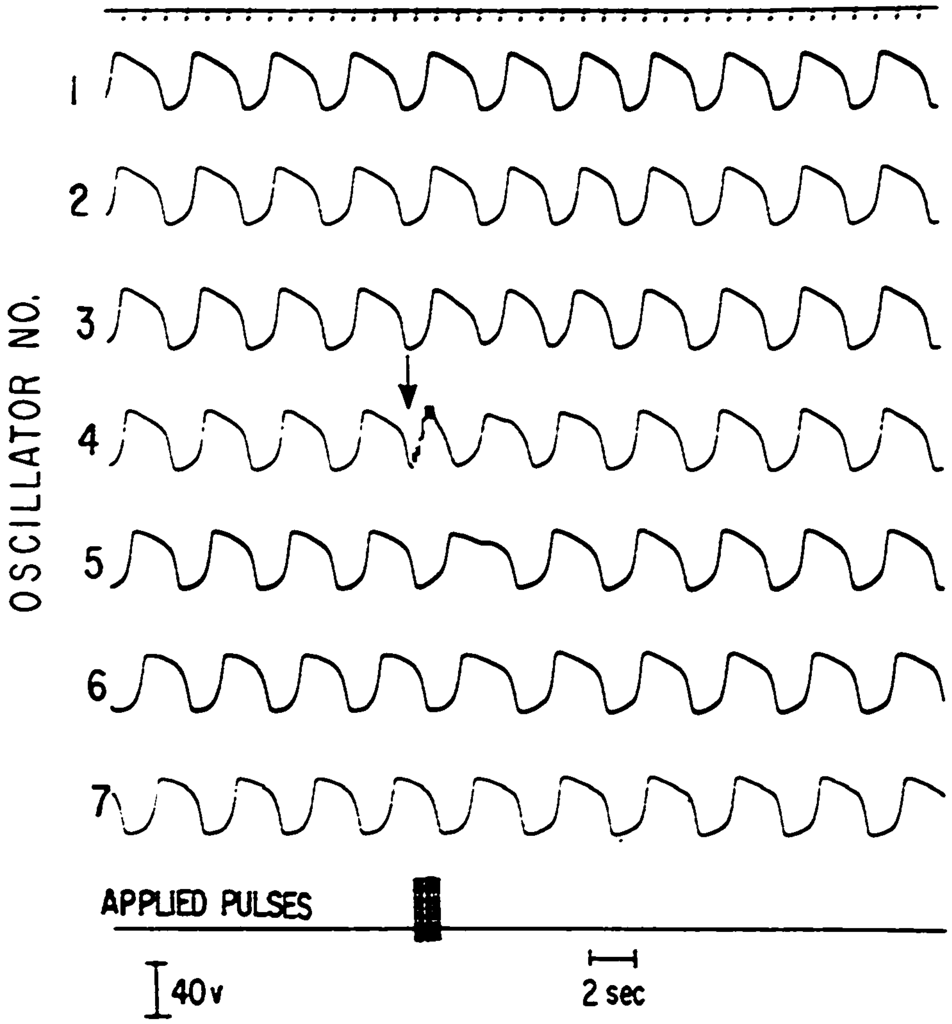

Figure 3.24

Recording showing the effect of applying pulses (simulated ERA) to the input of oscillator 4 in the second intestinal model. The pulses were applied at 2.0 sec (shown by arrow) and lasted for 1.0 sec. The application of pulses at this phase of the wave cycle caused unlocking of the distal control waves from the proximal ones.

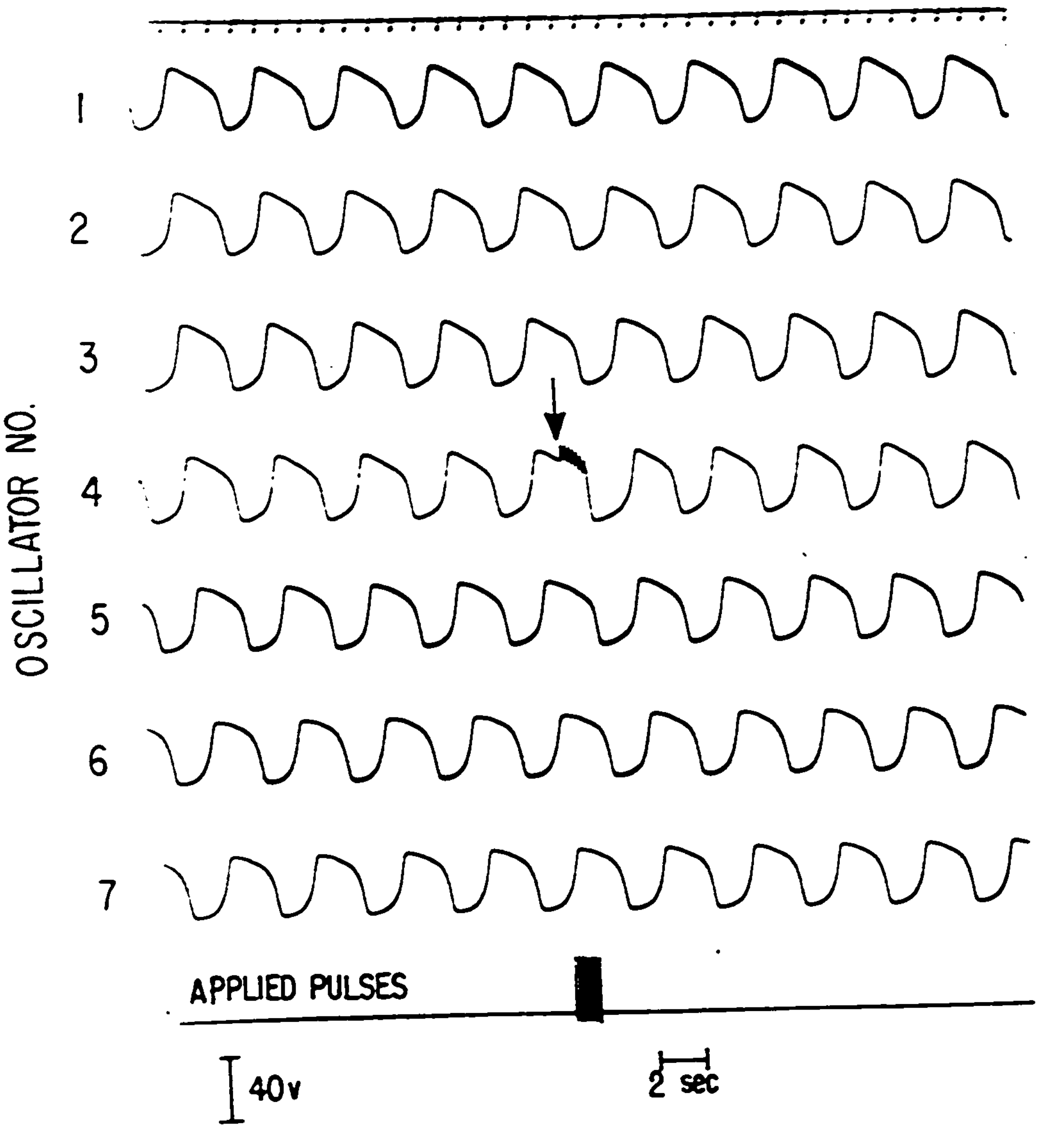

Figure 3.25

Recording showing the effect of applying pulses (simulated ERA) to the input of oscillator 4 in the second intestinal model. The pulses were applied at 1.0 sec and lasted for 1.0 sec. The application of pulses at this phase of the wave cycle had no effect on phase locking.

3.4 Discussion

The shape of ECA frequency gradient in the intact intestine has been a point of controversy. Some investigators have reported a continuous ECA frequency gradient, while others have reported multiple frequency plateaus (22-24, 33, 40-42).

We found only one stable frequency plateau in the intestine of dogs. The frequency plateau extended over the entire duodenum and part of the jejunum. Similar results were obtained by Szurszewski et al. (33) in unanesthetized dogs. The control waves recorded from successive electrodes in the frequency plateau region were phase locked in the sense that they never fell 360° or more out of phase. Distal to the frequency plateau, the control waves were phase locked temporarily. Distal control waves fell 360° or more out of phase from the proximal ones, thus preventing the formation of a stable frequency plateau.

Diamant and Bortoff (24) reported the existence of multiple plateaus in cat and dog intestine. Their results, however, showed that the frequency plateaus subsequent to the first one had a variable length and frequency. This apparently meant that those frequency plateaus were unstable. The apparent difference between their study and ours arises at least in part from our requirement that the waves be phase locked for the formation of a frequency plateau. This requirement distinguishes between stable and unstable frequency plateaus. Also they averaged the frequency over 5-minute periods, whereas we averaged it over 1-minute periods. Averaging over the longer period would tend to conceal the variation of frequencies distal to the first plateau, and could lead to the appearance of nearly constant average frequency.

The intrinsic frequency gradient in the dog intestine is not linear as reported by others (24). The intrinsic frequencies show a steep fall in the proximal part of the intestine up to about 90-120 cm from the pylorus, and a much smaller fall in the distal part.

The intrinsic frequency defined here is that of a small segment which may not be that of an individual oscillator. The exact size or the identity of an oscillator in the intestine is undefined as yet. The individual oscillator may be as small as one cell, or it may consist of a large collection of such cells oscillating in phase. The latter concept is based on the observation that control waves recorded at electrodes less than 5 mm apart longitudinally in the duodenum show very little or no phase lag.

Two models which simulate the intestinal ECA characteristics have been proposed in this thesis. Both, the bidirectional coupling and the phase shifted coupling, were used in the first model. The oscillator parameters in this model were such that if the phase shifted coupling was not used, the plateau frequency dropped with the addition of lower frequency oscillators in the chain, and thus prevented the formation of a stable frequency plateau. The physical analog of this coupling has been proposed to be the circular muscle layer. Although the effect of this layer on the longitudinal muscle layer has been simulated by feeding the inverted output of a distal oscillator into the next proximal oscillator, the arrangement in the physical system would certainly be more complex.

The circular muscle cells do not show control activity when isolated from longitudinal muscle cells (21). However, when connected to longitudinal muscle cells, they show control activity. Bortoff and Sachs (46) recorded the currents from the circular muscle in volume and showed them to be 180° out of phase with the currents from longitudinal muscle.

It is, therefore, possible that the circular muscle cells are not self-excitable, but can be excited in the presence of an external input. The activity so initiated may be called forced electrical control activity. This forced control activity could in turn influence the control activity of the longitudinal cells just like the bidirectional coupling among longitudinal cells. However, to include this effect would necessitate a two-dimensional model of the intestine. The first model approximated the effect of this second dimension by the phase shifted coupling. The total phase shift required to simulate this effect was found to be 180° or more, and hence this coupling was taken from the already lagging oscillator and inverted to get a further phase shift of at least 180°.

In a physical system, the control wave fed back from the circular muscle cells is not likely to hold a fixed phase relationship with the control wave of distal longitudinal cells. A more accurate representation of circular muscle cells would be to phase shift the inverted output of an oscillator and feed it back into itself. This idea was not pursued further at this stage because of the uncertainty that exists regarding the exact role of circular muscle cells, as discussed later.

In the second model, the oscillator parameters were such that when the first two oscillators were bidirectionally coupled, the resultant frequency was higher than that of either of them separately. No drop in frequency occurred when other lower intrinsic frequency oscillators were added to the chain. The model did not require phase shifted coupling. This model is based on the assumption that the circular muscle cells do not play an active role in the longitudinal spread of ECA. They may be acting as a current source for the longitudinal cells, as suggested by Bortoff and Sachs (46), or the control activity originating in longitudinal muscle cells may be passively spreading into the circular muscle cells. The suggestion of Bortoff and Sachs is questionable on the basis of experiments of Kobayashi _et al._ (21) who showed that isolated longitudinal muscle cells continued to show electrical control activity. It would, therefore, be necessary to ascertain the exact role of circular muscle cells to establish the validity of one model or the other.

A model with forward coupling alone was tried and found to lack several properties of the intestinal ECA—notably the rise of plateau frequency above the highest intrinsic frequency, absence of multiple plateaus, reversal of the direction of phase lag distal to a cut or constriction in the intestine of an unreserpinized dog. Also the hypothesis that in the situation where cells are in close proximity to one another, only the proximal ones should affect the distal ones, seems to be weak on _a priori_ and ultrastructural grounds (47).

The use of a general system of two first-order nonlinear differential equations to represent each oscillator rather than the Van der Pol equation was found necessary to obtain the observed characteristics of the intestinal ECA. In particular, the rise of plateau frequency above the highest intrinsic frequency in the model using bidirectional coupling alone could not be obtained without a proper choice of parameters in the equations. Furthermore, the shape of the oscillator wave can be made more similar to the intestinal waveform by an adjustment of these parameters. This is not possible with the Van der Pol equation whose solution, though non-sinusoidal, is symmetrical about the time axis.

The control activity characteristics, particularly the formation of a frequency plateau and proper phase lags, could not be obtained with voltage coupling alone, but were obtainable with current coupling alone or both couplings together (see Chapter V). Oscillator parameters in the models were such that only current coupling was present in the second model, while both current and voltage couplings were present in the first model. The ratio of current coupling to voltage coupling in the first model was 30:1.

Reduction of the ratio between current coupling and voltage coupling caused the models to exhibit characteristics not found in the animal intestine. For instance, when voltage coupling was introduced in the second model by making b_1 non-zero (current coupling to voltage coupling ratio 12.5:1) the model did not simulate the effect of response activity on the control activity. In this case, when response activity was introduced in an oscillator in the frequency plateau region, the distal oscillators unlocked and dropped to a lower frequency. These lowered frequency oscillators pulled down the frequency of proximal oscillators as well after a few cycles. The result was that the entire plateau frequency dropped to a value lower than the highest intrinsic frequency. This situation was, however, not stable; and after variable periods of time, the original frequency was restored. No similar observation was ever made in the animal. A dominant current coupling or current coupling alone is, therefore, suggested in the smooth muscle of the small intestine.

The models were kept simple in the form of a chain, since very little or no phase difference existed along the circumference in the duodenum. The ability of these oscillators to oscillate when arranged in the form of a closed chain, as would exist in the intestine in the circumferential direction, was studied by using 10 oscillators. The intrinsic frequencies of these oscillators were distributed at random between 18.0 c/min and 17.5 c/min. The oscillators were then coupled to form a closed chain; i.e., oscillator 1 was also coupled to oscillator 10. All oscillators were phase locked, and the phase lag between the most leading oscillator and the most lagging oscillator depended upon the coupling factor. The oscillator with the highest intrinsic frequency had the most leading wave. The most lagging wave existed approximately half-way along the circumference from this oscillator.

In order to simulate the temporal variation of frequencies distal to the frequency plateau region, the bidirectional coupling had to be reduced distally in the chain of oscillators. Reduction of coupling factor was partly justified by the observation that the control waves in the isolated segments of the distal jejunum and ileum were not phase locked even after the effect of higher frequency oscillators was removed by surgical cuts. Another possible reason for the temporal variation of frequencies in the distal part of the intestine could be that the oscillators in that region are comparatively less stable, causing their intrinsic frequencies to vary over a wider range. This aspect, though possible, was not included in the deterministic models described above.

When a cut was made in the variable frequency region of either model, the outputs of all the distal oscillators became phase locked. Such a long frequency plateau was not formed when a similar cut was made in the small intestine. This dissimilarity between the models and the dog intestine could be due to the relatively greater instability of the distal oscillators as discussed above. Other factors that could cause this dissimilarity are:

a) The ECA waves recorded from the ileum showed phase differences along the circumference. Such phase differences did not exist in the models because a single oscillator was used to represent the electrical activity of the entire circumference. It would be more appropriate to use a ring of oscillators to represent the ECA along the circumference of each small segment in the ileum. Such an arrangement could not be tried, due to the small number of oscillators that could be simulated on the computers.

b) The second reason is based on the electron microscope data (Daniel et al., unpublished) regarding the orientation of circular muscle cells in the small intestine. It was observed that the circular muscle cells were oriented perpendicular to the longitudinal muscle cells in the duodenum, but in the ileum they were oriented at different angles with the transverse axis. This difference of orientation would give rise to differences in the arrangement of couplings in the duodenum and in the ileum (Fig. 3.26), and hence could be a factor in preventing the formation of stable frequency plateaus.

The models suggested that the frequency plateau ended where the intrinsic frequency dropped below the value which the available coupling could entrain. Distal to the frequency plateau, the amplitude of waves varied a great deal, accompanied by unlocking. Diamant and Bortoff (24) referred to these as the areas of waxing and waning. We observed such variations in amplitude accompanied by a variation in frequency occurring very commonly in the distal jejunum and ileum. Similar changes, though less marked than in the animal, were observed in the control waves of the oscillators in the variable frequency regions of the models. It is, therefore, suggested that such changes of amplitude occur due to interactions between bidirectionally coupled relaxation oscillators. This view is different from that of Diamant and Bortoff (24) who proposed that

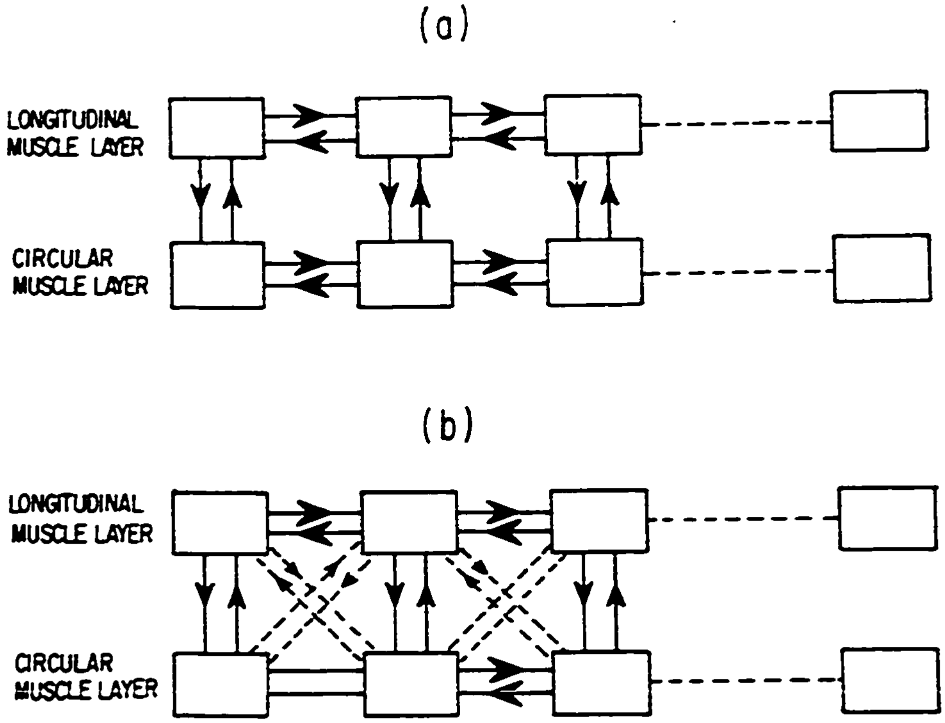
(a)
LONGITUDINAL MUSCLE LAYER
CIRCULAR MUSCLE LAYER
(b)
LONGITUDINAL MUSCLE LAYER
CIRCULAR MUSCLE LAYER

Figure 3.26

Diagram showing the probable manner of interaction between longitudinal and circular muscle layers in the small intestine: (a) in the duodenum; (b) in the ileum.

waxing and waning occurred due to the summation of two control waves at different frequencies.

The reversal in the direction of phase lag due to local heating or sympathetic reflex could be explained by the fact that in a chain of bidirectionally coupled relaxation oscillators, the oscillator with the highest intrinsic frequency dominates. The domination is in the sense that it pulls the frequency of the others to that of its own, or to higher values, and has the most leading wave.

The models also suggested a possible reason for the observed effects of response activity on control activity. The response potentials consist of positive going spikes. Soon after depolarization the control wave is in an absolutely refractory state to any positive electrical stimulus. The response potentials introduced in this phase which has been referred to as the relatively positive phase are, therefore, ineffective in altering the wave shape or the period of control wave. When the repolarization of the control wave has begun, or is about to begin, it is in a relatively refractory state to positive stimulus. Response potentials introduced in this phase cause it to depolarize again or to sustain the depolarization and thereby lengthen the period. This lengthening of the period unlocks the distal waves from proximal waves. Refractory properties of relaxation oscillators are discussed in further detail in the next chapter.

The models proposed here simulate the electrical control activity observed in the dog intestine. These models can, however, be easily modified to the cases of other species where different characteristics may exist. For instance, the stepwise frequency gradient reported by Diamant and Bortoff (24) in the cat, or the situation where the plateau frequency is equal to the highest intrinsic frequency can easily be simulated by adjusting oscillator parameters and coupling factors.

CHAPTER IV

ELECTRICAL CONTROL ACTIVITY OF THE STOMACH

4.1 General

The stomach is a musculoglandular organ interposed between the esophagus and the small intestine. The inlet of the stomach is called cardia and the outlet is called pylorus. The stomach stores and partly mixes the food, while its intrinsic glands intermittently add enzymes, mucus and hydrochloric acid. Along with mixing, it propels its contents aborally. The stomach has three functional regions which correspond roughly to its anatomic divisions. In caudad sequence they are fundus, corpus or body, and antrum (Fig. 3.1).

The fundus is the part of the stomach cephalad to the esophagogastric junction. It is a reservoir capable of large variations in size with little change in tension or intragastric pressure.

The corpus or central portion of the stomach is the largest region. Like the fundus it adapts to changing volume of contents, and so subserves the reservoir function. Also, and more importantly, it mixes and propels the contents with a vigor adapted to their nature.

The antrum is the most distal part of the stomach, ending in the pylorus. Its major function is propelling. Motor activity is present more often in the antrum than elsewhere, and contractions of the antrum are the most vigorous.

The stomach possesses dorsal and ventral walls and greater and lesser curvatures. The dorsal wall presents a convex outer surface which faces mostly dorsally but also caudodextrally. The ventral wall faces to the left and cranially as well as ventrally. The greater curvature is convex and extends from the cardia to the pylorus. The lesser curvature also runs from the cardia to the pylorus and is the shortest distance between these two parts.

The contractions of the stomach can be classified into two types. The first type is called peristaltic contractions or gastric peristalsis. Gastric peristalsis results from the contraction of a band of circular muscle fibres surrounding the stomach which moves in a caudad direction owing to progressive contraction and relaxation of contiguous strands of circular fibres (55). The width of the moving band is variable. It is usually 1-1.5 cm in dogs. The site of origin of peristaltic contractions of the stomach is not fixed, but migrates between the cardia and the terminal region of the antrum. The speed of movement of the ring of contraction increases distally. Peristaltic contractions are mainly responsible for the movement of gastric contents. The second type of contractions do not migrate. They occur over a segment several centimeters in length (55). They occur in two forms. One form has been designated "tone" contraction and can occur anywhere in the stomach. The other form is confined to the antrum and has been designated as the "terminal antral contraction" (56).

4.2 Animal Studies

4.21 Electrical control activity of the dorsal and ventral walls

Sixteen electrodes were implanted (Fig. 4.1) in a dog, eight on the ventral side and eight on the dorsal side, so that their positions were approximately identical with respect to the pylorus and with respect to the two curvatures. The control waves recorded at all the electrodes were phase locked. The ECA frequency was 5.5 c/min. The phase lag patterns were similar on both sides (see section 4.23).

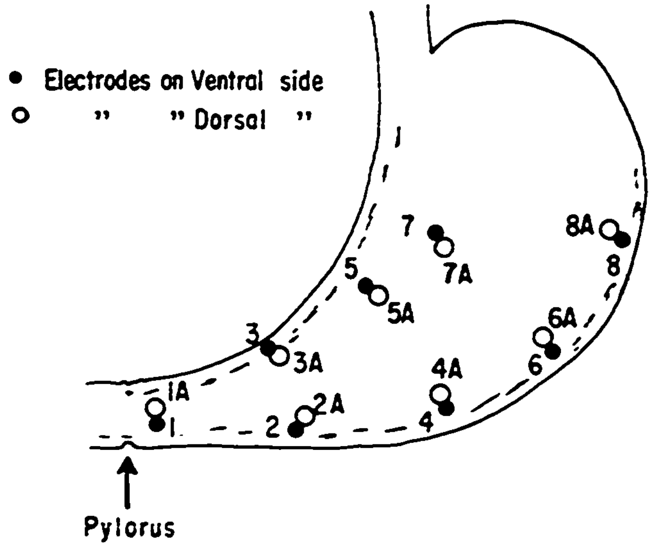

● Electrodes on Ventral side
○ " " Dorsal "
1
1A
2
2A
3
3A
4
4A
5
5A
6
6A
7
7A
8
8A
Pylorus

Figure 4.1

Diagram showing the position of electrodes implanted on the dorsal and the ventral sides. Distances of electrodes 1 to 8 from the pylorus were 1.0, 3.5, 3.8, 6.6, 6.1, 10.4, 8.7 and 12.2 cm, respectively. Distances between electrodes 2-3, 4-5 and 6-7 were 2.6, 2.1 and 2.5 cm, respectively. Corresponding electrodes on the dorsal side were identically located. Broken lines show the position of longitudinal cuts made on the dorsal side.

Longitudinal cuts (shown by broken lines in Fig. 4.1) in muscle layers only were made parallel to the two curvatures and 1-2 cm away from them on the dorsal side. The cuts were 15 cm long and were well beyond the most proximal site at which electrical control activity (MPSECA) could be recorded. Changes observed in the frequency and the phase lag/cm values on the ventral side before and after the cuts were insignificant, as shown in Table 4.1.

Table 4.1

EFFECT OF THE ISOLATION OF DORSAL AND VENTRAL SIDES ON ECA

	ECA Frequency in c/min	Phase Lag/cm near MPSECA	Phase Lag/cm near Pylorus
Before isolating dorsal side	5.5	79°	22.8°
After isolating dorsal side	5.75	75°	21.3°

Slight changes in the values of frequency and phase lag/cm could be attributed mainly to the changes in body tempeature. Since the ECA was identical on the ventral and dorsal sides, all the subsequent recordings were made from the ventral side only.

4.22 Intact frequency gradient

Electrodes were implanted on the ventral side in two or three rows to determine the intact frequencies in 9 dogs. When two rows of electrodes were implanted, one was near the greater curvature and the other on the midline between the greater and lesser curvatures. In 4 experiments a third row of electrodes near the lesser curvature was implanted. Regular and stable ECA could be recorded only up to a distance of 10-14 cm along the greater curvature in different dogs. This distance reduced to 8-10 cm on the midline and to 4-6 cm along the lesser curvature. For instance, in one of the dogs the distances were 12.8 cm on the greater curvature, 8.4 cm on the midline and 4.0 cm on the lesser curvature. The shape of the electrically active region in the dog stomach is shown in Figure 4.2. Figure 4.3 shows the control waves recorded at 6 electrodes implanted on the greater curvature. Distances of electrodes 1 to 6 from the pylorus were 0.4, 2.2, 4.0, 6.3, 8.0 and 10 cm, in that order.

Control waves at all sites that showed ECA had the same frequency and were phase locked. In other words, a single frequency plateau existed in the stomach. The ECA frequency in 9 different dogs was between 4.0 and 6.5 c/min (mean 5.1 ± 0.52 s.e.). The frequency also depended on the body temperature of the dogs. The amplitude of oscillation of control waves recorded was the largest in the antrum and the least in the region of the MPSECA.

4.23 Phase lag pattern

Electrodes were implanted approximately 1 cm apart to determine the phase lag pattern in 5 dogs. In the stomach, phase difference existed in the longitudinal and in the transverse directions. Longitudinally, the phase lag existed in the aboral direction and transversely, from the greater curvature to the lesser curvature. Phase lag per cm was of the order of 70° to 100° near the MPSECA and of the order of 8° to 20° near the pylorus

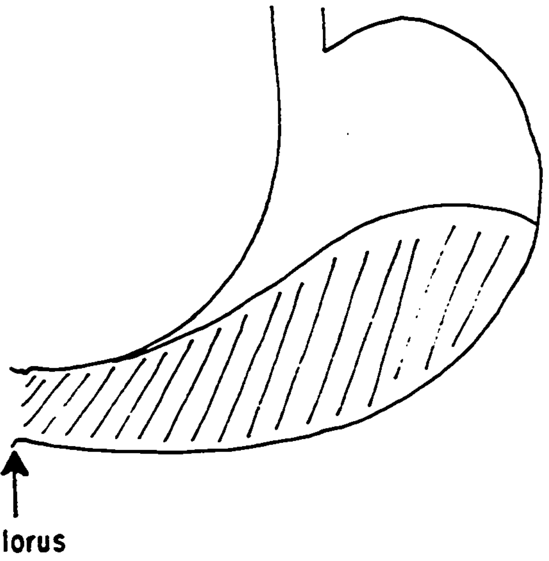

Figure 4.2

The hatched area shows the shape of the electrically active region in the dog stomach.

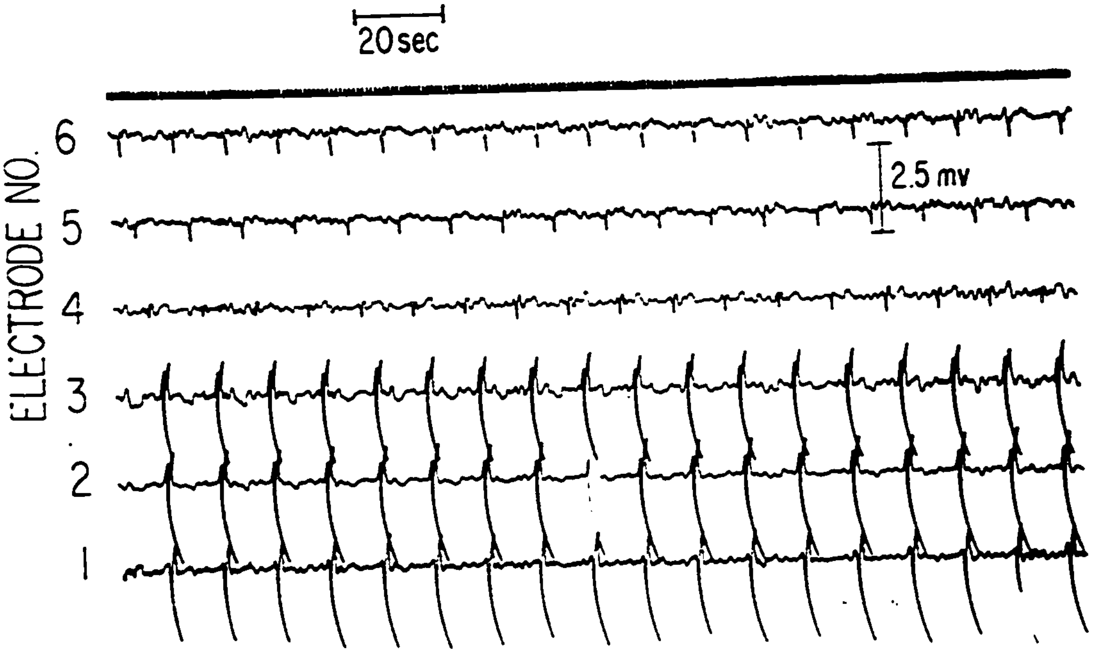

Figure 4.3

Control waves recorded from 6 electrodes implanted on the greater curvature. Distances of electrodes 1 to 6 from the pylorus were 0.4, 2.2, 4.0, 6.3, 8.0 and 10.0 cm, respectively. All the control waves were phase locked.

in different dogs. Phase lag patterns in two dogs are shown in Figure 4.4. Phase lag/cm was the largest near the MPSECA and decreased distally. Similar phase lag patterns were observed in other dogs. These results are in agreement with those of others (48) who interpreted it as a slower conduction velocity in the body and a faster conduction velocity in the antrum.

4.24 Intrinsic frequency gradient

The intrinsic frequency gradient was determined in 7 dogs by electrically isolating the stomach longitudinally and transversely into small segments. The stomach was first divided longitudinally by cuts all around the circumference. Each isolated segment contained two electrodes, one near the greater curvature and the other 2 cm away from it towards the lesser curvature. Control waves recorded from the electrodes in the same isolated segment were phase locked. The control wave near the greater curvature led the control wave near the midline. A longitudinal cut was then made in between the two rows of electrodes such that each isolated segment was divided into two parts (Fig. 4.5). The intrinsic frequency gradients along the greater curvature and along the midline in one dog are shown in Figure 4.6. The sites of cut are shown by arrows. Similar gradients were observed in other dogs.

The intrinsic frequency gradient was also determined by making one circumferential cut at a time and allowing the dog to recover before making the next cut (2 dogs). In one dog the first cut was made in the antrum and then the other proximal cuts, while in the other dog the first cut was made in the body and then the more distal cuts. This method was used to determine if the effect of trauma and any disruption in blood supply due to several cuts had an effect on the intrinsic frequencies. No

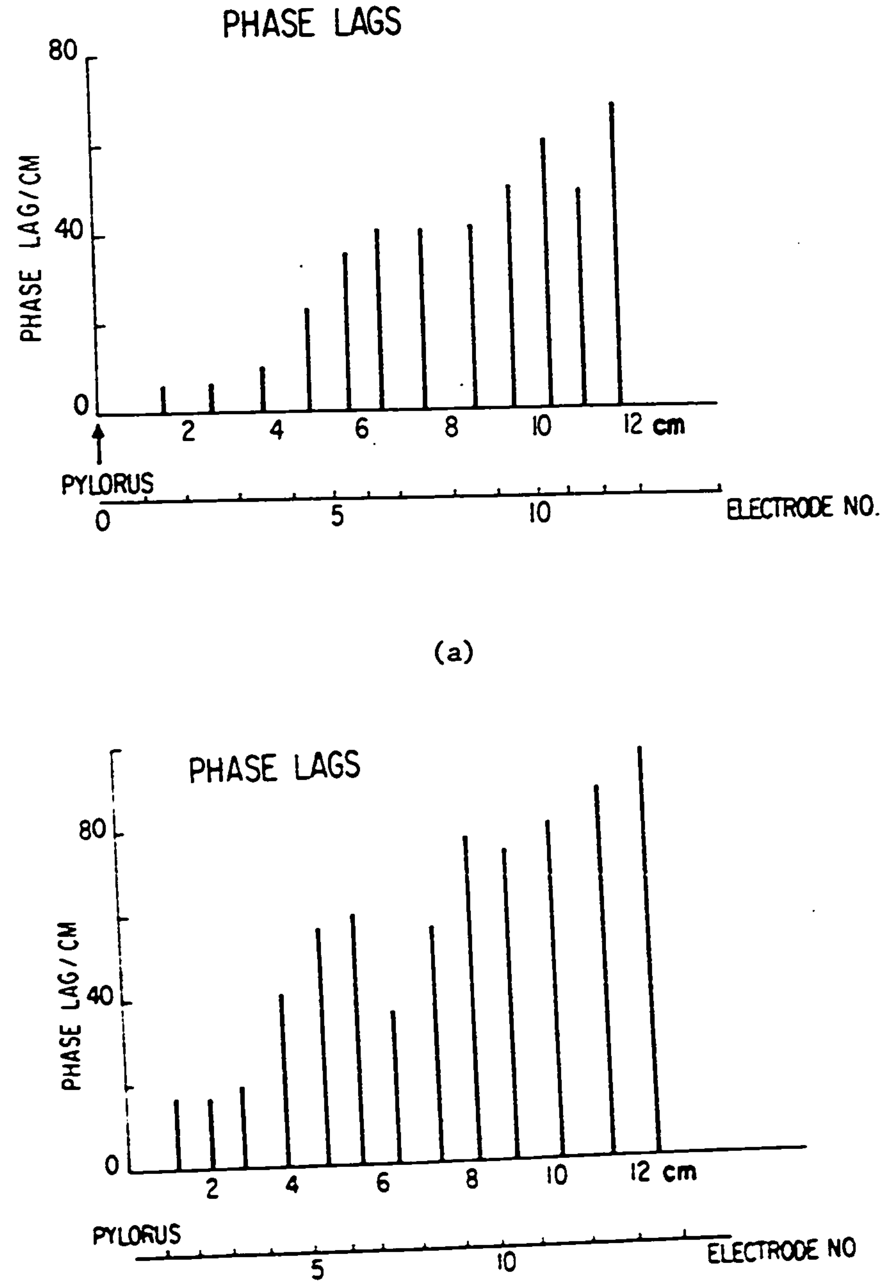

(a)

(b)

Figure 4.4

Phase lag patterns along the greater curvatures of two dogs. Electrodes were implanted 1-2 cm apart. Phase lag between two successive electrodes was divided by the distance between them, and plotted at the mean distance of the two electrodes from the pylorus.

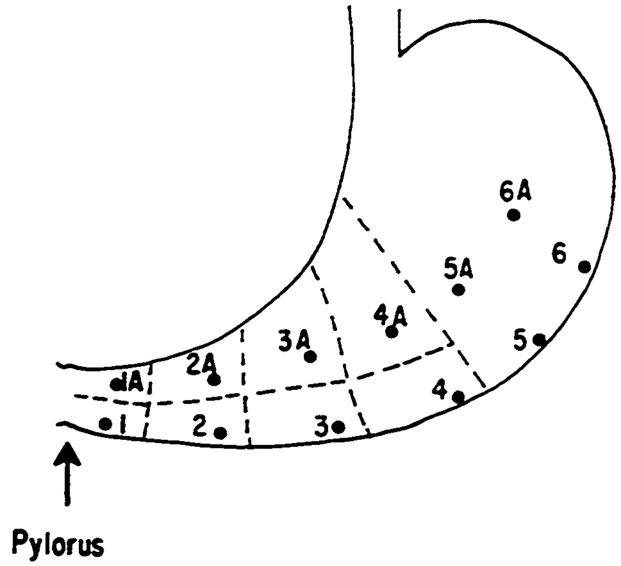
6A
6
5A
5
4A
4
3A
3
2A
2
1A
1
Pylorus

Figure 4.5

Diagram showing the longitudinal and the circumferential cuts made in the stomach to determine intrinsic frequencies. The diagram also shows the placement of electrodes and their numbers.

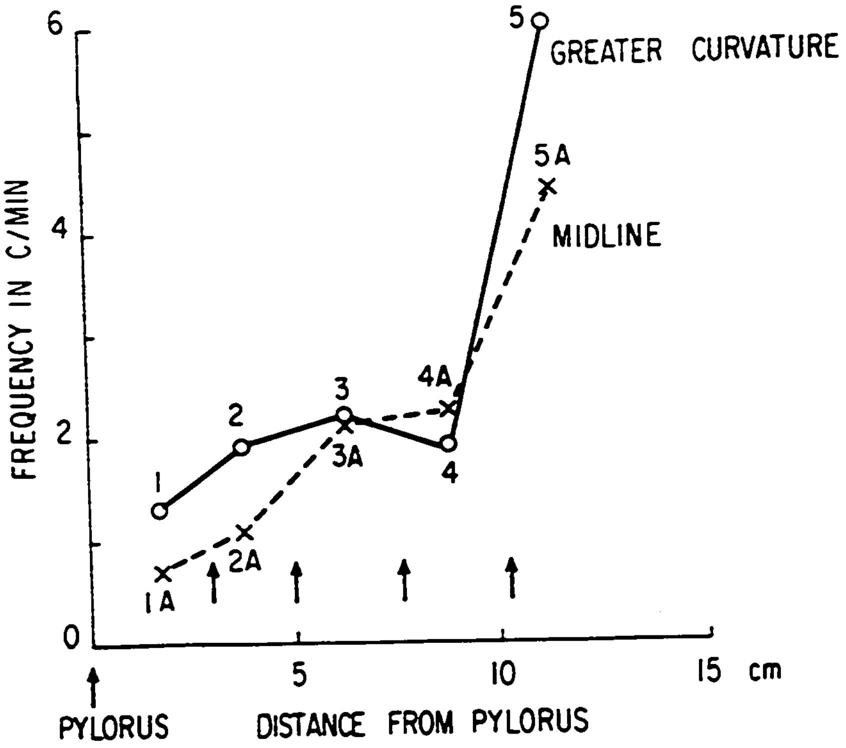

Figure 4.6

Diagram showing the intrinsic frequency gradients along the greater curvature (—) and on the midline (--) of the dog stomach. The sites of cuts are shown by arrows. Numbers refer to different electrodes (see Figure 4.5).

significant difference in the intrinsic frequency gradient was found by this method, although the intrinsic frequencies determined by this method were 5 to 15% higher than those determined by making all cuts simultaneously.

4.25 Partial circumferential cuts

Partial circumferential cuts were made in a variety of ways to determine the relative magnitudes of couplings in the longitudinal and transverse directions. In all cases, two rows of electrodes were implanted in the stomach. One row of electrodes was near the greater curvature, and the other row was approximately 2 cm away from it on the midline. The electrodes were numbered as shown in Figure 4.5. The cuts were made on both the dorsal and the ventral sides. The length of each cut at different stages was expressed as a percentage of the length of the circumference at the site of the cut. The results of these cuts are summarized below.

Dog 1.

No. of electrodes in each row = 6

ECA frequency of intact stomach = 5.3 c/min

1st stage:

A 50% cut was made from the greater curvature side at a distance of 3.0 cm from the pylorus. The cut was between electrodes 2 and 3. Prior to the cut, the control wave at electrode 3 led the control wave at electrode 3A, and the control wave at electrode 2 led the control wave at electrode 2A. Phase difference between control waves at electrodes 2 and 3 was 20°. After the cut, all control waves were still phase locked, and there was no change in ECA frequency. However, after the cut, the control wave at electrode 3 led the one at electrode 3A as before, but the control wave at electrode 2A led the control wave at electrode 2. Phase lag between the control wave at electrode 3 and that at electrode 2 increased to 68.6°. Evidently the oscillator at electrode 2 was now being driven by the oscillator at electrode 2A. This indicated that in the antrum area strong coupling existed in the transverse direction.

2nd stage:

The cut in the first stage was extended all around. The ECA frequency at electrodes 1, 1A, 2 and 2A dropped to 1.75 c/min. The ECA frequency proximal to the cut was not affected.

3rd stage:

Another 50% cut was made from the greater curvature side at a distance of 8.2 cm from the pylorus. The cut was between electrodes 4 and 5. The 50% cut in this area caused frequency pulling in the control waves at electrodes 3, 3A, 4 and 4A. The 5-minute average frequency at these electrodes was 3.4 c/min. ECA frequency at proximal electrodes, i.e., electrodes 5, 5A, 6 and 6A, was not affected. This cut suggested that the longitudinal coupling on the midline between electrodes 4A and 5A was not strong enough for entrainment. Control waves at electrodes 6 to 1 are shown in Figure 4.7. The phenomenon of frequency pulling is evident in the control waves recorded at electrodes 4 and 5.

4th stage:

The cut in the third stage was extended all around the circumference. No frequency pulling was observed at electrodes 3, 3A, 4 and 4A. The time periods of control waves at these electrodes were nearly uniform. Average frequency at these electrodes dropped to 2.4 c/min.

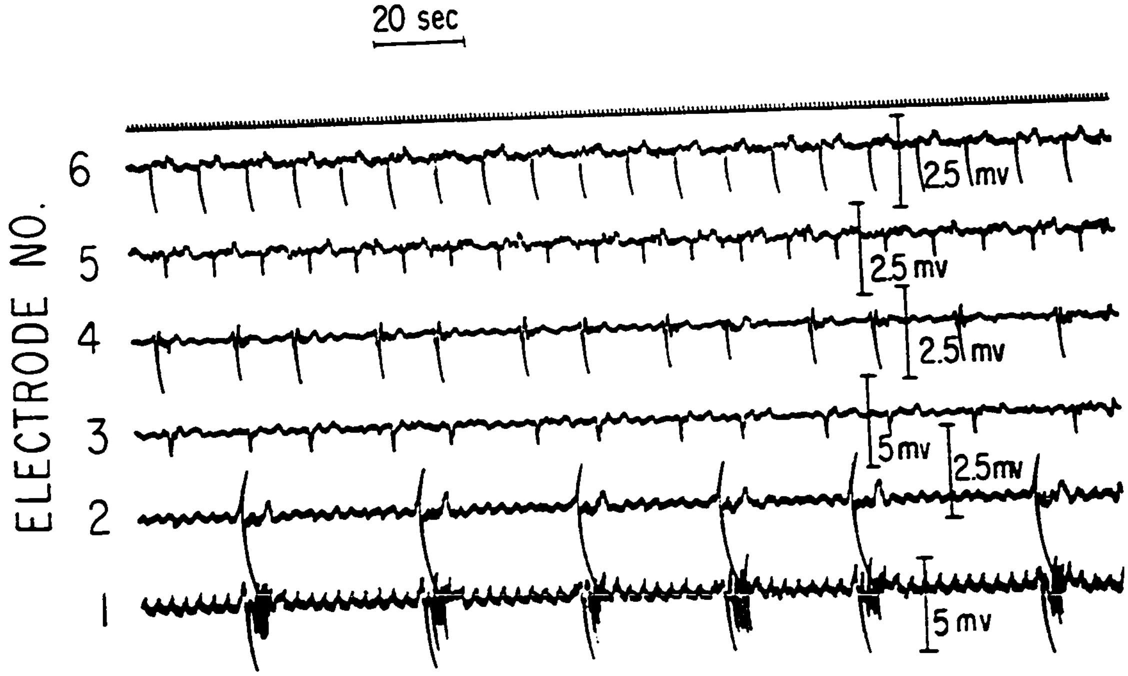

Figure 4.7

Control waves recorded from 6 electrodes implanted near the greater curvature (see Figure 4.5). A complete circumferential cut (3.0 cm from the pylorus) existed between electrodes 2 and 3, and a partial circumferential cut (8.2 cm from pylorus) existed between electrodes 4 and 5. Note the frequency pulling of control waves recorded at electrodes 3 and 4.

Dog 2.

No. of electrodes in each row = 5

ECA frequency of intact stomach = 4.75 c/min

1st stage:

A 35% cut was made between electrodes 2 and 3 from the greater curvature side. The cut was 4.5 cm from the pylorus. No effect on the ECA frequency was observed.

2nd stage:

The cut in the first stage was extended to 55%. ECA frequency at electrodes 1, 1A, 2 and 2A dropped to 2.7 c/min, while that at others remained unaffected.

Dog 3.

No. of electrodes in each row = 6

ECA frequency of intact stomach = 4.8 c/min

1st stage:

A 50% cut between electrodes 3A and 4A was made from the lesser curvature side. The cut was 5.9 cm from the pylorus. The control waves at all the electrodes were phase locked, and the ECA frequency was 6.1 c/min. The rise in ECA frequency was probably due to rise in body temperature. The phase lag between control waves at electrodes 3A and 4A increased from 137.5° before the cut to 173° after the cut. The control wave at electrode 3A led the control wave at electrode 3 before the cut by 12.2°, but there was no phase lag between them after the cut.

2nd stage:

The cut in the first stage was extended to 75%. The ECA frequency after this stage was 5.2 c/min, and all the control waves were still phase locked. Control wave at electrode 3 led the control wave at electrode 3A by 10.6°.

3rd stage:

The cut was extended to 90%. The ECA frequency dropped to 4.3 c/min, but all control waves were phase locked. The control wave at electrode 3 led the control wave at electrode 3A by 30.6°.

4th stage:

The cut was extended all around the circumference. The ECA frequency at electrodes 1, 1A, 2 and 2A dropped to 1.9 c/min, while at the other electrodes it was 4.3 c/min.

The above procedure of cuts was repeated in dog 4. Similar results were obtained; i.e., no unlocking of control waves proximal and distal to the cut occurred up to a 90% cut.

The results of experiments with dogs 2, 3 and 4 indicated that more circumferential length of muscle was required near the lesser curvature for phase locking of distal and proximal waves than was required near the greater curvature. This meant that more coupling was available near the greater curvature than near the lesser curvature. The results of experiment with dogs 3 and 4 also indicated that in the region 5-6 cm from the pylorus enough transverse coupling was available for the oscillator at electrode 3 to entrain the oscillator at electrode 3A when the latter was uncoupled from the oscillator at electrode 4A.

Dog 5.

No. of electrodes in each row = 6

ECA frequency of intact stomach = 5.25 c/min

1st stage:

A 50% cut was made from the lesser curvature side between electrodes 4A and 5A. The cut was 6.5 cm from the pylorus. The phase lag between control waves at electrodes 4A and 5A before the cut was 123°, and that after the cut was 117°. No change in ECA frequency occurred. All control waves remained phase locked after the cut.

2nd stage:

The cut was extended to 70%. The phase lag between control waves at electrodes 4A and 5A increased to 183°. The ECA frequency at all electrodes rose to 6.1 c/min.

3rd stage:

The cut was extended to 90%. Frequency pulling occurred distal to the cut. The average ECA frequency distal to the cut was 5.3 c/min, and proximal to the cut it was 5.6 c/min.

4th stage:

The cut was completed all around the circumference. The ECA frequency distal to the cut dropped to 2.8 c/min, while that proximal to the cut was unchanged.

Dog 6.

No. of electrodes in each row = 6
ECA frequency of intact stomach = 5.0 c/min

1st stage:

A 15% cut was made from the greater curvature side at a distance of 5 cm from the pylorus. The cut was between electrodes 3 and 4. The phase lag between control waves at electrodes 3 and 4 remained unchanged at 153°.

2nd stage:

The cut was extended to 40%. This caused unlocking of control waves. The ECA frequency at electrodes 1, 1A, 2, 2A, 3 and 3A dropped to 4.5 c/min, while at other electrodes it was 5.75 c/min.

3rd stage:

The cut was extended to 60%. The ECA frequency at electrodes 1, 1A, 2, 2A, 3 and 3A dropped further to 2.5 c/min, while at other electrodes it was 5.5 c/min.

4th stage:

The cut was extended to 90%. The ECA frequency at electrodes 1, 1A, 2, 2A, 3 and 3A dropped to 1.8 c/min, while at other electrodes it was 5.5 c/min.

The above cut was repeated in dog 7. Results are summarized in Table 4.2.

Dog 8.

No. of electrodes in each row = 6

ECA frequency of intact stomach = 4.1 c/min

1st stage:

A 20% cut was made from the greater curvature side between electrodes 4 and 5. The cut was 6.5 cm from the pylorus. The phase lag between electrodes 4 and 5 did not change after the cut (82°). Control waves at all electrodes were phase locked at a frequency of 4.1 c/min.

2nd stage:

The cut was extended to 40%. No change in ECA frequency was observed. All control waves remained phase locked. The phase lag between control waves at electrodes 3 and 4 increased to 135°.

3rd stage:

The cut was extended to 55%. This caused unlocking of control waves. The ECA frequency at electrodes 5, 5A, 6 and 6A was 4.25 c/min, while at distal electrodes it dropped to 2.15 c/min.

The above cut was repeated in dogs 9 and 10. The results are summarized in Table 4.2.

Dog 11.

No. of electrodes in each row = 6

ECA frequency of intact stomach = 5.8 c/min

1st stage:

A 50% cut was made between electrodes 1 and 2 from the greater curvature side (Fig. 4.8). The cut was 2.25 cm from the pylorus. There was no change in the ECA frequency. The phase lag between control waves at electrodes 1 and 2 increased from a value of 24.7° before the cut to a value of 85° after the cut.

2nd stage:

Another 50% cut was made between electrodes 2A and 3A from the lesser curvature side (Fig. 4.8). The cut was 3.5 cm from the pylorus. The ECA frequency was still unaffected. The control waves at all electrodes were phase locked. The phase lag between control waves at electrodes 2A and 3A increased from a value of 27.9° before the cut to a value of 103.2° after the cut. This cut eliminated the coupling between oscillators at electrodes 2A and 3A, and therefore increased the phase lag between control waves at these electrodes.

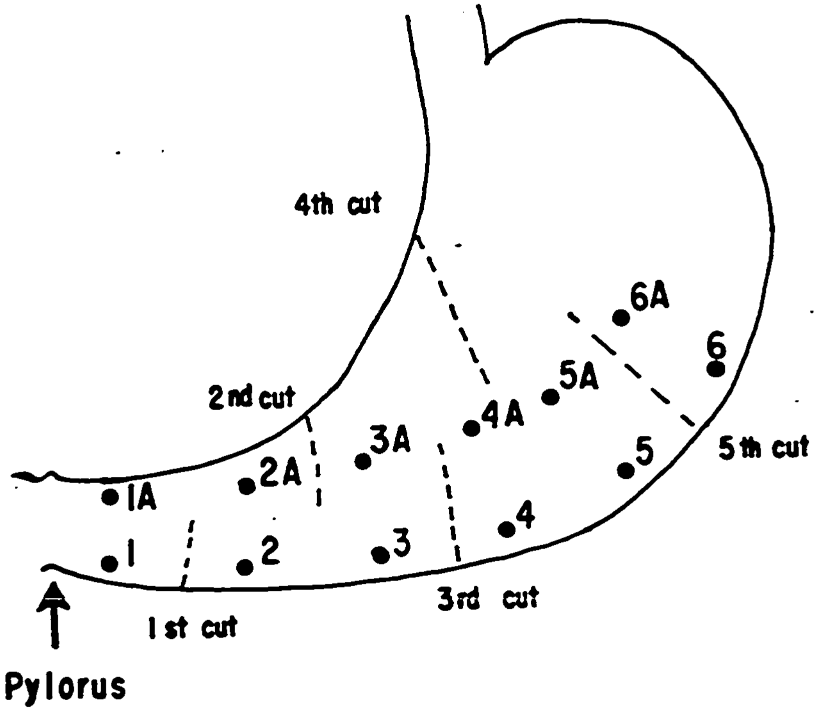
4th cut
6A
6
5A
2nd cut
4A
3A
5th cut
5
2A
1A
4
1
3
2
3rd cut
1st cut
Pylorus

Figure 4.8

Diagram showing successive 50% cuts in the stomach.

3rd stage:

Another 50% cut was made between electrodes 3 and 4 from the greater curvature side (Fig. 4.8). The cut was 6.3 cm from the pylorus. The control waves recorded at electrodes 1, 1A, 2, 2A, 3 and 3A showed frequency pulling at an average frequency of 4.5 c/min. ECA frequency at proximal electrodes was unaffected.

4th stage:

A 50% cut was made between electrodes 4A and 5A from the lesser curvature side (Fig. 4.8). The cut was 8 cm from the pylorus. No further change in ECA frequency occurred.

5th stage:

A 50% cut was made between electrodes 5 and 6 from the greater curvature side (Fig. 4.8). ECA frequency at electrodes 6 and 6A was unaffected by this cut. The control waves at distal electrodes showed frequency pulling at an average frequency of 2.6 c/min. They were all phase locked.

Dog 12.

No. of electrodes in each row = 7

ECA frequency of intact stomach = 5.25 c/min

1st stage:

Four 50% cuts were made simultaneously (Fig. 4.8), and the dog was allowed to recover for 1 hour. Distances of the cuts from the pylorus were:

1st cut: 2.0 cm
2nd cut: 5.5 cm
3rd cut: 8.0 cm
4th cut: 9.6 cm

The ECA frequency at electrodes 6, 6A and 7 remained unchanged after the cuts, while at other electrodes it showed frequency pulling at an average frequency of 4.1 c/min. No ECA existed at electrode 7A.

2nd stage:

The ends of all the cuts on the dorsal side were joined by another longitudinal cut. No effect on the ECA frequency of the ventral side was observed.

4.26 Premature control potentials

Premature control potentials (PCP) were produced in the stomach by close intraarterial (i.a.) injections of acetylcholine (0.05-0.5 μg). The i.a. injections were made at different phases of the control wave cycle. Two kinds of responses to i.a. injections of acetylcholine were observed, depending upon the phase in which the injection was made:

a) If acetylcholine was injected in an early phase of the cycle (0-50%; time was measured from the positive going zero crossing of the control wave and expressed as a percentage of the total period), a response potential consisting of prolonged negative going deflection (depolarization) occurred.

b) If acetylcholine was injected in the later phase of the cycle (50-100%), it resulted in a premature control potential.

The division of the cycle into two zones as described above is only approximate. There was an overlap of 5-10% of the two zones. The earliest that a PCP could be produced in the 7 dogs experimented on was at 41.7%. Markedly increasing the dose of acetylcholine injections in the early phase (less than 40%) disrupted the electrical activity of that region, and also of the distal region. In these cases no electrical activity existed for periods of

Table 4.2

RESULTS OF PARTIAL CUTS IN THE STOMACH

Dog No.	Cut on greater curvature (G.C.) or lesser curvature (L.C.)	Distance of cut from the pylorus	Max. length of cut at which no unlocking was observed	Min. length of cut at which unlocking was observed
1	G.C.	3.0 cm	50%	100%
1	G.C.	8.2 cm	--	50%
2	G.C.	4.5 cm	35%	55%
3	L.C.	5.9 cm	90%	100%
4	L.C.	5.2 cm	90%	100%
5	L.C.	6.5 cm	70%	90%
6	G.C.	5.0 cm	15%	40%
7	G.C.	6.5 cm	15%	35%
8	G.C.	6.5 cm	40%	55%
9	G.C.	6.5 cm	55%	70%
10	G.C.	6.5 cm	15%	30%

up to 2 minutes.

Acetylcholine was injected on the greater curvature side in 5 dogs, and on the lesser curvature side in 2 dogs. The results of an experiment on one dog are shown in Table 4.3. The results of injections on the greater curvature side in 5 dogs are summarized in Table 4.4. It is seen that the PCP was usually produced in the 65-80% phase of the cycle. The PCP propagated more often distally than proximally. The proximal propagation was usually up to a distance of 2 cm or so. In a few cases (5 in 5 dogs) the proximal propagation was up to a distance of 4 cm, and in one case it was up to a distance of 6 cm.

The occurrence of a PCP and its spread is shown in Figure 4.9. The electrodes were implanted as shown in Figure 4.5. The PCP due to i.a. injection of acetylcholine was produced in the region of electrode 4. In the proximal direction it propagated up to the region of electrode 5, and in the distal direction up to the region of electrode 2. When the PCP arrived in the region of electrode 6, a normal control potential (NCP) had already been initiated, and the oscillator was in an absolutely refractory state with respect to ECA (see section 4.38). This halted any further propagation in the proximal direction. Figure 4.10 shows the delay produced in the cycle when acetylcholine was injected in an early phase of the cycle in which the oscillator was in an absolutely refractory state.

The propagation of a PCP in the direction of the lesser curvature from the greater curvature was studied in 3 dogs (dogs 1, 3 and 4 in Table 4.4). Whenever a PCP propagated in the distal direction, it also propagated in the direction of the lesser curvature.

The propagation of a PCP from the lesser curvature to the greater

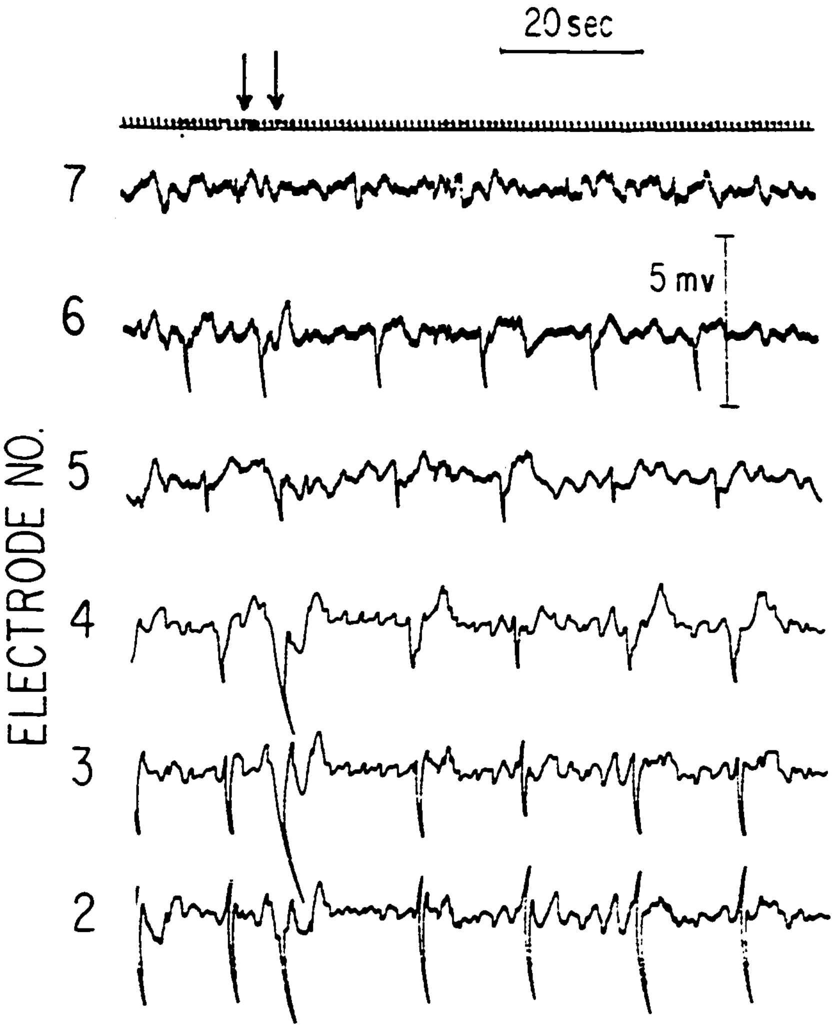

Figure 4.9

Recording showing the spread of a PCP in the proximal and distal directions. Distances of electrodes 2 to 7 from pylorus were 2.2, 4.2, 5.2, 6.7, 9.0 and 11.2 cm, respectively. Electrode 4 was in the perfused region. The first arrow from the left on the time scale indicates the injection of acetylcholine, and the second arrow indicates the injection of 0.5 cc of Krebs-Ringer solution to flush acetylcholine. The PCP propagated up to the region of electrode 5 proximally, and up to the region of electrode 2 distally. It probably spread to the pylorus distally, but the recording could not be made due to the availability of only 6 channels.

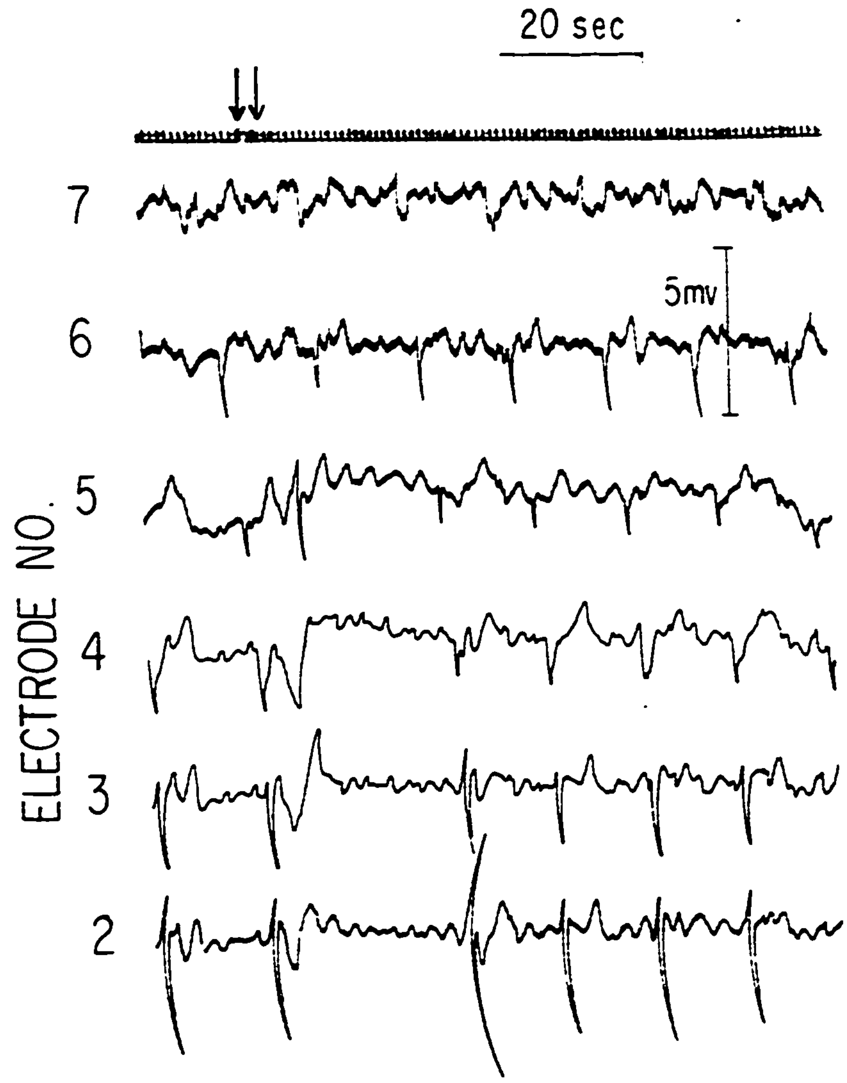

Figure 4.10

Recording showing the lengthening of wave period (electrodes 4, 3 and 2) due to the injection of acetylcholine. The positions of electrodes were the same as described in Figure 4.9. The two arrows on the time scale have also the same meaning as described in Figure 4.9. In this case the acetylcholine probably perfused into the regions of electrodes 4 and 5 simultaneously. A PCP was produced at electrode 5 because its control wave led the control wave at electrode 4 and hence was in a relatively less refractory phase. This PCP, however, did not propagate in any direction.

Table 4.3

INTRAARTERIAL INJECTIONS OF ACETYLCHOLINE ON THE GREATER CURVATURE SIDE

Electrodes 3 and 4 (Fig. 4.5) were in the perfused area

Per-fusion No.	Dose µg	PCP started at electrode No.	*Phase at which PCP produced	PCP produced at proximal electrode No(s).	PCP produced at distal electrode Nos.	Remarks
1	0.1	4	58.3%	—	3, 2	
2	0.1	—	—	—	—	Response potential
3	0.1	4	62.3%	5	3, 2	
4	0.1	4	46.7%	5	3, 2	
5	0.1	—	—	—	—	Response potential
6	0.1	4	51.3%	5	3, 2	
7	0.1	4	47.2%	5	3, 2	
8	0.1	4	62.7%	5	3, 2	
9	0.1	4	62.0%	5, 6	3, 2	
10	0.1	4	72.7%	5	3, 2	
11	0.1	4	84.0%	5	3, 2	
12	0.1	—	—	—	—	No effect
13	0.1	—	—	—	—	No effect
14	0.1	4	84.4%	—	3, 2	
15	0.1	4	89.5%	—	3, 2	

*Time lag between an acetylcholine injection and the production of a PCP was negligible.

Table 4.4

SUMMARY OF ACETYLCHOLINE INJECTION ON GREATER CURVATURE SIDE

Dog No.	Total injections	No. of times PCP produced	Average phase at which PCP produced	Minimum phase at which PCP produced	Maximum phase at which PCP produced	No. of times PCP propagated proximally	No. of times PCP propagated distally
			s.e.				
1	15	11	65.4 ± 14.18	47.2%	89.5%	8	11
2	21	12	80.5 ± 11.43	41.7%	96.0%	3	11
3	20	8	84.8 ± 7.5	69.3%	96.0%	0	8
4	32	21	76.7 ± 6.97	60.0%	87.3%	4	21
5	10	6	77.8 ± 8.16	66.6%	85.5%	2	5

curvature was studied in two dogs. A PCP produced on the lesser curvature side was found to propagate to the greater curvature. However, it was found that when acetylcholine was injected from the lesser curvature side the perfusion area was well up to the midline between the greater and lesser curvatures. This gave rise to the possibility that the PCP that propagated to the greater curvature might have been produced on the midline instead of on the lesser curvature. The premature control potentials produced on the lesser curvature propagated proximally and distally as described before.

Another observation of interest was made during the above experiments. The regions near the lesser curvature in the body did not normally show any ECA in fasted dogs. However, when acetylcholine was injected they showed control potentials. This suggested that the cells in this region are potential oscillators. They can be made to oscillate with an external stimulus.

4.27 Summary of results

To sum up the results of animal study, any model of the gastric control activity of dogs must show the following:

1) One frequency plateau in the entire electrically active region of the stomach.
2) A complete circumferential cut should not affect the ECA frequency of the proximal part, but the ECA frequency of the distal part should fall and form another frequency plateau.
3) The phase lag/cm in the longitudinal direction should decrease distally from the body of the stomach to the antrum.
4) The control waves should also show a phase lag in the transverse

direction.

5) The intrinsic frequency should decrease distally from the most proximal site of electrical control activity to the antrum. The intrinsic frequency should also show a small decrease from the greater curvature to the lesser curvature.

6) The length of a partial cut that unlocks the ECA of the distal part from that of the proximal part should be less if the cut is on the greater curvature side than if it is on the lesser curvature side.

7) A premature control potential produced in the later part of the control wave cycle should be able to initiate premature control potentials in the proximal and/or distal regions, depending on the phase at which it is produced. An attempt to produce a premature control potential in the early part of the cycle should lengthen the time period of control wave.

4.3 Computer Model of Gastric ECA

4.31 Arrangement of oscillators

An array of bidirectionally coupled relaxation oscillators is proposed as a model of the gastric ECA. The arrangement of oscillators in the array is shown in Figure 4.11. Oscillators 1 to 6 represent the ECA of the greater curvature side, oscillators 7 to 11 represent the ECA of the midline, and oscillators 10 to 13 represent the ECA of the lesser curvature side. Oscillators 10 and 11 represent the electrical activities of the midline and of the lesser curvature in the antrum because the stomach narrows down in this part.

Each oscillator was represented by equations 2.1 and 2.2. Current coupling alone was used to couple the oscillators (see Chapter V). The parameters of oscillators are given in Table 4.5, and the coupling factors are shown in Figure 4.11. The coupling factors were chosen to get the following:

1) One frequency plateau in the entire stomach model
2) The phase lag pattern in the model similar to that observed in the dog stomach
3) The results of partial cuts in the model similar to those observed in the dog stomach.

The dorsal and the ventral sides of the stomach were shown to be independent of each other in exhibiting the phase lags and the ECA frequency. Only one side (ventral) was, therefore, simulated in the model.

4.32 Frequency gradients

The intrinsic frequency gradients along the greater curvature, the midline and the lesser curvature are shown in Figure 4.12. The intrinsic

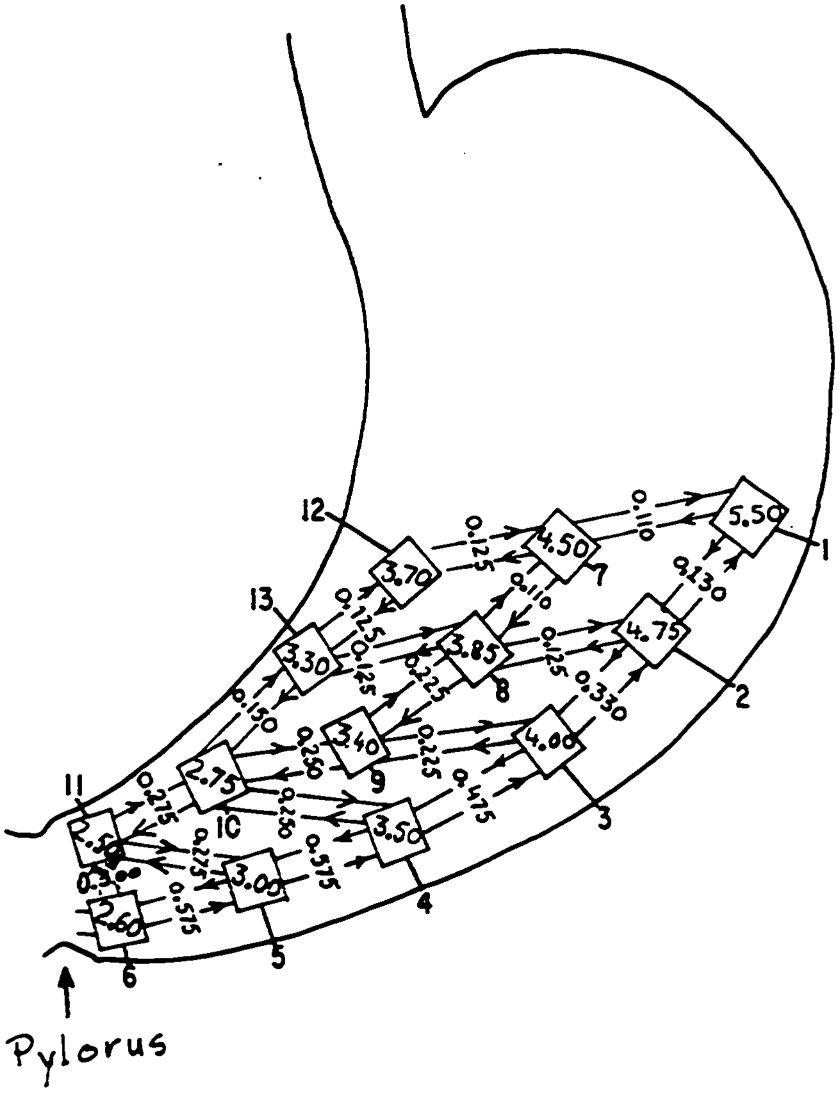
5.50
4.50
3.70
3.30
3.85
4.75
3.40
4.00
2.75
3.50
3.00
2.60
2.50
1
2
3
4
5
6
7
8
9
10
11
12
13
0.110
0.125
0.130
0.110
0.125
0.125
0.125
0.225
0.330
0.150
0.250
0.225
0.475
0.275
0.250
0.275
0.575
0.575
Pylorus

Figure 4.11

Arrangement of oscillators in the gastric ECA model. Oscillators 1 to 6 represent the ECA of the greater curvature; oscillators 7 to 11 represent the ECA of the midline; and oscillators 10-13 represent the ECA near the lesser curvature. Numbers inside the boxes indicate the intrinsic frequencies of oscillators, and those between them indicate coupling factors.

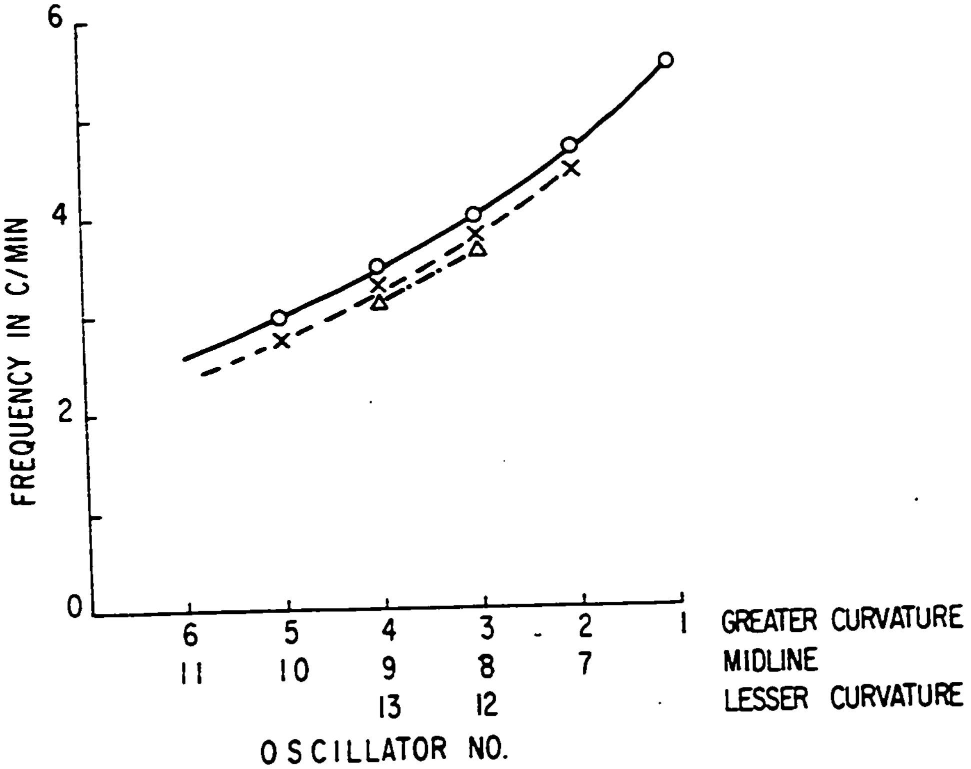

Figure 4.12

Diagram showing the intrinsic frequency gradients along the greater curvature (——), the midline (----), and the lesser curvature (-•-•-) used in the gastric ECA model.

Table 4.5

PARAMETERS OF OSCILLATORS FOR THE GASTRIC ECA MODEL

$a_2 = 1.0$, $b_1 = 0.0$, $b_2 = 3.50$, $b_3 = 0.0$, $b_4 = 0.0$,
$b_0 = 5.0$, $k = 10.0$ for all oscillators

Oscillator No.	a_1	a_3	a_4
1	1.344	0.6440	0.4636
2	1.202	0.7050	0.5022
3	1.038	0.8340	0.5600
4	1.017	0.8380	0.5600
5	0.827	1.1400	0.6730
6	0.934	0.8800	0.6095
7	1.120	0.9200	0.5800
8	1.030	0.9015	0.5820
9	0.950	1.0270	0.6340
10	0.730	0.9840	0.5925
11	0.700	1.1150	0.6625
12	1.000	1.1150	0.6820
13	0.910	1.0070	0.5580

frequency reduced from a value of 5.5 c/min in oscillator 1 to a value of 2.5 c/min in oscillator 6. A slight gradient of intrinsic frequency was also kept in the transverse direction as observed in the dog stomach.

When the oscillators were coupled as described before, their outputs were phase locked at a frequency of 5.0 c/min. Oscillator 1, with the largest intrinsic frequency, had the most leading control wave. Outputs of oscillators 1 to 6 in the uncoupled and coupled stages are shown in Figure 4.13.

4.33 Phase lag pattern

The phase lag between oscillators in the proximal part of the array representing the body of the stomach was large, and it decreased distally. Phase lags among oscillators representing the greater curvature are shown in Figure 4.14. Phase lags also existed in the transverse direction as observed in the dog stomach.

4.34 Complete circumferential cuts

As for the intestinal models, a cut between two oscillators was simulated by reducing the coupling factor between them to zero. The ECA frequency distal to a complete circumferential cut dropped to a lower value in all cases. Very small change in the proximal ECA frequency was observed unless the complete cut isolated oscillator 1. In this case the ECA frequency of oscillator 1 rose to 5.5 c/min. The control waves in each part after a complete circumferential cut were phase locked in all cases. The results of cuts are summarized in Table 4.6.

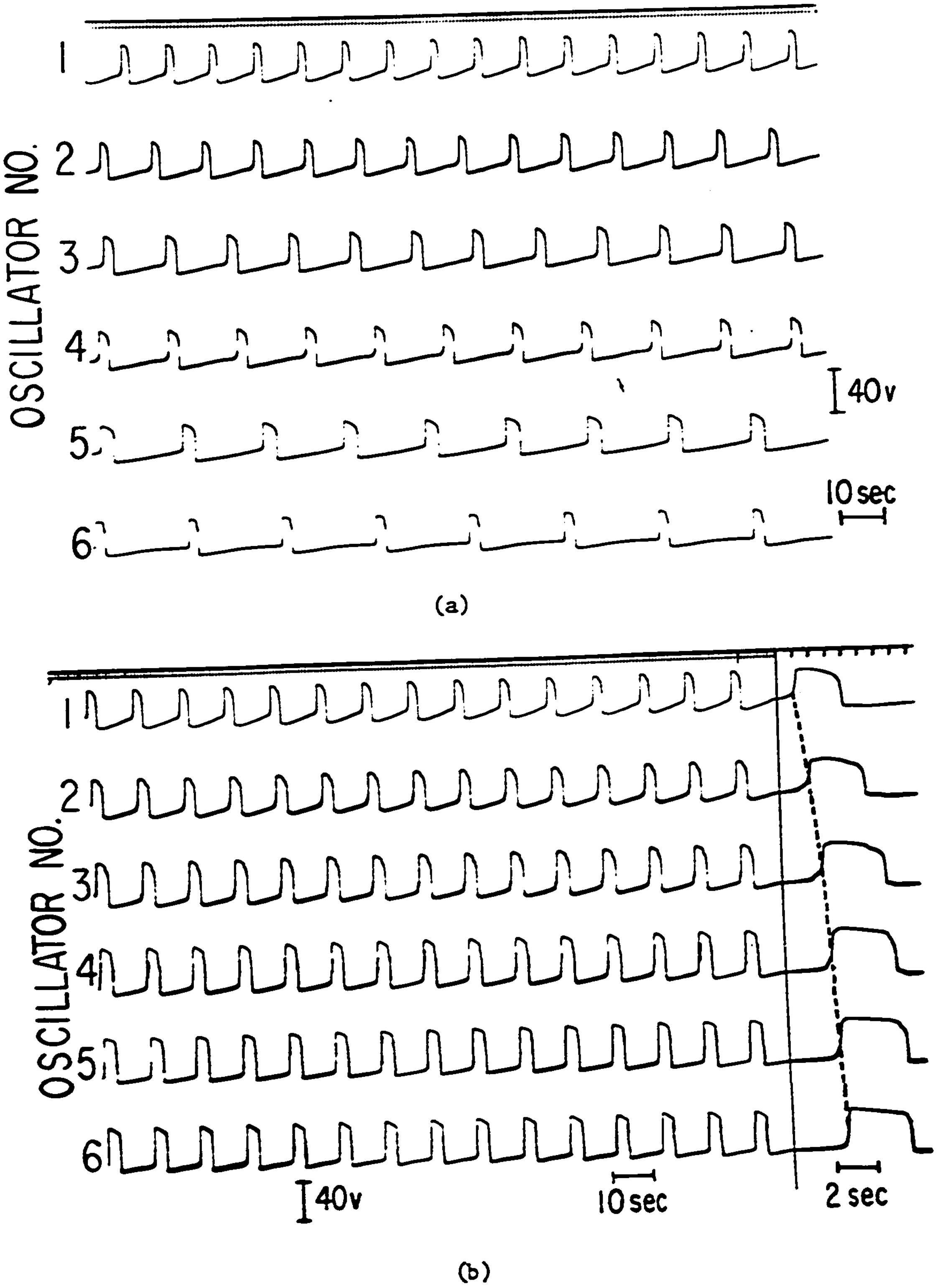

Figure 4.13

Outputs of oscillators 1 to 6 (see Figure 4.11): (a) the oscillators were uncoupled; (b) the oscillators were coupled as shown in Figure 4.11. The recording on the right side made at a faster paper speed shows the reduction in phase lags among distal oscillators.

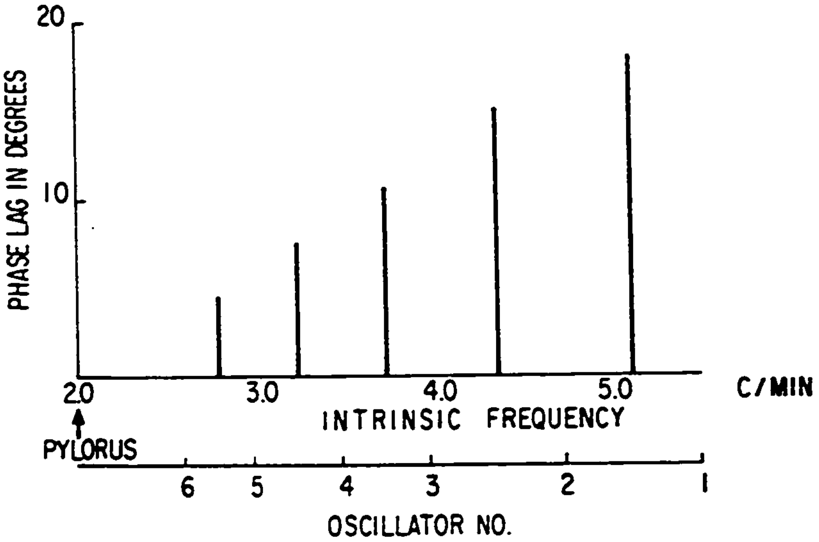

Figure 4.14

Phase lag patterns among oscillators 1 to 6, representing ECA of the greater curvature in the model.

Table 4.6

COMPLETE CIRCUMFERENTIAL CUTS IN THE GASTRIC MODEL

No.	Cut between oscillators	Proximal frequency in c/min	Distal frequency in c/min
1	5-6, 6-11	5.00	2.70
2	4-5, 10-11	5.00	2.90
3	3-4, 9-10, 10-13	5.00	3.10
4	2-3, 8-9, 10-13	5.15	3.30
5	5-11, 5-6, 10-11	5.00	2.72
6	10-13, 9-10, 4-10, 4-5	5.00	2.92
7	3-4, 3-9, 8-9, 8-13, 12-13	5.10	3.33
8	2-3, 2-8, 7-8, 7-12	5.20	3.75

4.35 Partial cuts

The results of partial cuts were similar to those obtained in the dog stomach. The results are summarized below.

1 (a) Cut between oscillators 5-6

No change in the ECA frequency was observed. The phase lag between control waves of oscillators 5 and 6 increased from 4.5° to 13.6° as a result of this cut. Before the cut the control wave of oscillator 11 lagged the control wave of oscillator 6 by 1.5°. After the cut the control wave of oscillator 11 led the control wave of oscillator 6 by 4.4°.

(b) Cut extended to 5-11

The frequency of oscillators 6 and 11 showed frequency pulling after the cut at an average frequency of 4.4 c/min (Fig. 4.15).

2 (a) Cut between oscillators 10-11

The cut had no effect on ECA frequency. All control waves remained phase locked. The phase lag between control waves of oscillators 10 and 11 increased from 7.5° before the cut to 19.5° after the cut.

(b) Cut extended to 5-11

All control waves remained phase locked without any change in ECA frequency. The phase lag between control waves of oscillators 6 and 11 increased to 13.5° from a value of 1.5° before any cut. The phase lag between control waves of oscillators 10 and 11 increased to 25.5°.

The above two cuts showed similarity with observations made in the dog stomach. The cut starting at the lesser curvature was longer than

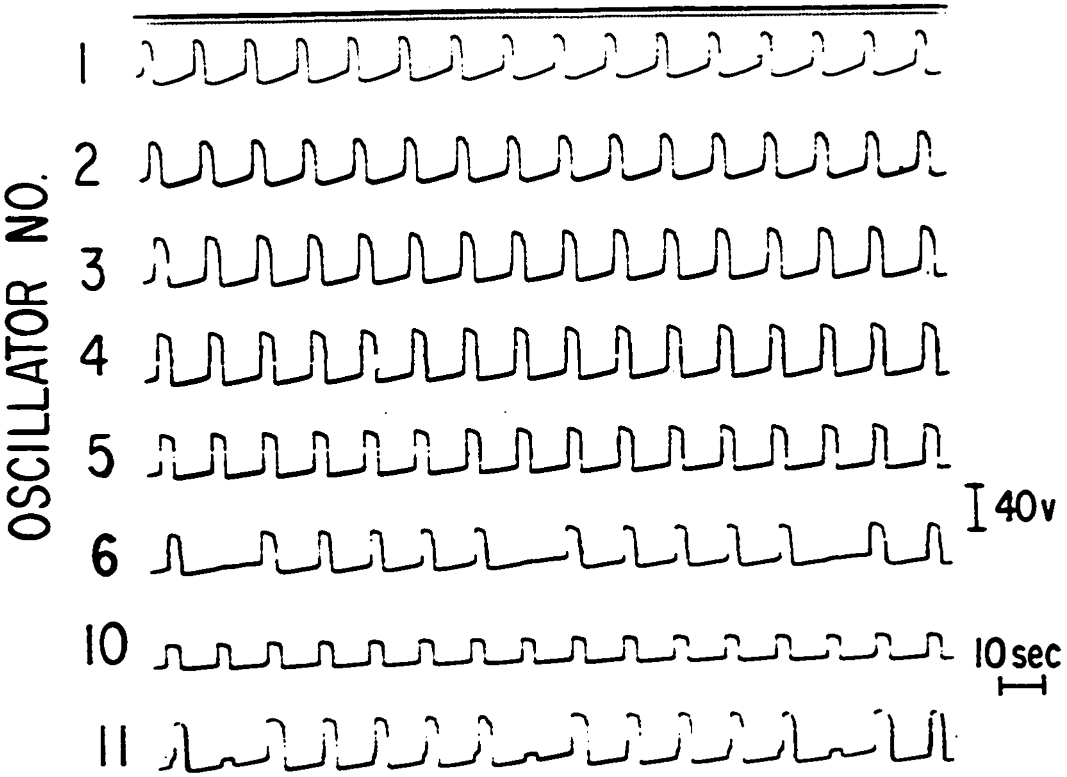

Figure 4.15

Typical recording showing the phenomenon of frequency pulling (in oscillators 6 and 11). A simulated cut (by setting the coupling factor to 0) existed between oscillators 5 to 6 and 5 to 11 (see Figure 4.11 for arrangement of oscillators).

the cut starting at the greater curvature to cause unlocking. Other cuts also showed effects similar to those observed in the dog stomach.

3 (a) Cut between oscillators 4-5

This cut caused frequency pulling in the ECA of oscillators 5, 6 and 11 at an average frequency of 3.0 c/min.

(b) Cut extended to 4-10

No further change in ECA frequency was observed.

(c) Cut extended to 9-10

The frequency of oscillator 10 also dropped to that of oscillators 5, 6 and 11 which was still unchanged.

4 (a) Cut between oscillators 13-10

All the control waves remained phase locked without any change in ECA frequency.

(b) Cut extended to 9-10

The control waves remained phase locked without any change in ECA frequency.

(c) Cut extended to 4-10

There was still no effect on ECA frequency or the phase locking of control waves. The phase lag between the control waves of oscillators 5 and 10 increased from a value of 1.5° before any cut to a value of 25.5° after the cut.

5) Cut between oscillators 3-4

The frequency of oscillators 4, 5, 6, 9, 10 and 11 dropped to 3.3 c/min.

6 (a) Cut between oscillators 12-13

This cut had no effect on the ECA frequency or the phase locking of control waves.

(b) Cut extended to 8-13

All control waves remained phase locked without any change of ECA frequency.

(c) Cut extended to 8-9

The frequency of oscillators 4, 5, 6, 9, 10, 11 and 13 dropped to 4.25 c/min, while that of others remained unaffected.

7 (a) Cut between oscillators 5-6

No change in ECA frequency or the phase locking of waves was observed.

(b) Another cut added between oscillators 10-13

Still no change in ECA frequency or the phase locking of waves was observed.

(c) Cut in 7 (b) extended to 9-10

All control waves remained phase locked without any change in ECA frequency.

(d) Another cut added between oscillators 3-4

The frequency of oscillators 4, 5, 6, 10 and 11 dropped to a value of 3.15 c/min. No change was observed in the frequency of other oscillators.

(e) Another cut added between oscillators 12-7 and 8-7

The frequency of oscillators 1, 2, 3 and 7 was 5.2 c/min. The frequency of other oscillators was 3.30 c/min.

4.36 Premature control potentials

Premature control potentials were produced by applying a pulse of duration 1 second and amplitude 60 V at the input of an oscillator. The pulse was applied at different phases of the control wave cycle. The earliest that a PCP could be produced was at 75% of the wave cycle. Time was measured from the positive going zero of the control wave and expressed as a percentage of the time period. Premature control potentials were produced in oscillators 2-5 and 10-13. The results of producing premature control potentials at the output of oscillator 4 are summarized in Table 4.7.

When the pulse was applied at an early phase of the cycle, i.e., up to 6 sec (50%), no effect on control waves was observed. When the pulse was applied at 7 and 8 sec (58.3% and 66.6%), it caused unlocking by lengthening the time period. When the pulse was applied at 9 and 10 sec (75% and 83.3%), a PCP was produced which propagated proximally, distally and sidewise. When the pulse was applied at 11 sec (91.6%), the PCP produced propagated distally and sidewise. Similar results were obtained when pulses were applied at the inputs of oscillators 2, 3 and 5.

Premature control potentials produced at the output of oscillator 10 did not propagate in any direction. Pulses applied at the inputs of oscillators 12 and 13, which lengthened its time period (see Fig. 4.17 for oscillator 4) did not affect the time periods of other oscillators. Premature control potentials produced at the output of oscillator 12 propagated to oscillators 7 and 1. These premature control potentials were produced by applying pulses at 10 and 11 sec (83.3% and 91.6%). Similarly, the premature control potentials produced at the output of oscillator 13 (pulses applied at 10 and 11 sec) propagated to oscillators 12, 8, 7, 2 and 1.

4.37 Effect of response activity on control activity

The response activity in the antrum of dog consists of bursts of

Table 4.7

PREMATURE CONTROL POTENTIALS IN THE GASTRIC MODEL

Time at which pulse applied to oscillator 4	PCP produced or not	Remarks
1-6 sec	no	No effect on control waves (Fig. 4.16)
7 sec	no	Control waves of oscillators 3-6, 9-11 and 13 had a longer time period than usual and were unlocked from proximal waves (Fig. 4.17)
8 sec	no	Same as for 7 sec
9 sec	yes	The PCP propagated proximally up to oscillator 2, distally up to oscillator 6 and sidewise to oscillators 9, 10 and 11 (Fig. 4.18)
10 sec	yes	Same as for 9 sec
11 sec	yes	No proximal propagation. The PCP propagated distally up to oscillator 6 and sidewise to oscillators 10 and 11 (Fig. 4.19)

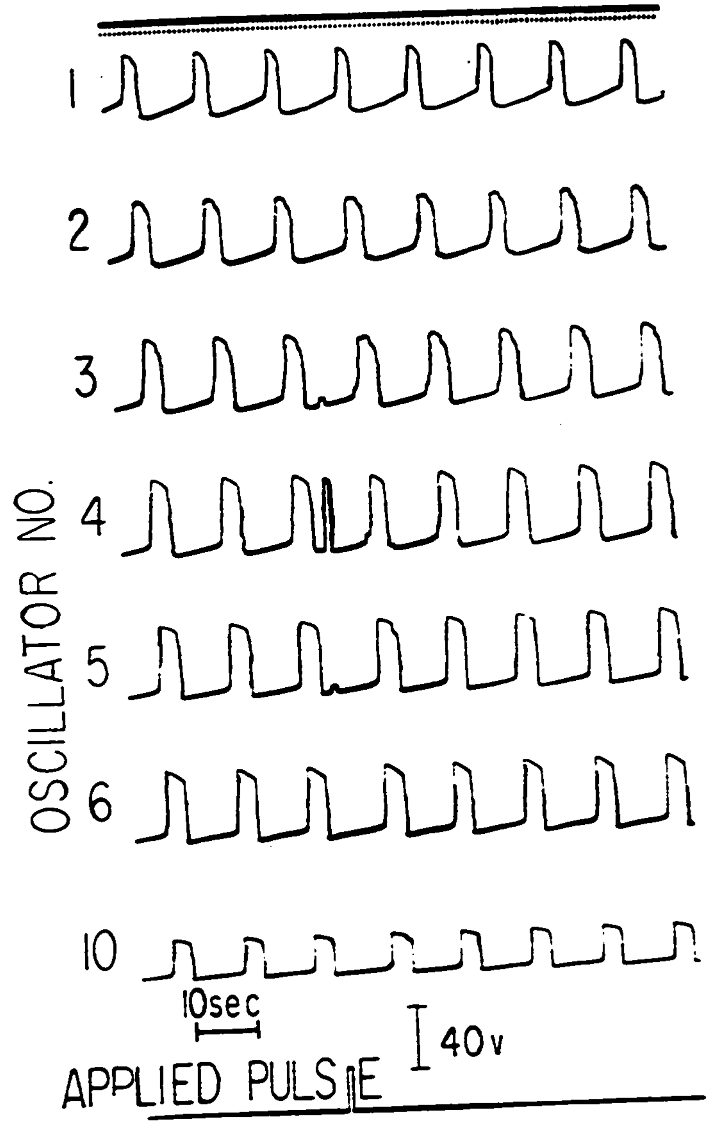

Figure 4.16

Recording showing the application of pulse to the input of oscillator 4 at 4.0 sec. No PCP was produced, and no unlocking of control waves occurred. The pulse amplitude was 60 V and the pulse width 1.0 sec. The voltage scale in recordings showing applied pulse or pulses does not apply to the amplitude of pulses.

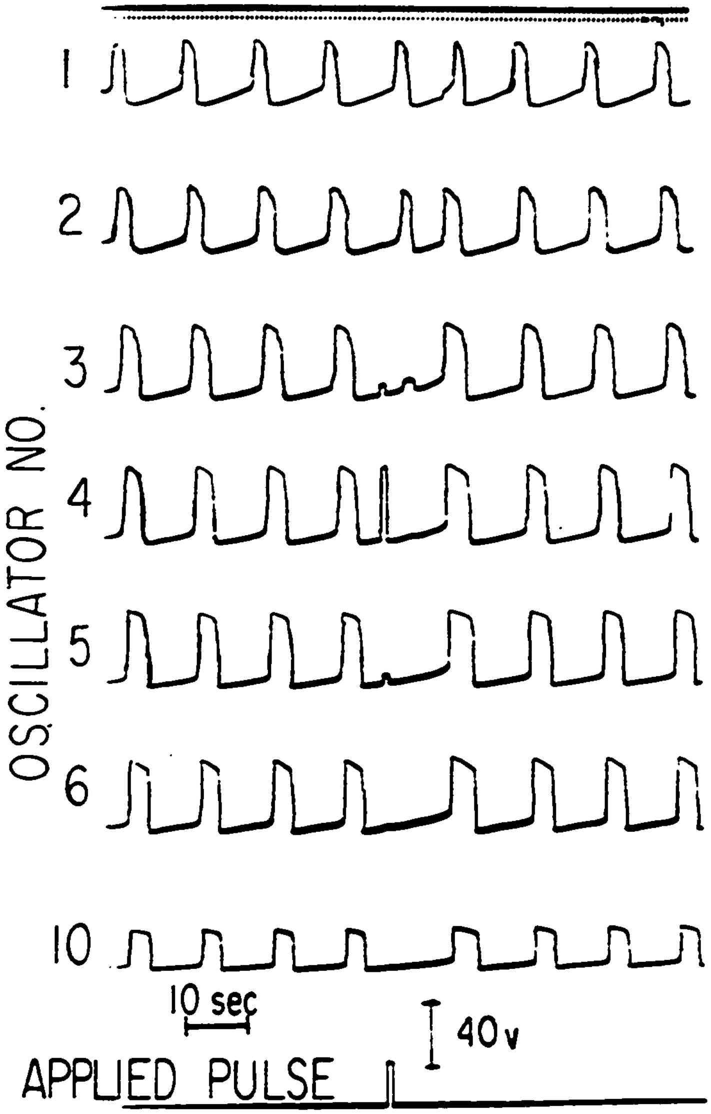

Figure 4.17

Recording showing the application of pulse to the input of oscillator 4 at 7.0 sec. The control waves of oscillators 3 to 6 had a longer time period after the application of the pulse, and were unlocked from the control waves of oscillators 1 and 2. The pulse amplitude was 60 V, and the pulse width 1.0 sec.

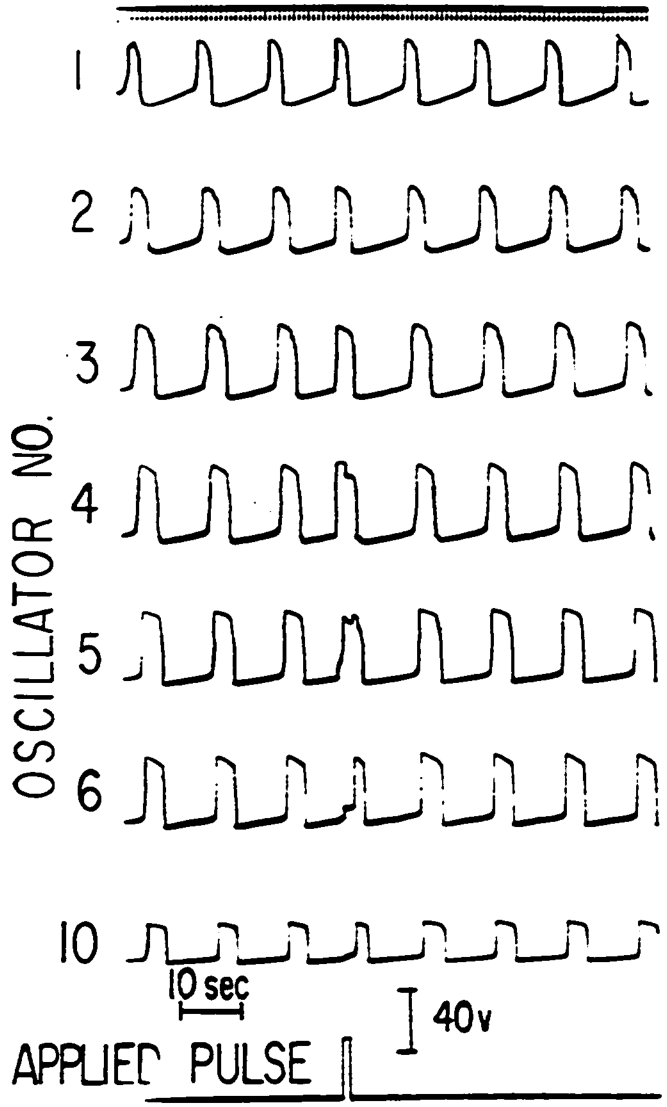

Figure 4.18

Recording showing the application of pulse to the input of oscillator 4 at 9.0 sec. A PCP was produced which propagated proximally up to oscillator 2 and distally up to oscillator 6. It also propagated sidewise to oscillators 9, 10 and 11 (not shown in this recording). The pulse amplitude was 60 V, and the pulse width 1.0 sec.

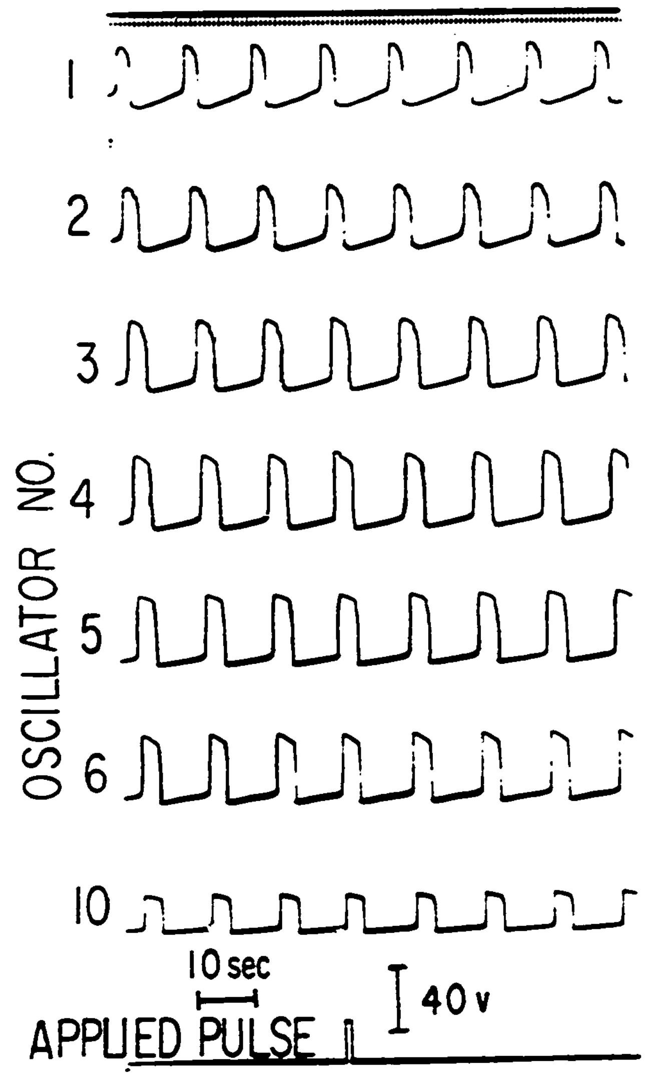

Figure 4.19

Recording showing the application of pulse to the input of oscillator 4 at 11.0 sec. A PCP was produced which propagated distally up to oscillator 6. It did not propagate proximally. The PCP propagated sidewise to oscillators 10 and 11 (not shown in this recording). The pulse amplitude was 60 V, and the pulse width 1.0 sec.

spikes, while that in the body consists of sustained depolarizations. The effect of response activity on the control activity was studied in the model by applying bursts of pulses (10 c/sec and pulse duration 30 msec) at the input of an oscillator. The bursts of pulses were applied at different phases of the ECA cycle in oscillator 4. It had no effect on control waves. Figure 4.20 shows the case when response activity was applied at 3 sec. The duration of response activity was 2.0 seconds. The response activity in the animal occurs soon after the occurrence of a control potential.

4.38 Refractoriness of oscillators

The refractoriness and threshold properties of the oscillators were studied by applying a single pulse of width 0.5 sec at various phases of the control wave cycle. The following observations were made:

a) At every phase of the cycle (after repolarization) a threshold value of the input pulse amplitude existed that could produce an output response of amplitude comparable (within 10%) with a normal control potential.

b) In the early part of the control wave cycle, the output response lasted only as long as the input pulse (Fig. 4.21). This was not considered to be a premature control potential. This part of the cycle was called absolutely refractory. In the later part of the wave cycle, the output response had the same shape and width as a normal control potential. This output response was called premature control potential, and this part of the cycle relatively refractory. The transition from the absolutely refractory part to the relatively refractory part was gradual (transition period lasted for 1-2 sec). The relatively refractory period was considered to start when the

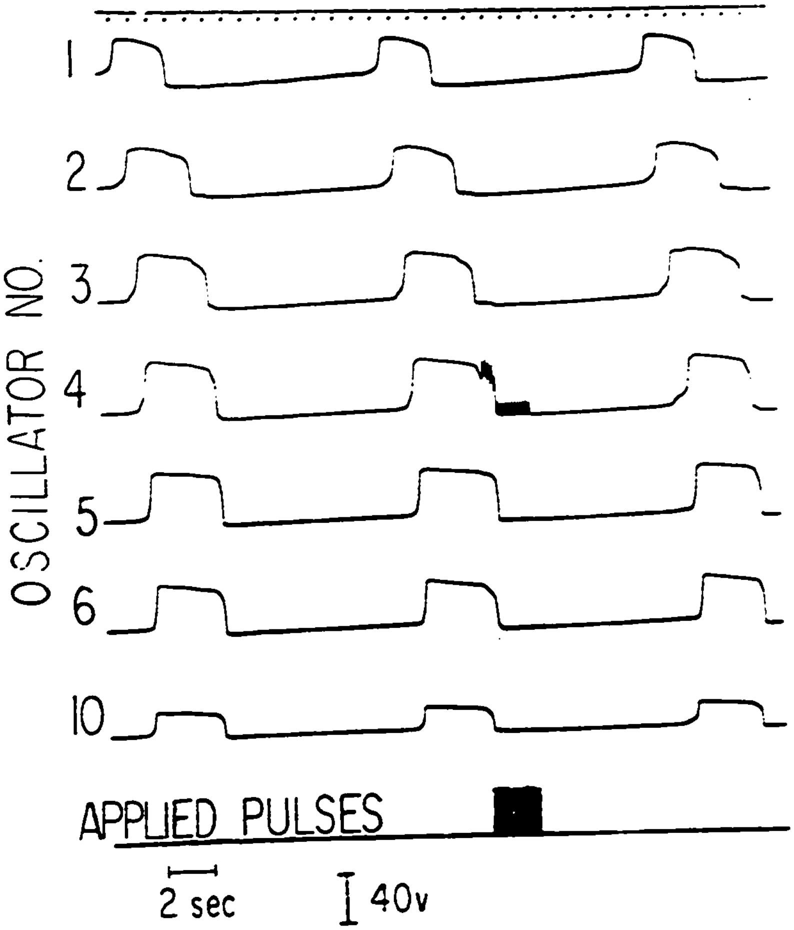

Figure 4.20

Recording showing the effect of applying a burst of pulses to the input of oscillator 4. The pulses were applied at 3.0 sec, and they lasted for 2.0 sec. The application of pulses which simulated ERA had no effect on ECA. The amplitude of pulses was 80 V, the pulse frequency 10 c/sec, and the pulse width 30 msec.

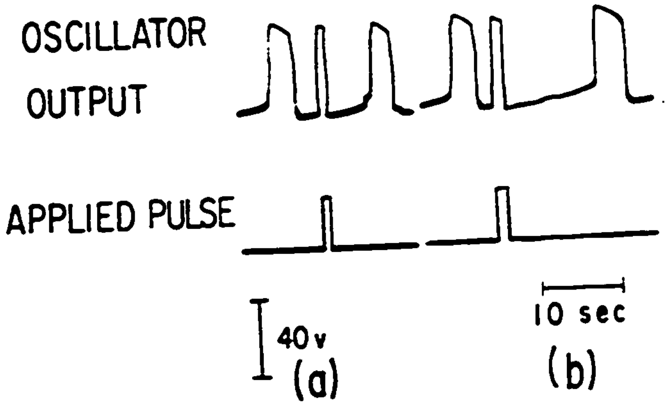

Figure 4.21

Recording showing the application of pulse in the absolutely refractory part of the wave cycle. The width of output response was nearly equal to the width of applied pulse: (a) pulse width was 1.0 sec; (b) pulse width was 1.5 sec.

width of output response was twice the width of the applied pulse, which was 0.5 sec. This definition was chosen for convenience and was arbitrary otherwise.

c) The phenomenon of the production of an output response was not completely of the all-or-none type. It was possible to produce output responses of intermediate amplitudes (i.e., between no output and an output of amplitude equal to the amplitude of a normal control potential) with a fine control of input pulse amplitude.

The refractory curve of an oscillator (of frequency 3.5 c/min) showing threshold values at various phases of the cycle is shown in Figure 4.22. The absolutely refractory part of the period is shown by the broken line, and the relatively refractory part by the continuous line. The abscissa shows the phase of the cycle expressed as a percentage of the total time period.

When an oscillator was coupled with another, its refractoriness increased. Figure 4.23 shows the refractory curves when different numbers of oscillators (all at 3.5 c/min) were coupled with a coupling factor of 0.3. Curve 1 shows the refractory curve for the uncoupled oscillator. Curves 2, 3 and 4 show the refractory curves for the arrangement of oscillators shown in Figures 4.24 (a), (b) and (c) respectively. When the oscillators are coupled, not only the threshold values increase, but also the absolutely refractory part of the period is lengthened. Increasing the value of the coupling factor had similar effects. The refractory curves for the arrangement of oscillators shown in Figure 4.24 (c), but with different coupling factors, are shown in Figure 4.25. Curves 1, 2 and 3 show the threshold values when coupling factors were 0.1, 0.3 and 0.5, respectively.

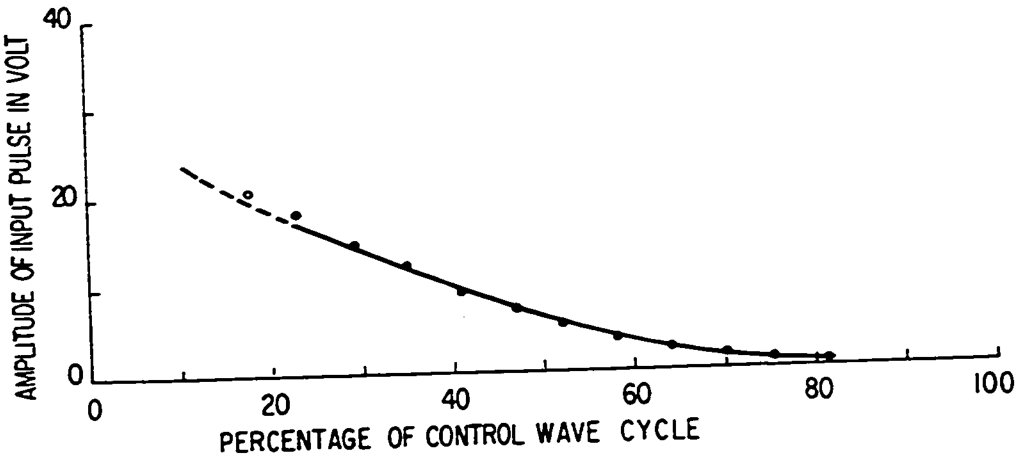

Figure 4.22

The refractory curve of an oscillator of frequency 3.5 c/min, showing threshold values for the initiation of a PCP at various phases of the wave cycle. The broken line shows the absolutely refractory part, and the continuous line shows the relatively refractory part. The pulse width was 0.5 sec.

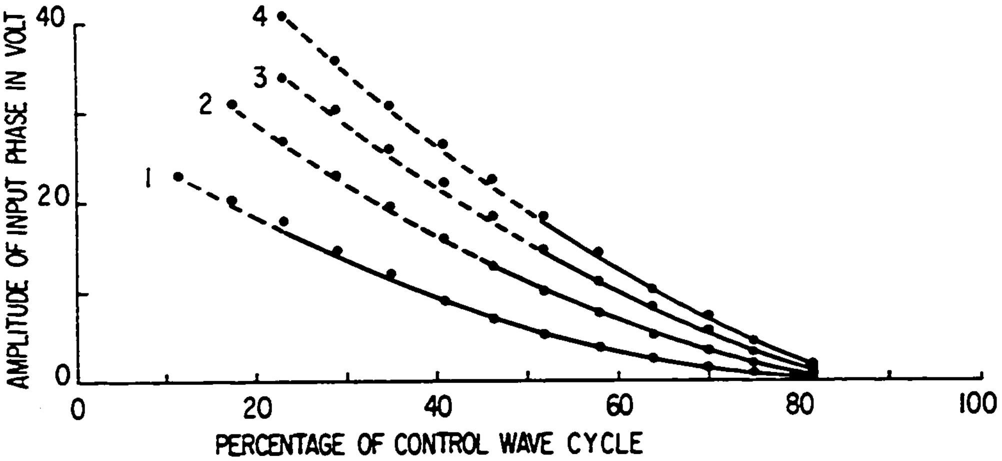

Figure 4.23

Effect of coupling to other oscillators on the refractoriness of oscillator 1. All coupling factors were 0.3. Curve 1 shows the refractory curve of oscillator 1 alone, while curves 2, 3 and 4 show the refractory curves for the arrangement of oscillators in Figures 4.24 (a), (b) and (c), respectively. The broken lines show the absolutely refractory parts, and the continuous lines show the relatively refractory parts. The pulse width was 0.5 sec.

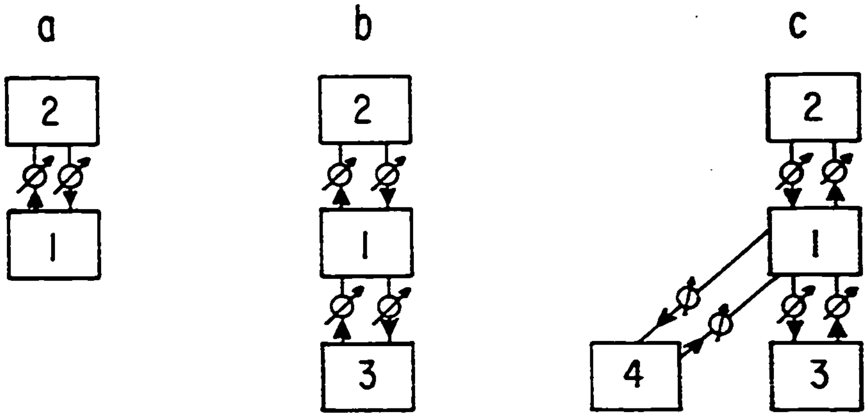

Figure 4.24

Diagram showing the arrangement of oscillators referred to in Figure 4.23. The intrinsic frequencies of all oscillators were 3.5 c/min.

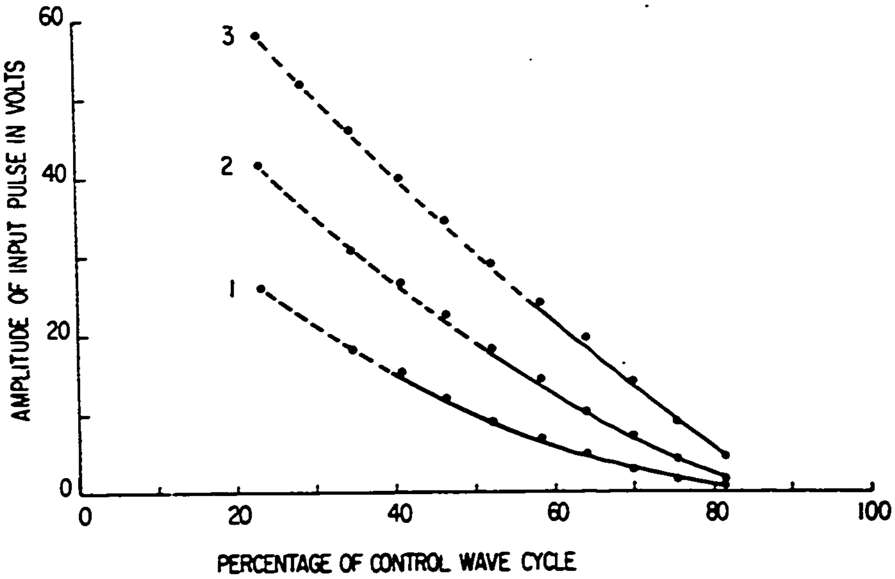

Figure 4.25

Refractory curves of oscillator 1 for different coupling factors. Oscillator 1 was coupled with oscillators 2, 3 and 4 as shown in Figure 4.24 (c). Coupling factors were 0.1, 0.3 and 0.5 for curves 1, 2 and 3, respectively. Broken lines show the absolutely refractory parts, and the continuous lines show the relatively refractory parts. The pulse width was 0.5 sec.

The threshold values and the length of absolutely refractory part reduced if the input pulse was applied simultaneously at the inputs of several oscillators instead of at the input of one oscillator. Figure 4.26 shows the threshold values when the pulse was applied to oscillator 1 of Figure 4.24 (c) (curve 1), and when it was applied to oscillators 1, 2 and 3 of Figure 4.24 (c) (curve 2). The coupling factor was 0.5 for all oscillators.

4.39 Frequency of coupled oscillators

In the stomach model, as for the second intestinal model, the resultant frequency of two bidirectionally coupled relaxation oscillators depended on the parameters of oscillators. The effect of varying b_0 on the resultant frequency of two coupled oscillators was studied. The results are shown in Figure 4.27. The frequency of oscillator 1 was kept at 5.5 c/min. Curves 1, 2 and 3 show the resultant frequencies when the frequency of oscillator 2 was 4.5, 5.0 and 5.5 c/min. It is seen that the resultant frequency increased as the value of b_0 was increased. Also, for a given value of b_0, the resultant frequency was higher for a smaller difference of intrinsic frequency between the two oscillators. The coupling factor was kept constant at 0.1.

4.40 Interaction between duodenal and antral electrical control activities

The interaction between the duodenal and the antral control activities was studied by coupling the two models as shown in Figure 4.28. The second model (see section 3.31) was used to represent the duodenal ECA. Four oscillators were used (oscillators 14 to 17). The outputs of these oscillators were phase locked and had a frequency of 18.7 c/min, just like

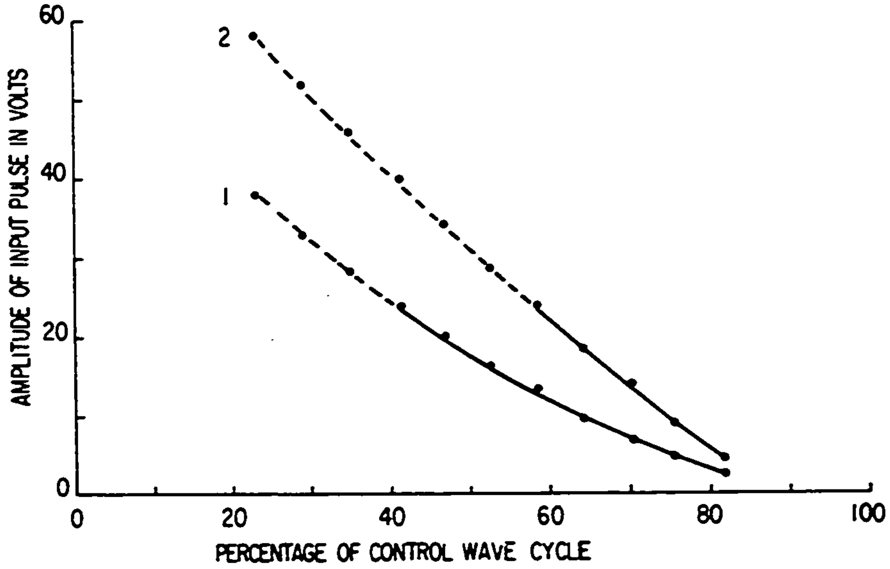

Figure 4.26

Effect of applying pulse to more than one oscillator on the refractoriness of oscillator 1. Oscillator 1 was coupled with oscillators 2, 3 and 4 as shown in Figure 4.24 (c). Curve 1 shows the refractory curve when the pulse was applied to the input of oscillator 1 only. Curve 2 shows the refractory curve when the pulse was applied simultaneously to the inputs of oscillators 1, 2 and 3. The broken lines show the absolutely refractory parts, and the continuous lines show the relatively refractory parts. The pulse width was 0.5 sec. The coupling factor was 0.5 for all oscillators.

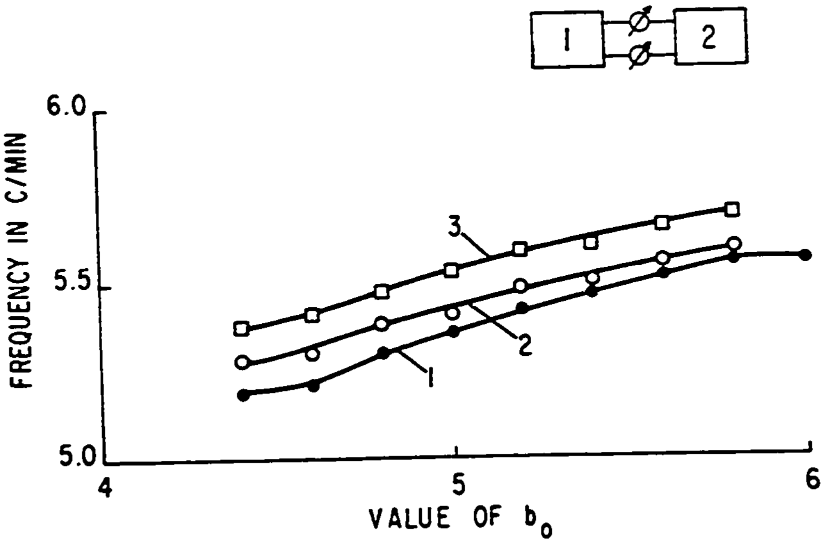

Figure 4.27

Diagram showing the effect of varying parameter b_0 on the resultant frequency of two bidirectionally coupled relaxation oscillators. The coupling factor was 0.1. The frequency of one of the oscillators was kept constant at 5.5 c/min, while that of the other was kept at 4.5, 5.0 and 5.5 c/min (curves 1, 2 and 3, respectively).

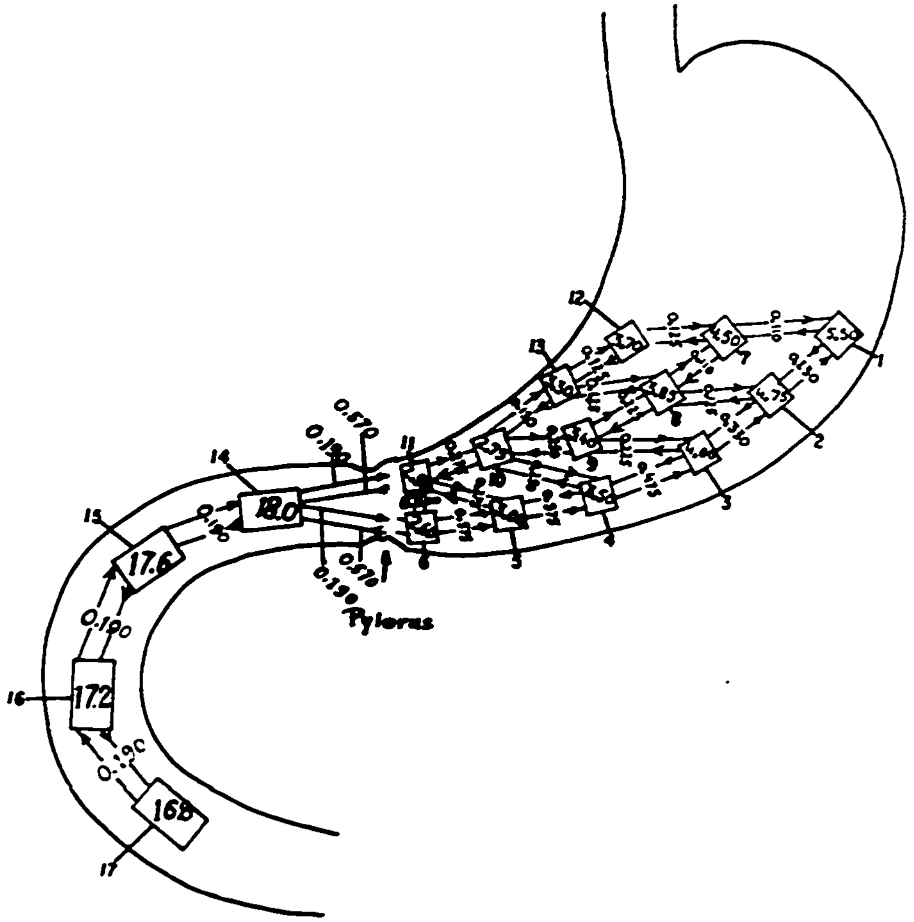
12
13
5.50
4.50
4.75
0.130
0.350
1
2
3
4
5
6
7
8
9
10
11
0.570
0.190
18.0
0.570
0.190
Pylorus
14
15
17.6
0.190
0.190
16
17.2
0.190
16.8
17

Figure 4.28

Diagram showing the coupled gastric and second intestinal ECA models. The intrinsic frequencies and the coupling factors in the two models were the same as described before (Figures 3.10 and 4.11).

the complete intestinal model. The intrinsic frequencies of oscillators 14 to 17 were 18.0, 17.6, 17.2 and 16.8 c/min, respectively. The coupling factor in the intestine was 0.190 as before.

The ratio of the amplitudes of control waves in the antrum and in the duodenum of dog was of the order of 3:1 by our recording technique, as well as by intracellular electrodes (17). However, in the computer models, the amplitude of the control waves in the antrum and the duodenum was the same. In order to simulate a situation in the model similar to that in the animal, the coupling factor from the stomach to the intestine (0.570) was always kept 3 times the coupling factor from intestine to the stomach (0.190). This simulated the condition of equal forward and backward coupling as discussed in Chapter III.

The following effects of antral ECA on the duodenal ECA were observed in the model:

1) It made the control waves of the two proximal oscillators irregular in shape, time period and the amplitude of oscillation. The effects were most marked in the most proximal duodenal oscillator, less in the next distal oscillator, and were absent in the subsequent ones (Fig. 4.29). When an antral control wave occurred, the amplitude of oscillation of the control wave of the most proximal oscillator increased (Fig. 4.30). The above effects increased with an increase in the coupling factor between the gastric and the intestinal models.
2) The outputs of the third and the fourth intestinal oscillators were phase locked. The average frequency of these oscillators was constant at 18.1 c/min. These oscillators formed the intestinal frequency plateau. The output of the second intestinal oscillator remained phase locked with those of the third and the fourth most of the time,

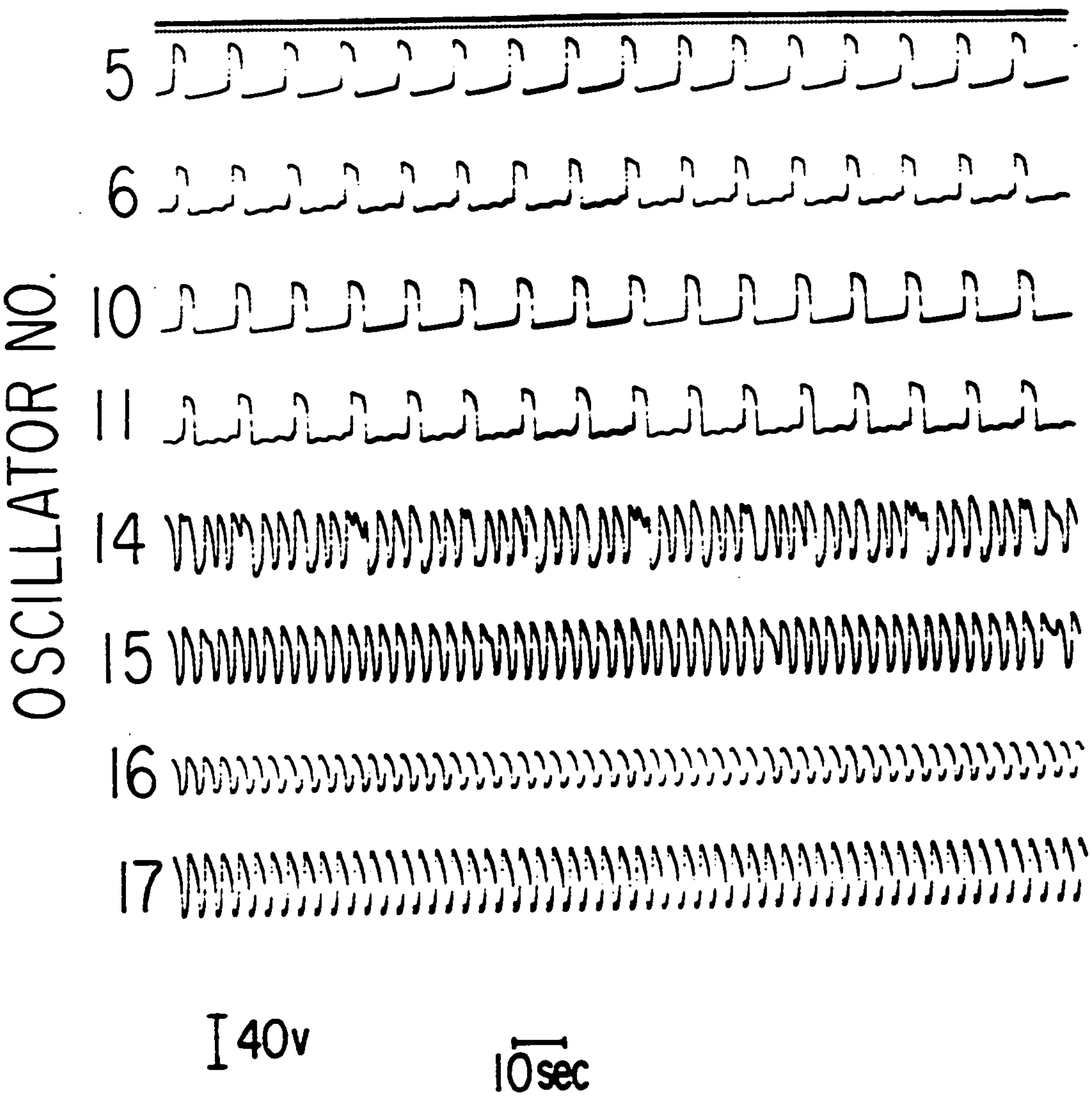

Figure 4.29

Recording of the outputs of oscillators 5, 6, 10, 11 and 14 to 17 when the gastric and the second intestinal models were coupled. Labelling of oscillators as in Figure 4.28.

and occasionally became unlocked. The average frequency of this oscillator varied between 17.6 c/min and 18.1 c/min. The output of the first intestinal oscillator was not phase locked with that of any other intestinal oscillator. The average frequency of this oscillator varied between 17.0 and 18.0 c/min. Thus the first and the second oscillators were not in the frequency plateau.

The plateau frequency, when the intestinal and the gastric models were coupled, was 18.1 c/min as compared to 18.7 c/min in the uncoupled intestinal model. This was due to the fact that when the two models were coupled, the first two intestinal oscillators were affected by the gastric electrical activity and, therefore, they were not in the frequency plateau. The most proximal oscillator that was in the frequency plateau had an intrinsic frequency of 17.2 c/min instead of 18.0 c/min in the uncoupled intestinal model. The plateau frequency was, therefore, proportionally smaller. A similar situation is not likely in the animal because the effect of the antral activity is observed for only a few mm (less than 1 cm) from the pylorus (51, 53). Because of a small gradient of intrinsic frequency in this region (see section 3.21), there is not likely to be much difference between the intrinsic frequency at the pylorus and that at 1 cm distal to it. This means that in the dog intestine the most proximal oscillator in the frequency plateau would have nearly the same intrinsic frequency as that of the pyloric region on the intestinal side.

3) There was no harmonic entrainment of stomach oscillators and the oscillators in the intestinal frequency plateau. This means that the frequency of the two can vary independently of each other. The first oscillator was, however, harmonically entrained with the gastric ECA

(7:2).

4) When the first duodenal oscillator was uncoupled from the other duodenal oscillators, it was harmonically entrained with the gastric ECA at 3:1. The increase in its amplitude of oscillation corresponding to a control wave in the antrum was more than that prior to uncoupling (Fig. 4.30). The average frequency of this oscillator was 15.0 c/min. The frequency of the other three oscillators, the outputs of which were phase locked, was 18.4 c/min.

5) When the second duodenal oscillator was uncoupled from the third but the first two were coupled, the variations in the time period, etc., of the second oscillator were also marked. Both oscillators were harmonically entrained with the gastric ECA at 3:1. The plateau frequency was 18.0 c/min.

The effect of duodenal ECA on the antral ECA was to produce a ripple in the control wave of two oscillators (oscillators 6 and 11) that were nearest to the pylorus. There was no effect on the gastric ECA frequency or on the phase relationships. However, when oscillators 5 and 10 were uncoupled from oscillators 6 and 11 to simulate a complete circumferential cut, the duodenal ECA raised the ECA frequency of the isolated antral area. Figure 4.31 shows the control waves of oscillators 6, 11, 14 and 15 after the complete circumferential cut mentioned above. The frequency of oscillators 6 and 11 was 4.4 c/min. Figure 4.32 shows the control waves of the same oscillators as above, but oscillators 6 and 11 were also uncoupled from oscillator 14. The frequency of oscillators 6 and 11 dropped to 2.7 c/min. The rise in frequency of the isolated antrum depended on the coupling factor between the gastric and the intestinal models, as shown in Table 4.8.

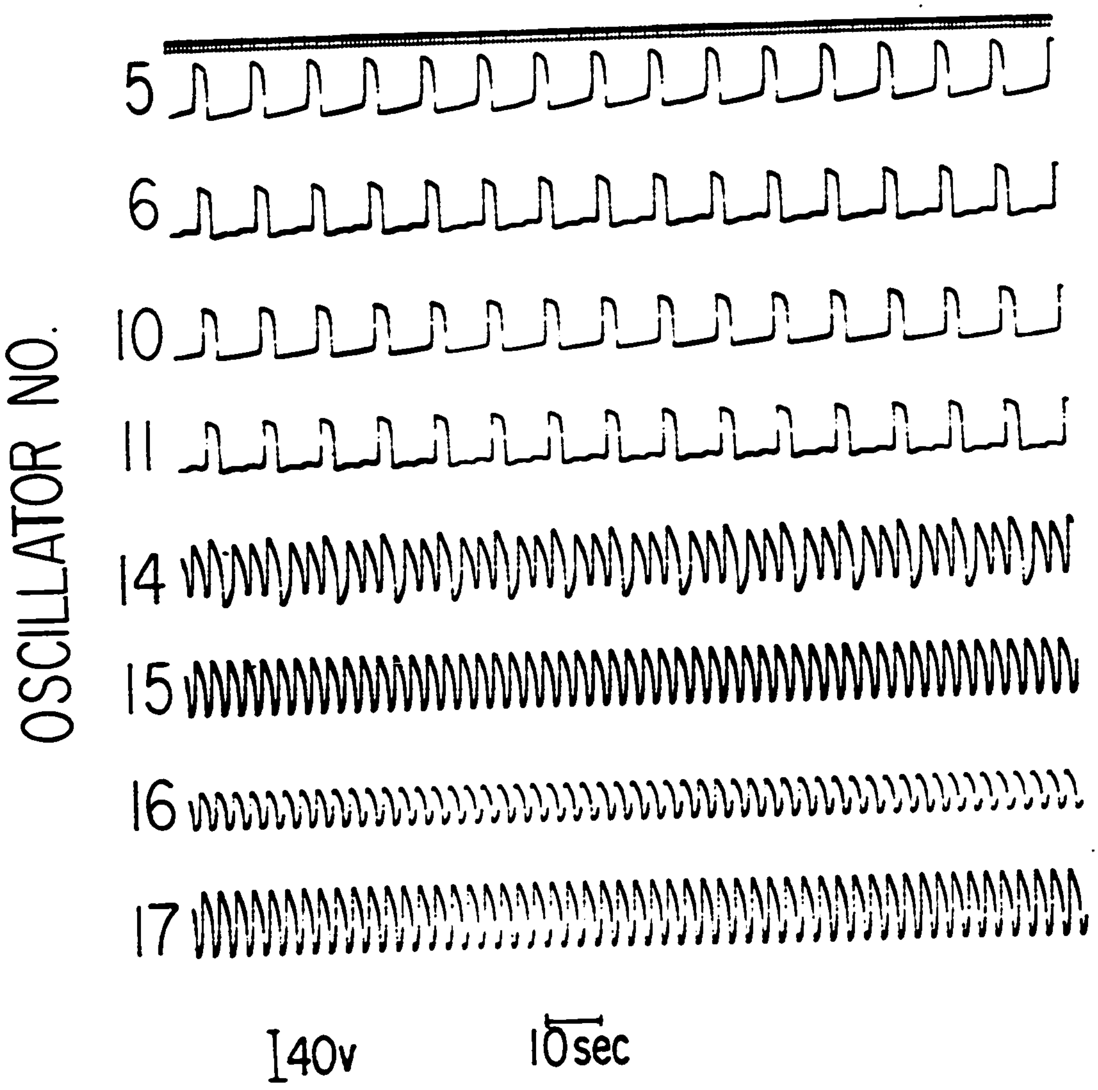

Figure 4.30

Recording of the outputs of oscillators 5, 6, 10, 11 and 14 to 17 as described in Figure 4.29, but oscillator 14 was uncoupled from oscillator 15. Labelling of oscillators as in Figure 4.28.

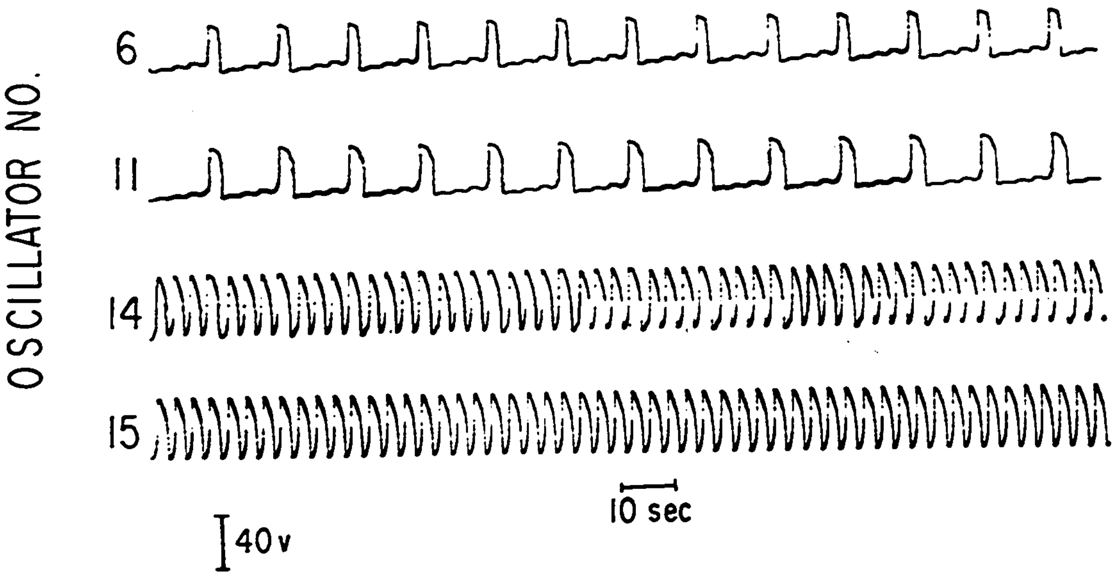

Figure 4.31

Recording of the outputs of oscillators 6, 11, 14 and 15 when the gastric and the second intestinal models were coupled, but a complete simulated circumferential cut existed between oscillators 5-6, 5-11, and 10-11. Labelling of oscillators as in Figure 4.28.

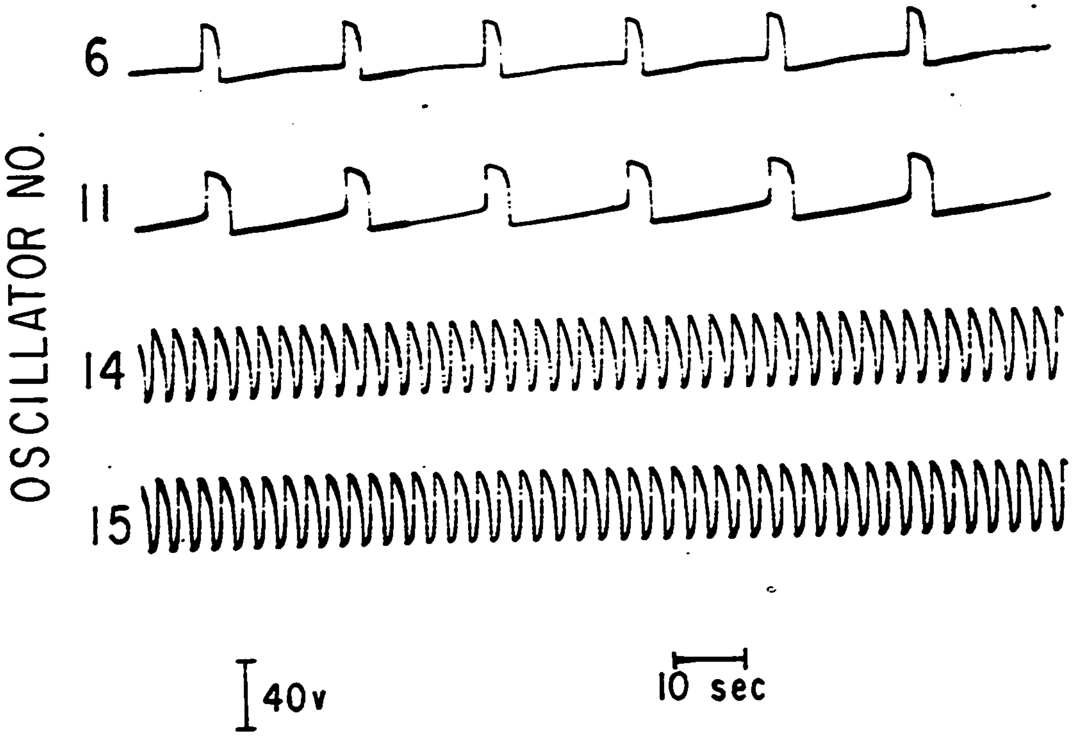

Figure 4.32

Recording of the outputs of oscillators 6, 11, 14 and 15 as described in Figure 4.31, but oscillator 14 was uncoupled from oscillators 6 and 11. Labelling of oscillators as in Figure 4.28.

Table 4.8

EFFECT OF THE COUPLING FACTOR BETWEEN GASTRIC AND INTESTINAL MODELS ON THE FREQUENCY OF A SMALL ISOLATED SEGMENT OF ANTRUM

Coupling factor from the gastric to the intestinal model	Coupling factor from the intestinal to the gastric model	Frequency of oscillators 6 and 11
0.570	0.190	4.4 c/min
0.450	0.150	3.1 c/min
0.270	0.090	2.9 c/min
0.0	0.0	2.7 c/min

4.4 Discussion

This study showed that the gastric ECA behaved like one frequency plateau. This result was in agreement with those of others (16, 48-50). A marked intrinsic frequency gradient was found along the axis of the stomach and a slight intrinsic frequency gradient along the circumference. The site of the highest intrinsic frequency was found to be on the greater curvature in all dogs. This site had the most leading control wave in the stomach. This site has been called the pacemaker by other investigators (48-50). It has been referred to as the most proximal site of electrical control activity (MPSECA) in this thesis. The distance of this site from the pylorus varied in different dogs, but was close to two-thirds of the total length of the stomach along the greater curvature, as reported by Kelly _et al._ (49).

In the stomach, phase lags existed in the longitudinal as well as in the transverse directions. For this reason it was necessary to use an array of oscillators rather than a chain to model the gastric ECA. The model also showed phase lags in both directions. Although the pattern of phase lag in the model and in the dog stomach was similar, i.e., the phase lag/cm reduced distally, yet there was a significant difference between the total amounts of phase lags between the MPSECA and the pylorus in the two cases. The total phase difference between the MPSECA and the pylorus in 5 dogs was 375°, 655°, 932°, 456° and 687°. Thus it varied over a wide range. In the model, the total phase lag between oscillator 1 and oscillator 6 was 55.5°. The difference between the two was due to the much smaller number of oscillators used in the model than would exist in the animal stomach.

To simulate the pattern of phase lag in the dog stomach, i.e., more phase lag/cm in the proximal part and less in the distal one, the coupling factor among oscillators had to be kept less in the proximal part of the array than that in the distal part. Attempt was made to determine if variation in any oscillator parameter had an effect on phase lag. The phase lag between two bidirectionally coupled oscillators seemed to be independent of variation in parameters within a small range. Larger variations in parameters could not be tried, since they affected other properties of oscillators and also their waveshape.

The results of partial cuts indicated that the longitudinal coupling was stronger along the greater curvature than on the midline or near the lesser curvature. This was due to the fact that the minimum width of muscle layers necessary for the entrainment of distal oscillators was smaller on the greater curvature side than on the lesser curvature side. For this reason, the longitudinal coupling factor was kept less on the lesser curvature side than that on the greater curvature side in the model. The transverse coupling factors were chosen to get the results of partial cuts in the model similar to those obtained in the dog stomach. The transverse coupling factor reduced proximally and in the direction of the lesser curvature.

The dorsal and the ventral sides showed identical electrical control activity patterns. No change in the ECA of the ventral side was observed when the dorsal side was isolated from it. This showed that in the intact stomach the ECA on one side was not affected by the ECA of the other side. Because of the small number of oscillators available, only one side was simulated in the model.

In the body of the stomach, ECA was very weak or did not exist near the lesser curvature. However, when acetylcholine was injected intra-arterially in this region, one or two control potentials could be recorded immediately after the injection. It is probable that the cells in this region are potential oscillators but are not self-excitable. They oscillate only when stimulated externally. Under normal conditions in the fasted dogs, the transverse coupling is not strong enough for the oscillators on the midline to excite them.

In the antrum, the ECA could be recorded all around the circumference. The stomach in this part behaved much like the duodenum except that a phase lag existed along the circumference.

In the model described above, oblique instead of horizontal coupling was used in the transverse direction. For instance, oscillator 2 was coupled to oscillator 8 instead of to oscillator 7. The reason for this was that the longitudinal muscle layers in the dog stomach are also oriented in a similar manner (50). A model with horizontal coupling was also tried, and it gave similar results. This suggested that determination of the exact direction of the transverse coupling was not critical for the model.

The muscular coat of the stomach consists essentially of an outer longitudinal and an inner circular layer of smooth muscle fibres. To these layers are added oblique fibres over the body of the stomach (57). The oblique layer is adjacent to submucosa. It is generally agreed that the ECA is generated in the longitudinal muscle layer. Very little work has so far been done to determine the electrical activity of the oblique and circular muscle layers, or the role that they might have in the spread of the ECA of the longitudinal muscle layer. The effects of the electrical activity of these muscle layers on the ECA of the longitudinal muscle layer were, therefore, not included in the model. However, since the model simulated all the characteristics of the dog stomach, it is possible that the electrical activity of these muscle layers does not affect the ECA of the longitudinal muscle layer in any significant manner. A possible role of these muscle layers is discussed in the sixth chapter.

The earliest that a premature control potential could be produced in the dog stomach was at 41.7%, while in the model it was at 75%. The difference could be due to the fact that when acetylcholine was injected, it perfused an area 1-2 cm in length and 2-3 cm in width. In doing so, it is possible that it would have excited more than one oscillator simultaneously, and hence the threshold value for excitation of these oscillators reduced. A similar observation was made in the model when the input pulse was applied to more than one oscillator simultaneously.

The propagation of premature control potentials in the proximal and in the distal directions depended on the time of their occurrence. This could be explained on the basis of refractory curves drawn for the oscillators in the model. If a PCP occurred early in the cycle (shown by 1 in Fig. 4.33), the proximal oscillators would be in a less refractory state than the distal oscillators because of their leading control waves. It would, therefore, be possible for the PCP to propagate proximally until it arrives at an oscillator which has produced a normal control potential and is in an absolutely refractory state. Further propagation would be halted. The distal oscillators would at the time of initiation of the PCP be in a relatively more refractory state due to their lagging control waves. They, therefore, would not initiate a premature control potential. Instead, their time period would be lengthened, as seen in Figure 4.10. If a PCP occurred in the later part of the cycle (shown by (2) in Fig. 4.33), the proximal oscillators would have already produced normal control potentials and, therefore, would be in a relatively more refractory state. This

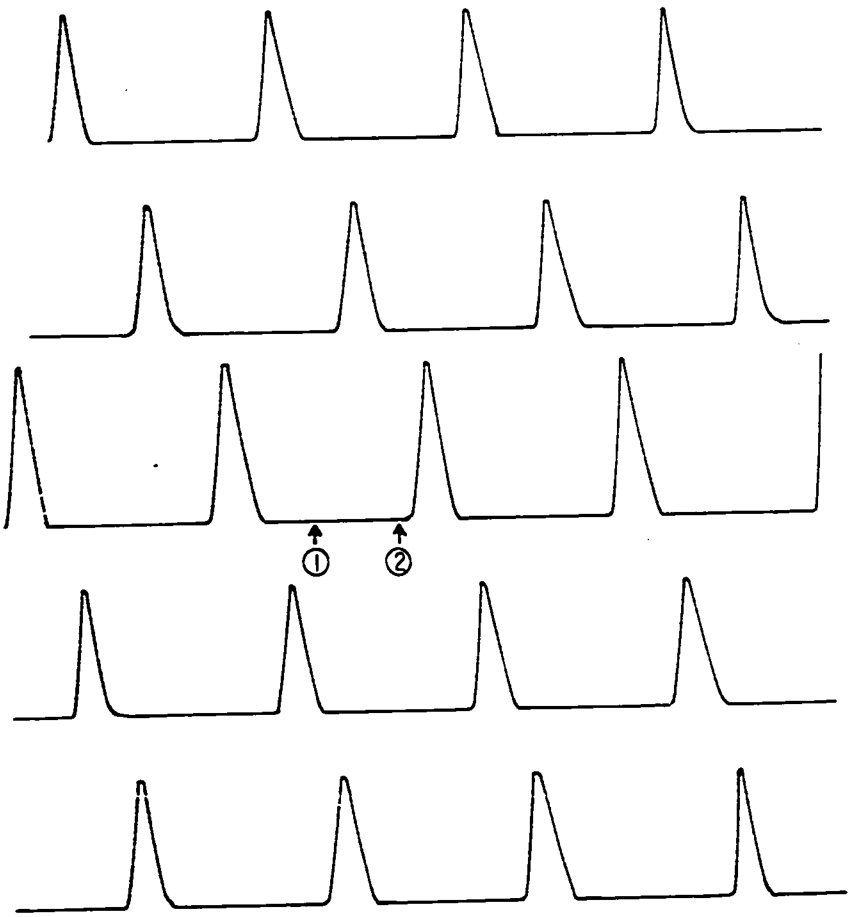

Figure 4.33

Diagram of control waves to explain the proximal and distal propagation of premature control potentials on the basis of refractoriness of oscillators. A PCP produced at (1) will propagate proximally, while that produced at (2) will propagate distally.

would prevent propagation in that direction. The distal oscillators would be in a sensitive or relatively less refractory state at this time, and the PCP would propagate in that direction. In between these two states, a state would exist in which a PCP could propagate in both directions.

The computer model, like the stomach, showed the above three different cases, but the three different zones were shorter in duration than those found in the dog stomach. A quantitative comparison of the lengths of proximal and distal propagations in the model and in the dog stomach could not be made, due to the smaller number of oscillators present in the former than in the latter.

The coupled models of the stoamch and the small intestine simulated the ECA of the pyloric region. The models suggested that the pyloric region did not act as an electrical insulator as suggested by Bass *et al.* (52). The model is consistent with the findings of Bortoff and Davis (51) who reported that the antral ECA was myogenically transmitted across the gastroduodenal junction. They reported the irregularity in the waveshape, time period, etc., of control waves recorded from electrodes implanted close to the pylorus (less than 9 mm). No such effects were, however, observed when we implanted electrodes further away from the pylorus.

It was sometimes observed that if the antrum was isolated by a complete circumferential cut, its frequency did not fall to the intrinsic value. In this situation, the leading control wave existed near the pylorus, and the direction of phase lag was oral up to the cut. It is possible that this leading control wave and the high frequency was due to the effect of the duodenal ECA on the antral ECA. It was shown in the model that if enough coupling is available, the duodenal ECA can raise the frequency of the control waves in isolated antrum.

This study has shown that an array of bidirectionally coupled relaxation oscillators simulates all the characteristics of the gastric ECA in dogs and hence is an appropriate model of it.

CHAPTER V

MATHEMATICAL ANALYSIS

5.1 Necessary and Sufficient Conditions for the Existence of a Limit Cycle

The necessary conditions for the existence of a limit cycle were derived by using state space analysis, while the sufficient conditions were derived by using the theorem of Dragilev (60, 61).

5.11 Necessary conditions

The system equations are:

$$\dot{x} = k(a_1 y + a_2 x + a_3 x^2 + a_4 x^3) \tag{5.1}$$

$$\dot{y} = -\frac{1}{k}(b_1 y + b_2 x + b_3 x^2 + b_4 x^3 - b_0) \tag{5.2}$$

The singular points can be found by putting $\dot{x} = \dot{y} = 0$; i.e.,

$$a_1 y + a_2 x + a_3 x^2 + a_4 x^3 = 0 \tag{5.3}$$

$$b_1 y + b_2 x + b_3 x^2 + b_4 x^3 - b_0 = 0 \tag{5.4}$$

Eliminating y from equations (5.3) and (5.4) leads to a cubic equation in x:

$$(a_4 b_1 - a_1 b_4)x^3 + (a_3 b_1 - a_1 b_3)x^2 + (a_2 b_1 - a_1 b_2)x + a_1 b_0 = 0 \tag{5.5}$$

The system would, therefore, have three singular points. To make the phase plane analysis for the existence of a limit cycle simple, the coefficients in equation (5.5) could be constrained so that the system has one real and two imaginary singular points. Apart from simplicity, this constraint would be desirable for the models described above. The constraint would ensure that each oscillator trajectory would return to its limit cycle after any disturbance. This constraint requires that

$$q^3 + r^2 > 0 \qquad \text{where}$$

$$q = \frac{1}{3}\frac{(a_2b_1 - a_1b_2)}{(a_4b_1 - a_1b_4)} - \frac{1}{9}\left\{\frac{(a_3b_1 - a_1b_3)}{(a_4b_1 - a_1b_4)}\right\}^2$$

$$r = \frac{1}{6}\left\{\frac{(a_2b_1 - a_1b_2)(a_3b_1 - a_1b_3)}{(a_4b_1 - a_1b_4)^2} - \frac{3(a_1b_0)}{(a_4b_1 - a_1b_4)}\right\} - \frac{1}{27}\left\{\frac{(a_3b_1 - a_1b_3)}{(a_4b_1 - a_1b_4)}\right\}^3$$

Assume the real singular point to be (x_1, y_1) and denote

$$x - x_1 = \xi \;, \qquad y - y_1 = \eta \;.$$

Equations (5.1) and (5.2) can be expanded about this singular point by using a Taylor series as follows:

$$\begin{aligned}\dot{\xi} = k\Big\{& a_1y_1 + a_1(y - y_1) + a_2x_1 + a_2(x - x_1) + a_3x_1^{\,2} \\ &+ \frac{2a_3x_1(x - x_1)}{1!} + \frac{2a_3(x - x_1)^2}{2!} + a_4x_1^{\,3} \\ &+ \frac{3a_4x_1^{\,2}(x - x_1)}{1!} + \frac{6a_4x_1(x - x_1)^2}{2!} \\ &+ \frac{6a_4(x - x_1)^3}{3!}\Big\}\end{aligned}$$

$$= k\left\{(a_1\eta + (a_2 + 2a_3x_1 + 3a_4x_1^2)\xi + (a_3 + 3a_4x_1)\xi^2 + a_4\xi^3\right\} \tag{5.6}$$

$$\dot{\eta} = -\frac{1}{k}\left\{b_1 y_1 + b_1(y - y_1) + b_2 x_1 + b_2(x - x_1) + b_3 x_1^{\,2} + \frac{2b_3 x_1 (x - x_1)}{1!} + \frac{2b_3 (x - x_1)^2}{2!} + b_4 x^{\,3} + \frac{3b_4 x_1^2 (x - x_1)}{1!} + \frac{6b_4 x_1 (x - x_1)^2}{2!} + \frac{6b_4 (x - x_1)^3}{3!} - b_0\right\}$$

$$= -\frac{1}{k}\left\{b_1 \eta + (b_2 + 2b_3 x_1 + 3b_4 x_1^{\,2})\xi + (b_3 + 3b_4 x_1)\xi^2 + b_4 \xi^3\right\} \tag{5.7}$$

Lyapunov has shown that so long as the linear terms are present and the system is structurally stable (i.e., no singular point is a center), the second and higher order terms may be neglected close to the singular point in equations (5.6) and (5.7) (58). Thus close to the singularity, the equations reduce to

$$\dot{\xi} = k\left\{(a_2 + 2a_3 x_1 + 3a_4 x_1^{\,2})\xi + a_1 \eta\right\} \tag{5.8}$$

$$\dot{\eta} = -\frac{1}{k}\left\{(b_2 + 2b_3 x_1 + 3b_4 x_1^{\,2})\xi + b_1 \eta\right\} \tag{5.9}$$

A necessary condition for a closed curve to be a limit cycle is that its Poincare index be +1. This criterion is not sufficient, however. Since the system has only one singular point, it must be a node or a focus for the Poincare index to be +1 (center is not realizable in physical systems because of its structural instability).

The condition for the singular point to be a node or a focus is (61):

$$-\frac{b_1}{k}(a_2 + 2a_3x_1 + 3a_4x_1{}^2) + \frac{a_1}{k}(b_2 + 2b_3x_1 + 3b_4x_1{}^2) > 0$$

or

$$a_1(b_2 + 2b_3x_1 + 3b_4x_1{}^2) - b_1(a_2 + 2a_3x_1 + 3a_4x_1{}^2) > 0 \tag{5.10}$$

For oscillations to build up from any initial condition inside the limit cycle, the node or the focus should be unstable. This constraint requires that

$$k(a_2 + 2a_3x_1 + 3a_4x_1{}^2) - \frac{b_1}{k} > 0$$

or

$$k^2(a_2 + 2a_3x_1 + 3a_4x_1{}^2) - b_1 > 0 \tag{5.11}$$

5.12 Sufficient conditions

The set of two first order differential equations (5.1) and (5.2) can be reduced to the following second order differential equation:

$$\ddot{x} + (\frac{b_1}{k} - ka_2 - 2ka_3x - 3ka_4x^2)\dot{x} + (a_1b_2 - b_1a_2)x + (a_1b_3 - b_1a_3)x^2$$
$$+ (a_1b_4 - b_1a_4)x^3 - a_1b_0 = 0 \tag{5.12}$$

The constant term can be eliminated by change of axis:

Let $x = Z + p$, then

$$\begin{aligned}\ddot{Z} &+ \left(\frac{b_1}{k} - ka_2 - 2ka_3p - 3ka_4p^2 - 2ka_3Z - 3ka_4Z^2 - 6ka_4Zp\right)\dot{x} \\ &+ \left\{(a_1b_2 - b_1a_2) + 2(a_1b_3 - b_1a_3)p + 3(a_1b_4 - b_1a_4)p^2\right\} Z \\ &+ \left\{(a_1b_3 - b_1a_3) + 3(a_1b_4 - b_1a_4)p\right\} Z^2 \\ &+ (a_1b_4 - b_1a_4)Z^3 + (a_1b_4 - b_1a_4)p^3 \\ &+ (a_1b_3 - b_1a_3)p^2 + (a_1b_2 - b_1a_2)p - a_1b_0 = 0 \qquad (5.13)\end{aligned}$$

For the constant term to be zero,

$$(a_1b_4 - b_1a_4)p^3 + (a_1b_3 - b_1a_3)p^2 + (a_1b_2 - b_1a_2)p - a_1b_0 = 0 \qquad (5.14)$$

This reduces equation (5.13) to

$$\ddot{Z} + f(Z)\dot{Z} + g(Z) = 0 \qquad (5.15)$$

where

$$f(Z) = \left(\frac{b_1}{k} - ka_2 - 2ka_3p - 3ka_4p^2\right) - 2k(a_3 + 3a_4p)Z - 3ka_4Z^2$$

$$\begin{aligned}g(Z) = &\left\{(a_1b_2 - b_1a_2) + 2(a_1b_3 - b_1a_3)p + 3(a_1b_4 - b_1a_4)p^2\right\} Z \\ &+ \left\{(a_1b_3 - b_1a_3) + 3(a_1b_4 - b_1a_4)p\right\} Z^2 \\ &+ (a_1b_4 - b_1a_4)Z^3\end{aligned}$$

Dragilev's theorem can now be used to find sufficient conditions for the existence of at least one limit cycle for equation (5.15).

Theorem of Dragilev (60, 61):

$$\text{Let } F(Z) = \int_0^Z f(Z)dZ, \qquad G(Z) = \int_0^Z g(Z)dZ$$

The differential equation (5.15) has at least one limit cycle if the following conditions are satisfied:

1) (a) g(Z) satisfies Lipschitz conditions

   (b) $Zg(Z) > 0$ for $Z \neq 0$

   (c) $G(\infty) = \infty$

2) (a) F(Z) is uniquely defined in the interval $-\infty < Z < \infty$

   (b) F(Z) satisfies the Lipschitz conditions in any finite interval

   (c) for sufficiently small $|Z|$,

   $F(Z) < 0$ if $Z > 0$ and $F(Z) > 0$ if $Z < 0$

3) (a) There exists a number M and there exist numbers k and k', $k' < k$, such that

   $F(Z) \geqslant k$, when $Z > M$,

   $F(Z) \leqslant k'$, when $Z < -M$

The following constraints are established to satisfy the above conditions for the existence of at least one limit cycle:

1) (a) g(Z) is a polynomial, so it satisfies the Lipschitz conditions

   (b) g(Z) passes through the origin. Hence for $Zg(Z) > 0$, g(Z) must lie in the first and the third quadrants. Also g(Z) should not intersect the Z-axis.

   g(Z) is of the form

   $g(Z) = AZ + BZ^2 + CZ^3$ where

$$A = \left\{(a_1b_2 - b_1a_2) + 2(a_1b_3 - b_1a_3)p + 3(a_1b_4 - b_1a_4)p^2\right\}$$

$$B = \left\{(a_1b_3 - b_1a_3) + 3(a_1b_4 - b_1a_4)p\right\}$$

$$C = (a_1b_4 - b_1a_4)$$

$$\frac{d}{dZ}\, g(Z)\Big|_{Z=0} = A$$

For the above conditions to be satisfied,

$$A > 0 \tag{5.16}$$

and the equation

$$(A + BZ + CZ^2) = 0$$

should have imaginary roots; i.e.,

$$B^2 < 4AC \tag{5.17}$$

(c) $$G(Z) = \frac{AZ^2}{2} + \frac{BZ^3}{3} + \frac{CZ^4}{4}$$

$$\text{for } G(\infty) = \infty , \quad C > 0 \tag{5.18}$$

2 (a) and (b)

$$f(Z) = P + QZ + RZ^2$$

where

$$P = (\frac{b_1}{k} - ka_2 - 2ka_3p - 3ka_4p^2)$$

$$Q = -2k(a_3 + 3a_4p)$$

$$R = -3ka_4$$

Therefore,

$$F(Z) = PZ + \frac{QZ^2}{2} + \frac{RZ^3}{3}$$

Since F(Z) is a polynomial, both these conditions are satisfied.

(c) This condition requires that

$$\left.\frac{d}{dZ}F(Z)\right|_{Z=0} < 0 \; ; \quad \text{i.e.,}$$

$$P < 0 \tag{5.19}$$

3(a) Since F(Z) is a polynomial of third degree, this condition is evidently satisfied if

$$R > 0 \tag{5.20}$$

The constraints on the parameters of oscillators are summarized below:

1) Constraints for one real singular point

C1: $q^3 + r^2 > 0$

where q and r are as defined above.

2) Necessary conditions

NC1: $a_1(b_2 + 2b_3x_1 + 3b_4x_1{}^2) - b_1(a_2 + 2a_3x_1 + 3a_4x_1{}^2) > 0$

NC2: $k^2(a_2 + 2a_3x_1 + 3a_4x_1{}^2) - b_1 > 0$

3) Sufficient conditions

SC1: $(a_1b_2 - b_1a_2) + 2(a_1b_3 - b_1a_3)p + 3(a_1b_4 - b_1a_4)p^2 > 0$

SC2: $$\left\{(a_1b_3 - b_1a_3) + 3(a_1b_4 - b_1a_4)p\right\}^2$$
$$< 4\left\{(a_1b_2 - b_1a_2) + 2(a_1b_3 - b_1a_3)p + 3(a_1b_4 - b_1a_4)p^2\right\}$$
$$\left\{(a_1b_4 - b_1a_4)\right\}$$

SC3: $(a_1 b_4 - b_1 a_4) > 0$

SC4: $\frac{b_1}{k} - ka_2 - 2ka_3 p - 3ka_4 p^2 < 0$

SC5: $- 3ka_4 > 0$

The parameters of the oscillators were chosen subject to the above constraints, while keeping in view the desired properties and waveshapes to be obtained. The parameters of the first oscillator in the second intestinal ECA model are shown below to satisfy the above constraints; the parameters are:

$a_1 = 1.339,\quad a_2 = 1.0,\quad a_3 = 0.3725,\quad a_4 = -0.3725$

$b_1 = 0.0,\quad b_2 = 2.40,\quad b_3 = 0.6,\quad b_4 = 0.75$

$b_0 = 6.0,\quad k = 5.0$

C1:

$q = 0.993,\quad r = -3.569$

Thus $q^3 + r^2 > 0$

NC1:

The value of x_1 obtained from the solution of equation (5.5) is 1.33.

Therefore,

$a_1(b_2 + 2b_3 x_1 + 3b_4 x_1^{\,2}) - b_1(a_2 + 2a_3 x_1 + 3a_4 x_1^{\,2}) = 10.7$

which is greater than 0.

NC2:

$k^2(a_2 + 2a_3 x_1 + 3a_4 x_1^{\,2}) - b_1 = 0.375$

which is greater than 0.

SC1:

The value of p obtained from equation (5.14) is 1.33.

$A = (a_1 b_2 - b_1 a_2) + 2(a_1 b_3 - b_1 a_3)p + 3(a_1 b_4 - b_1 a_4)p^2 = 10.70$

which is greater than 0.

SC2:

$B = (a_1 b_3 - b_1 a_3) + 3(a_1 b_4 - b_1 a_4)p = 4.82$

$C = (a_1 b_4 - b_1 a_4) = 1.005$

Therefore,

$$B^2 < 4AC$$

SC3:

$(a_1 b_4 - b_1 a_4) = 1.005$

which is greater than 0.

SC4:

$$\frac{b_1}{k} - ka_2 - 2ka_3 p - 3ka_4 p^2 = 0.075$$

which is greater than 0.

SC5:

$-3ka_4 = 5.585$

which is greater than 0.

5.2 Coupling of Oscillators

The set of equations representing each oscillator has two state variables, the x-state variable and the y-state variable. The x-state variable is also the output variable. Let the resultant of the outputs of the other oscillators which are fed into the nth oscillator be I_n. The forcing function I_n can be added either to equation (5.1) or to equation (5.2). The coupled equations of the nth oscillator in the two cases then become

$$\dot{x}_n = k(a_1 y_n + a_2 x_n + a_3 x_n^2 + a_4 x_n^3 + I_n) \tag{5.21}$$

$$\dot{y}_n = -\frac{1}{k}(b_1 y_n + b_2 x_n + b_3 x_n^2 + b_4 x_n^3 - b_0) \tag{5.22}$$

and

$$\dot{x}_n = k(a_1 y_n + a_2 x_n + a_3 x_n^2 + a_4 x_n^3) \tag{5.23}$$

$$\dot{y}_n = -\frac{1}{k}(b_1 y_n + b_2 x_n + b_3 x_n^2 + b_4 x_n^3 - b_0 + I_n) \tag{5.24}$$

respectively.

y_n can be eliminated from the two sets of equations to yield the following two second order differential equations, respectively:

$$\ddot{x} + f(x_n)\dot{x}_n + g(x_n) = b_1 I_n + k\frac{dI_n}{dt} \tag{5.25}$$

and

$$\ddot{x} + f(x_n)\dot{x}_n + g(x_n) = -a_1 I_n \tag{5.26}$$

$$f(x_n) = \frac{b_1}{k} - ka_2 - 2ka_3 x_n - 3ka_4 x_n^2$$

$$g(x_n) = (a_1 b_2 - b_1 a_2)x_n + (a_1 b_3 - b_1 a_3)x_n^2 + (a_1 b_4 - b_1 a_4)x_n^3 - a_1 b_0$$

It is, therefore, seen that adding the forcing function to equation (5.2) implies that the outputs of the other oscillators directly affect the forced oscillator. This can be compared to the case where two neighboring cells are in close contact at the nexus, and the potential variation across the membrane of one cell directly affects the other. This coupling has been referred to as voltage coupling.

Adding the forcing function to equation (5.1) implies that the outputs of other oscillators and their first derivatives affect the forced oscillator. This coupling has been referred to as the current coupling. The derivative part is similar to the case where the potential variations across the membrane set up currents in the extracellular fluid proportional to the first derivative of the potential variations. The parameter b_1 was zero for the second intestinal ECA model and the gastric ECA model. Hence only the derivative part was present for the coupling of oscillators.

The terms, voltage coupling and current coupling, have been used to distinguish the two cases described above, but the implications of these terms are purely speculative at this stage. No experimental or theoretical evidence exists at present to indicate that the extracellular current close to the cell membrane is proportional to the first derivative of membrane potential. The exact manner in which interaction between cells takes place is also uncertain yet. Barr (54) has proposed four possibilities which depend upon whether there is a continuity of membrane from cell to cell, or whether each cell is a separate entity.

CHAPTER VI

CONCLUSIONS, LIMITATIONS AND APPLICATIONS

This study has shown that the electrical control activity of the gastrointestinal tract behaves like a system of coupled relaxation oscillators. The muscle layers in this tract are a complex of relaxation type oscillators, each one of which is capable of oscillating at its own frequency but is influenced in frequency and in phase by the neighboring oscillators.

This model is different from the one in which the small intestine and the stomach are considered to behave like a cable. The cable model implies that the control waves generated at special regions known as pacemakers conduct through these organs. The cable model fails to explain the following:

1) End of the frequency plateau in the small intestine (see pages 20, 40, 69).
2) The response activity is local in nature; i.e., it can be recorded only at the site of its generation or a few mm away from it. This activity does not conduct even though the same conduction path is available to it as is available to the control activity.
3) A partial cut in the stomach or the small intestine may cause unlocking of distal and proximal waves even when a path is available for the control wave to conduct.
4) Different conduction velocities in different parts of the stomach and the small intestine.
5) Conduction taking place in the absence of membrane continuity in the longitudinal muscles of the duodenum (Daniel et al., unpublished).

The above phenomena were explained on the basis of models consisting of coupled relaxation oscillators.

The animal and the computer studies show that the terms Electrical Control Activity and Electrical Response Activity are the most appropriate terms to refer to the electrical activities of the gastrointestinal tract. These terms are descriptive as well as explanatory of the functions of the activities being referred to. The use of these terms was, therefore, preferred to the use of other terms like slow wave activity, basic electrical rhythm, pacesetter activity, fast activity and spike activity.

The models proposed in this thesis show qualitatively that with an appropriate choice of parameters, they can simulate the characteristics of the gastrointestinal electrical control activity. The differences between the models and the results of animal studies were the following:

1) The total phase lags in the stomach and the frequency plateau region of the small intestine were less in the models than in the animals.
2) A long frequency plateau was formed in the intestinal ECA models when a cut was made in the variable frequency region. No such frequency plateau was formed in the variable frequency region of the dog intestine.

These differences between the models and the animal results were mainly due to the following reasons:

1) The number of oscillators used in the models was small as compared to an unknown large number of oscillators in the animal organs.
2) Various parameters in these organs, e.g., intrinsic frequencies of cells, coupling factors between cells, are not fixed but vary about some mean value, probably at random, for a variety of reasons. Such variations were not incorporated into the models.
3) Each oscillator in the models was represented by a general system of

two first order nonlinear differential equations. No attempt was made at this stage to compare the parameters used in the equations with the basic constants of these organs.

4) Additional unknown structural and functional complexities may exist in the animal; e.g., a role for nerves in influencing control waves; a role for interaction between longitudinal and circular muscle layers.

Improvements of the models to take into account the above factors is an area of future work. Other areas of future work, related to this study, are mentioned below:

1) To determine the phase relationships between the electrical activities of the longitudinal muscle cells and the circular muscle cells in the stomach and the small intestine by using intracellular electrodes.
2) To represent the electrical activity of circular muscle cells by appropriate oscillators (they should oscillate only when driven by the oscillators representing the electrical activity of longitudinal muscle cells) and couple them with the oscillators representing the ECA of the longitudinal muscle cells.
3) To drive the oscillators in the stomach and the small intestine by electronic oscillators.
4) To do various operations in the animals like reversal of segments of different lengths in various parts of the small intestine, transfer of segments from ileum to duodenum and vice versa, excision of small intestinal and gastric segments, etc., and comparison of the results with those of similar operations in the models.

The animal studies and the models suggest a possible mechanism for the movement of the gastric and the intestinal contents. The control waves in the frequency plateau region of the small intestine and the stomach are phase locked. The phase lag under normal conditions is in the aboral direction. Since response activity, and hence contractions, occur in a relatively positive phase of the cycle, the contractions in successive regions of the small intestine (when a large region of small intestine is active) or of the stomach will also show similar phase lags. It will, therefore, appear as if a band of contraction is moving aborally. Similarly, temporary phase locking and frequency gradient would cause movements of intestinal contents in the distal jejunum and ileum.

A probable role of circular muscle cells in the stomach and the small intestine could be to synchronize the control activity along the circumference. If the control waves along the circumference are synchronized, the contraction in a small segment will also be simultaneous along the circumference. A simultaneous contraction along the circumference will be more effective in moving the contents than if it occurred along the circumference with a phase lag, or if it occurred only on a part of the circumference. Tight junctions which could be low resistance connections exist among circular cells (Daniel et al., unpublished). These low resistance connections would facilitate rapid spread of electrical activity in this direction.

The nature of electrical control mechanisms suggested by these models could have important applications in clinical medicine and in surgery. Many disorders of the stomach and the small intestine could have been caused by altered frequency gradients with consequent disturbances in mixing and propulsive movements. Postoperative effects of surgical operations like partial gastrectomy, gastric resection, excision of a segment of small intestine in case of ulcers, etc., could be explained on the basis of these models. The undesirable effects of these operations or altered frequency gradients in the diseased state could possibly be normalized with external oscillators.

BIBLIOGRAPHY

1. Alvarez, W. C. and L. J. Mahoney. Action currents in stomach and intestine. Am. J. Physiol. 58: 476, 1921.
2. Puestow, C. B. Studies on the origin of the automaticity of the intestine; the action of certain drugs on isolated intestinal transplants. Am. J. Physiol. 106: 682, 1932.
3. Bozler, E. The relation of the action potentials to mechanical activity in intestinal muscle. Am. J. Physiol. 146: 496-501, 1946.
4. Milton, G. W. and A. W. M. Smith. The pacemaking area of duodenum. J. Physiol. London 132: 100-114, 1956.
5. Milton, G. W., A. W. M. Smith and H. I. O. Armstrong. The origin of the rhythmic electropotential changes in the duodenum. Quart. J. Exptl. Physiol. 40: 79-88, 1955.
6. Daniel, E. E., D. R. Carlow, B. T. Wachter, W. H. Sutherland and A. Bogoch. Electrical activity of the small intestine. Gastroenterology 37: 268-281, 1959.
7. Daniel, E. E. and K. M. Chapman. Electrical activity of the gastrointestinal tract as an indication of mechanical activity. Am. J. Digest. Diseases 8: 54-102, 1963.
8. Daniel, E. E., B. T. Wachter, A. J. Honour and A. Bogoch. The relationship between electrical and mechanical activity of the small intestine of dog and man. Can. J. Biochem. Physiol. 38: 777-801, 1960.
9. Bass, P. Electrical activity of smooth muscle of the gastrointestinal tract. Gastroenterology 49: 391-394, 1965.

10. Bass, P., C. F. Code and E. H. Lambert. Motor and electrical activity of the duodenum. Am. J. Physiol. 201: 287-291, 1961.

11. Bortoff, A. Slow potential variations of the small intestine. Am. J. Physiol. 201: 203-208, 1961.

12. Bortoff, A. Configuration of intestinal slow waves obtained by monopolar recording techniques. Am. J. Physiol. 213: 157-162, 1967.

13. Bass, P., C. F. Code and E. H. Lambert. Electric activity of gastroduodenal junction. Physiologist 2: 8, 1959.

14. Bozler, E. The action potentials of the stomach. Am. J. Physiol. 144: 693-700, 1945.

15. Daniel, E. E. The electrical and contractile activity of the pyloric region in dogs and the effects of drugs. Gastroenterology 49: 403-418, 1965.

16. Daniel, E. E. and J. Irwin. Electrical activity of gastric musculature. In: HANDBOOK OF PHYSIOLOGY, Alimentary Canal. Washington, D. C. Am. Physiol. Soc., 1968. Sect. 6, Vol. IV, p. 1969-1984.

17. Daniel, E. E., A. J. Honour and A. Bogoch. Electrical activity of the longitudinal muscle of dog small intestine studied in vivo using microelectrodes. Am. J. Physiol. 198: 113-118, 1960.

18. Prosser, C. L. and A. Bortoff. Electrical activity of intestinal muscle under in vitro conditions. In: HANDBOOK OF PHYSIOLOGY, Alimentary Canal. Washington, D. C. Am. Physiol. Soc., 1968. Sect. 6, Vol. IV, p. 2025-2050.

19. Burnstock, G., M. E. Holman and C. L. Prosser. Electrophysiology of smooth muscle. Physiol. Rev. 43: 482-527, 1963.

20. Van Harn, G. L. Responses of muscles of cat small intestine to autonomic nerve stimulation. Am. J. Physiol. 204: 352-358, 1963.

21. Kobayashi, M., T. Nagai and C. L. Prosser. Electrical interaction between muscle layers of cat intestine. Am. J. Physiol. 211: 1281-1291, 1966.

22. Holaday, D. A., H. Volk and J. Mandell. Electrical activity of the small intestine with special reference to the origin of rhythmicity. Am. J. Physiol. 195: 505-515, 1958.

23. Nelson, T. S. and J. C. Becker. Simulation of the electrical and mechanical gradient of the small intestine. Am. J. Physiol. 217: 749-757, 1968.

24. Diamant, N. E. and A. Bortoff. Nature of the intestinal slow wave frequency gradient. Am. J. Physiol. 216: 301-307, 1969.

25. Diamant, N. E. and A. Bortoff. Effects of transection on the intestinal slow wave frequency gradient. Am. J. Physiol. 216: 734-743, 1969.

26. Diamant, N. E., P. K. Rose and E. J. Davison. Computer simulation of slow wave frequency gradient. Am. J. Physiol. 219: 1684-1690, 1970.

27. Sarna, S. K., E. E. Daniel and Y. J. Kingma. Simulation of slow wave electrical activity of the small intestine. Am. J. Physiol. In press.

28. Sarna, S. K., E. E. Daniel and Y. J. Kingma. A matrix of relaxation oscillators as a model of the electrical control activity of the stomach. 72nd Annual Meeting of American Gastroenterological Association. May 1971.

29. Van der Pol, B. and J. Van der Mark. The heart beat considered as a relaxation oscillator and an electrical model of the heart. Phil. Mag. Suppl. 6: 763-775, 1928.

30. Fitzhugh, R. Impulses and physiological states in theoretical models of nerve membrane. Biophys. J. 1: 445-466, 1961.

31. Winfree, A. T. Biological rhythms and the behaviour of populations of coupled oscillators. J. Theoret. Biol. 16: 15-42, 1967.

32. Bass, P. In vivo electrical activity of the small bowel. In: HANDBOOK OF PHYSIOLOGY. Alimentary Canal. Washington, D. C. Am. Physiol. Soc., 1968. Sect. 6, Vol. IV, p. 2051-2074.

33. Szurszewski, J. H., L. R. Elveback and C. F. Code. Configuration and frequency gradient of electrical slow wave over canine small bowel. Am. J. Physiol. 218: 1468-1473, 1970.

34. Roberge, F. A. and R. A. Nadeau. Simulation of sinus node activity by an electronic relaxation oscillator. Can. J. Physiol. Pharmacol. 44: 301-305, 1966.

35. McCoy, E. J. and R. D. Baker. Intestinal slow waves. Decrease in propagation velocity along upper small intestine. Am. J. Digest. Diseases 14: 9-13, 1969.

36. Barr, L., W. Berger and M. M. Dewey. Electrical transmission at the nexus between smooth muscle cells. J. Gen. Physiol. 51: 347-368, 1968.

37. Kobayashi, M., C. L. Prosser and T. Nagai. Electrical properties of intestinal muscle as measured intracellularly and extracellularly. Am. J. Physiol. 213: 275-286, 1967.

38. Holman, M. E. Introduction to electrophysiology of smooth muscle. In: HANDBOOK OF PHYSIOLOGY. Alimentary Canal. Washington, D. C. Am. Physiol. Soc., 1968. Sect. 6, Vol. IV, p. 1665-1708.

39. Bortoff, A. Electrical transmission of slow waves from longitudinal to circular intestinal muscle. Am. J. Physiol. 209: 1254-1260, 1965.

40. Bunker, C. F., L. P. Johnson and T. S. Nelson. Chronic in situ studies of the electrical activity of the small intestine. Arch. Surg. 95: 259-268, 1967.

41. Christensen, J., H. P. Schedl and J. A. Clifton. The small intestinal basic electrical rhythm (slow wave) frequency gradient in normal man and in patients with a variety of diseases. Gastroenterology 50: 309-315, 1966.

42. Hasselbrach, R. and J. E. Thomas. Control of intestinal rhythmic contractions by a duodenal pacemaker. Am. J. Physiol. 201: 955-960, 1961.

43. Roberge, F. A. Simulation of the phenomenon of concealed conduction in heart. Computers for Biomedical Research, Vol. 2, No. 4, June 1969, by Academic Press, 362-372.

44. Hodgkin, A. L. and A. F. Huxley. A quantitative description of membrane current and its application to conduction and excitation in nerve. J. Physiol. 117: 500-544, 1952.

45. Noble, D. Applications of Hodgkin-Huxley equations to excitable tissues. Physiol. Reviews. American Physiol. Soc., Vol. 46, No. 1, 1966.

46. Bortoff, A. and F. Sachs. Electrotonic spread of slow waves in circular muscle of small intestine. Am. J. Physiol. 218: 576-581, 1970.

47. Daniel, E. E., K. Robinson, G. Duchon and R. M. Henderson. The possible role of close contacts (nexuses) in the propagation

of control electrical activity in the stomach and small intestine. Am. J. Digest. Diseases. In press.

48. Kelly, K. A., C. F. Code and L. R. Elveback. Patterns of canine gastric electrical activity. Am. J. Physiol. 217: 461-470, 1969.

49. Kelly, K. A. and C. F. Code. Canine gastric pacemaker. Am. J. Physiol. 220: 112-118, 1971.

50. Weber, J. Jr. and S. Kohatsu. Pacemaker localization and electrical conduction patterns in the canine stomach. Gastroenterology 59: 717-726, 1970.

51. Bortoff, A. and R. S. Davis. Myogenic transmission of antral slow waves across the gastroduodenal junction in situ. Am. J. Physiol. 215: 889-897, 1968.

52. Bass, P., C. F. Code and E. H. Lambert. Electric activity of gastroduodenal junction. Am. J. Physiol. 201: 587-592, 1961.

53. Allen, G. L., E. W. Poole and C. F. Code. Relationships between electrical activities of antrum and duodenum. Am. J. Phsyiol. 207: 906-910, 1964.

54. Barr, L. Propagation in vertebrate visceral smooth muscle. J. Theoret. Biol. 4: 73-85, 1963.

55. Code, C. F. and H. C. Carlson. Motor activity of the stomach. In: HANDBOOK OF PHYSIOLOGY. Alimentary Canal. Washington, D. C. Am. Phsyiol. Soc., 1968. Sect. 6, Vol. IV, p. 1903-1916.

56. Carlson, H. C., C. F. Code and R. A. Nelson. Motor action of the canine gastroduodenal junction: A cineradiographic, pressure and electric study. Am. J. Digest. Diseases 11: 155-172, 1966.

57. Miller, M. E., G. C. Christensen and H. E. Evans. ANATOMY OF THE DOG. W. B. Saunders Company, 1964.

58. Gibson, J. E. NONLINEAR AUTOMATIC CONTROL. McGraw-Hill, New York, 1963.

59. LaSalle, J. and S. Lefschetz. STABILITY BY LYAPUNOV'S DIRECT METHOD WITH APPLICATIONS. Academic Press, New York, 1961.

60. Bogoliubov, N. N. and Y. A. Mitropolsky. ASYMPTOTIC METHODS IN THE THEORY OF NONLINEAR OSCILLATIONS. Hindustan Publishing Corp., Delhi, 1961.

61. Minorsky, N. NONLINEAR OSCILLATIONS. D. Van Nostrand Co., Inc., Princeton, New Jersey, 1962.

62. Truxal, J. G. CONTROL ENGINEERS' HANDBOOK. McGraw-Hill, New York, 1958.

APPENDIX

PDP-8 COMPUTER PROGRAM FOR MULTIPLIERS

THIS PROGRAM STARTS BY READING THE INPUT AT A/D CHANNEL 0. IN RESPONSE, IT GIVES (8*X↑2)/10 AT D/A CHANNEL 0 AND (32*X↑3)/100 AT D/A CHANNEL 1. INPUTS AT SUCCESSIVE A/D CHANNELS ARE THEN READ AND SIMILAR OUTPUTS GIVEN AT THE CORRESPONDING D/A CHANNELS. PUT THE NO. OF CHANNELS TO BE PROCESSED IN LOCATION CNT1 (8'S COMPLIMENT)

```
0200  7402            HLT
0201  7200  START,    CLA
0202  3313            DCA  DACHAN
0203  1306  ADCON,    TAD  CNT1   /READ NO. OF CHANNELS TO BE
                                  /PROCESSED
0204  3307            DCA  CNT2
0205  6416            6416        /SET A/D CONVERTER AND
                                  /MULTIPLEXER TO ZERO
0206  6421            6421        /ZERO A/D FLAG
0207  6422  HERE,     6422        /A/D CONVERT
0210  6411            6411        /WAIT 10 MICRO SEC FOR
                                  /CONVERTION
0211  5214            JMP   .-1
0212  6421            6421        /RESET THE FLAG
0213  7200            CLA
0214  6434            6434        /DATA TO AC
0215  3310            DCA  TEMP
0216  1310            TAD  TEMP
0217  7510            SPA         /CHECK IF AC POSITIVE
0220  7041            CIA         /NO: MAKE IT POSITIVE
0221  3232            DCA  NUM1
0222  1232            TAD  NUM1
0223  3241            DCA  NUM2
0224  1232            TAD  NUM1
0225  7425            7425
0226  0000  NUM1,     0000
0227  7415            7415
0230  0007            0007
0231  7701            7701
0232  3311            DCA  X2
0233  1311            TAD  X2
0234  7425            7425
0235  0000  NUM2,     0000
0236  7415            7415
0237  0010            0010
0240  7100            CLL
0241  1310            TAD  TEMP
0242  7710            SPA CLA
0243  7120            STL
0244  7501            7501
0245  7430            SZL
```

```
0246  7041              CIA
0247  3312              DCA  X3
0250  1311              TAD  X2
0251  6422  DACON,      6462       /RESET DATA AND ADDRESS
                                   /BUFFERS AND FLAG
0252  6464              6464       /LOAD DATA
0253  7200              CLA
0254  1313              TAD  DACHAN
0255  6451              6451       /LOAD ADDRESS BUFFER
0256  6454              6454       /D/A CONVERT
0257  6441              6441       /WAIT 10 MICRO SEC FOR
                                   /CONVERSION
0260  5263              JMP  .-1
0261  2313              ISZ  DACHAN
0262  7000              7000
0263  7200              CLA
0264  1312              TAD  X3
0265  6462              6462
0266  6464              6464       /LOAD DATA
0267  7200              CLA
0270  1313              TAD  DACHAN
0271  6451              6451       /LOAD ADDRESS BUFFER
0272  6454              6454       /D/A CONVERT
0273  6441              6441       /WAIT 10 MICR0 SEC FOR
                                   /CONVERSION
0274  5277              JMP  .-1
0275  2313              ISZ  DACHAN
0276  7000              7000
0277  2307              ISZ  CNT2  /ALL A/D CHANNELS PROCESSED?
0300  5213              JMP  HERE  /N0: PROCESS NEXT CHANNEL
0301  5201              JMP  START /YES: GO TO CHANNEL 0
0302  0000  CNT1,       0000
0303  0000  CNT2,       0000
0304  0000  TEMP,       0000
0305  0000  X2,         0000
0306  0000  X3,         0000
0307  0000  DACHAN,     0000
```